Vietnamese-German University

COPYRIGHT WARNING

RUHR-UNIVERSITÄT BOCHUM

Vietnamese-German University

DESIGN OF PLASTIC INJECTION MOLD WITH COMMERCIAL CAD/CAE PROGRAM

BACHELOR THESIS

BINH DUONG 28.04.2023

Submitted by: Ho Hoang Long

RUB Student ID: 19220266

VGU Student ID: 14473

Supervisor: Prof. Dr. Nguyen Quoc Hung

Co-supervisor: MsE. Do Minh Hieu

Design of plastic injection mold with commercial CAD/CAE program

A Thesis Presented
By
Long Ho Hoang

Submitted to the department of Mechanical Engineering of the
RUHR-UNIVERSITÄT BOCHUM and VIETNAMESE-GERMAN UNIVERSITY
in partial fulfillment of the requirement for the degree of
BACHELOR IN MECHANICAL ENGINEERING

April 2023

Major: Mechanical Engineering

Affirmation in lieu of oath

I hereby certify that this Bachelor thesis is my independent work with the sources and assistance listed in this paper. Any sentences, figures or tables stated in my work from published or unpublished sources are all marked and listed in the reference section. I declare that my thesis has not been submitted to any other board of examiners in the same or a similar format and has not been published yet.

Name: Long Ho Hoang

Place, date: Binh Duong, April 26

Signature:

_____

Acknowledgements

First of all, I would like to express my sincere gratitude to my advisor, Prof. Nguyen Quoc Hung for his advices, encouragement of the thesis, and support along the study courses throughout my university years.

Secondly, I would like to express a special thank to Mr. Hieu, who has provided me with additional assistance throughout the early study of this thesis. I now have the necessary tool for the mold flow analysis thanks to his recommendation and guidance of the mold analysis program.

Finally, I am very grateful for my friends' and family's advice and moral support, which have helped me revitalized and boost my energy during my time writing this thesis.

ABSTRACT

The purpose of this thesis is to design a plastic injection mold and apply commercial CAD/CAE software into the designing procedure. The designed injection mold produces a cover that protects the printed circuit board and electrical components of a LED light. To produce a plastic object with proper quality and reduce defects via the injection molding method, a proper feed system is required. This research introduces and applies the mold flow analysis program into designing a suitable feed system to achieve good quality products. When a sufficient feed system is achieved, the mold components including the mold plates, injection pin and the cores are designed with CAD program. These mold parts are subjected to various stresses, and they are analyzed with the CAD program's FEM analysis. The analysis results suggest the optimization for the mold components design and an assembly model of the plastic injection mold is obtained at the end of this thesis.

Table of contents

Acknowledgements 1

Abstract 2

List of figures 5

List of tables 9

Abbreviation 10

1. Introduction

    1.1. Injection molding definition 11

    1.2. Product description 12

    1.3. Goal and scope 14

2. Mold flow analysis 15

    2.1. Introduction of the feed system and the feed system analysis 15

    2.2. Autodesk Moldflow Insight 15

    2.3. Meshing 16

    2.4. Meshing procedure 16

    2.5. Gate location analysis 16

    2.6. Molding window analysis 19

    2.7. Fill + pack analysis 24

    2.8. Fill time analysis 24

    2.9. Pressure analysis 25

    2.10. Volumetric shrinkage 26

    2.11. Weld lines 27

    2.12. Frozen layer fraction 27

    2.13. Process optimization 30

3. Designing the feed system 39

    3.1. Feed system definition 39

    3.2. Feed system analysis 41

        3.2.1. Pressure drop analysis 41

        3.2.2. Feed system material's consumption 44

3.2.3. Runner balance analysis 44
3.2.4. Runner cooling time analysis 47
3.3. Designing the feed system's gate 50
3.3.1. Calculate the gate shear rate 52
3.3.2. Calculate the gate pressure drop 54
3.3.3. Calculate the gate freeze time 55
4. Selection of the cooling system 59
4.1. Calculation of the estimated cooling time 61
4.2. Calculation of the cooling line diameter 62
4.3. Selection of the cooling line depth 65
4.4. Selection of the cooling line pitch 65
5. Designing the mold components with NX 67
5.1. Introduction of the computer aided designing program 67
5.2. Designing the mold plates 67
5.2.1. Mold plates modeling process 68
5.2.2. Mold plates stress analysis using NX 69
5.2.3. Plate bending analysis 75
5.3. Designing the ejector pins 87
5.3.1. Calculating the ejector pin's push area and perimeter 87
5.3.2. Ejector pin modeling process 91
5.4. Designing the core insert 92
5.4.1. Core insert modeling process 93
5.4.2. Core insert stress analysis with NX 93
5.5. Selection of the spring for the ejection system 95
5.6. Plastic injection mold assembly model 98
6. Discussion 100
7. Conclusion 100
8. Reference 102

List of figures

Figure 1-1: The illustration of the LED light 12

Figure 1-2: The isometric view of the targeted product model 12

Figure 1-3: The top view of the targeted product model 13

Figure 1-4: The bottom view of the targeted product model 13

Figure 2-1: Illustration of the part cavities and feed system 15

Figure 2-2: The flow resistance indicated on the LED model 17

Figure 2-3: The flow resistance between the two screw pillars 17

Figure 2-4: The gating suitability result 18

Figure 2-5: The pink cone indicates the gate location 18

Figure 2-6: The zone (molding window) graph 20

Figure 2-7: The quality (molding window): XY plot 21

Figure 2-1: The shear stress at the recommended process conditions 21

Figure 2-2: The shear rate at the recommended conditions 22

Figure 2-3: The maximum cooling time at the cavity 23

Figure 2-4: Visualization of the product's filling time 25

Figure 2-5: The pressure and time graph at the gate location 26

Figure 2-6: The volumetric shrinkage of the product 27

Figure 2-7: The weld lines develop on the product's wall 28

Figure 2-8: The frozen layer fraction plot 29

Figure 2-9: The frozen layer fraction: XY plot of a cavity 30

Figure 2-10: The pressure: XY plot taken at the thin-wall section 30

Figure 2-11: The new gate location 31

Figure 2-12: The reduced number of weld lines 32

Figure 2-113: The new recommended molding conditions 33

Figure 2-14: The quality: XY plot for the new gate location 33

Figure 2-15: The new shear stress value 34

Figure 2-16: The new shear rate value 34

Figure 2-17: The new maximum cooling time 35

Figure 2-18: The new fill time of the cavities 36

Figure 2-19: The pressure plot taken at the similar position of each cavity 36

Figure 2-20: The new volumetric shrinkage of the products 37

Figure 2-21: The reduced number of weld lines 37

Figure 2-22: The frozen layer fraction visualization at different areas 38

Figure 2-23: The frozen layer fraction: XY plot taken at the analyzing positions 38

Figure 3-1: A general feed system 40

Figure 3-2: Demonstration of a two-plate mold 41

Figure 3-3: Demonstration of a three-plate mold 41

Figure 3-4: The sprue bushing provided by MISUMI 43

Figure 3-5: The pressure drop at the sprue 45

Figure 3-6: The pressure drop at the primary runner 45

Figure 3-7: The pressure drop at the secondary runner 45

Figure 3-8: The target pressure for the runner balance analysis 47

Figure 3-9: The modified feed system 47

Figure 3-10: The visualization of the time to reach ejection temperature 49

Figure 3-11: The new time to reach ejection temperature 50

Figure 3-12: The finalized model of the feed system and part cavities 51

Figure 3-13: The sprue gate design 52

Figure 3-14: The pin-point gate design 52

Figure 3-15: The edge gate design 53

Figure 3-16: The shear rate result of the 1 mm gate 54

Figure 3-17: The shear rate result of the 2 mm gate 55

Figure 3-18: The pressure drop at the gate: XY plot 56

Figure 3-19: The gate design of the feed system 58

Figure 3-20: Visualization of the finalized feed system 59

Figure 4-1: The cooling system with the continuously looped cooling lines 60

Figure 4-2: The cooling system with short return loop 60

Figure 4-3: The main distribution and accumulation line cooling layout 61

Figure 4-4: The peripheral cooling line layout 61

Figure 4-5,6,7: The cooling system of the plate A and plate B 67

Figure 5-1: The mold plates of the injection mold 69

Figure 5-2: The applied force and the fixed constraint for the FEM analysis 71

Figure 5-3: The von Mises stress on the spacer block 72

Figure 5-4: The von Mises stress on the bottom clamp plate 73

Figure 5-5: The von Mises stress on the support plate 73

Figure 5-6: The von Mises stress on the B plate 74

Figure 5-7: The von Mises stress on the A plate 74

Figure 5-8: The von Mises stress on the stripe plate 75

Figure 5-9: The von Mises stress on the runner plate 75

Figure 5-10: The von Mises stress on the top clamp plate 76

Figure 5-11: The bottom clamp plate's bending by compression 78

Figure 5-12: The plate B's bending by compression 78

Figure 5-13: The plate bending by compression on the plate A 79

Figure 5-14: The plate bending by compression on the stripe plate 79

Figure 5-15: The plate bending by compression on the runner plate 80

Figure 5-16: The plate bending by compression on the top clamp plate 80

Figure 5-17: The bending value of the support plate 82

Figure 5-18: The bottom clamp plate 83

Figure 5-19: The space block 83

Figure 5-20: The support plate 84

Figure 5-21: The plate B 84

Figure 5-22: The ejector plate 85

Figure 5-23: The ejector retainer plate 85

Figure 5-24: The plate A 86

Figure 5-25: The stripe plate 86

Figure 5-26: The runner plate 87

Figure 5-27: The top clamp plate 87

Figure 5-28: The side view of the ejection system 88

Figure 5-29: Ejector pin's dimension provided by MISUMI 93

Figure 5-30: The Isometric view of the ejector pin model 93

Figure 5-31: The von Mises stress result of the core 95

Figure 5-32: The displacement result on the core 95

Figure 5-33: The 2D projection views of the mold core 96

Figure 5-34: The die springs in the ejection system 99

Figure 5-35: The exploded view of the plastic injection mold model 99

Figure 1-24: The assembly model of the plastic injection mold 100

Figure 5-37: The 2D CAD of the injection mold 100

List of tables

Table 1-1: The material properties of LUPOY GN1008RF 15

Table 2-1: The recommended values from the molding window analysis 24

Table 2-2: The molding window analysis results with the new gate location 35

Table 3-1: The required input for runner system wizard 44

Table 3-2: Comparison between the estimated and calculated pressure drop values 46

Table 3-3: The balanced runner's diameter 48

Table 3-4: The old and new pressure drop values of the adjusted feed system 49

Table 3-5: The dimension of the feed system 50

Table 3-6: The shear rate in correspondence with the increasing gate's diameter 55

Table 3-7: The gate's dimension 58

Table 3-8: The finalized dimension of the feed system 58

Table 4-1: Specifications of Typical Cooling Plugs 66

Table 4-2: The cooling line's parameter 67

Table 5-1: The estimated deflection value of the fully supported plates 77

Table 5-2: The spring technical datasheet provided by Raymond manufacturer 98

Abbreviation

CAD: computer aided design

CAE: computer aided engineering

FEM: finite element method

PC: Polycarbonate

1. Introduction

This chapter introduces the definition of injection molding process and its utilization in the production industry. The targeted product is then described and the plastic injection mold design procedure is briefly described. For this thesis, the mold design procedure is assisted by the mold flow analysis program and CAD/CAE program to create a plastic injection mold model that produces high quality products.

1.1. Injection molding definition

Plastic products are one of the most widely consumed products and provides considerable profits. In order to achieve the required level of productivity, plastic processing industry has evolved with various processes have been developed to deliver a sufficient productivity. Injection molding is considered to be a particularly important part of the plastic industry.

Injection molding is a repetitive process, and its cycle consists of four phases: filling, packing, cooling and ejection phases. Prior to the injection of the resin, two halves of the mold are pressed together and held by the clamping unit. During the filling phase, the molten plastic is injected into the mold cavity. Throughout the packing phase, the material is held under pressure, allowing additional material to enter to compensate for the shrinkage. When the gate is completely frozen, which prevents more material to enter the cavity, the material continues to cool and solidify by contacting the mold's cold interior in the course of the cooling phase. The ejection phase starts when sufficient cooling time is reached and the parts become stiff enough to be ejected from the mold with the ejection system, basically duplicating the shape of the mold's cavity. The mold is then closed and the cycle repeats.

1.2. Product description

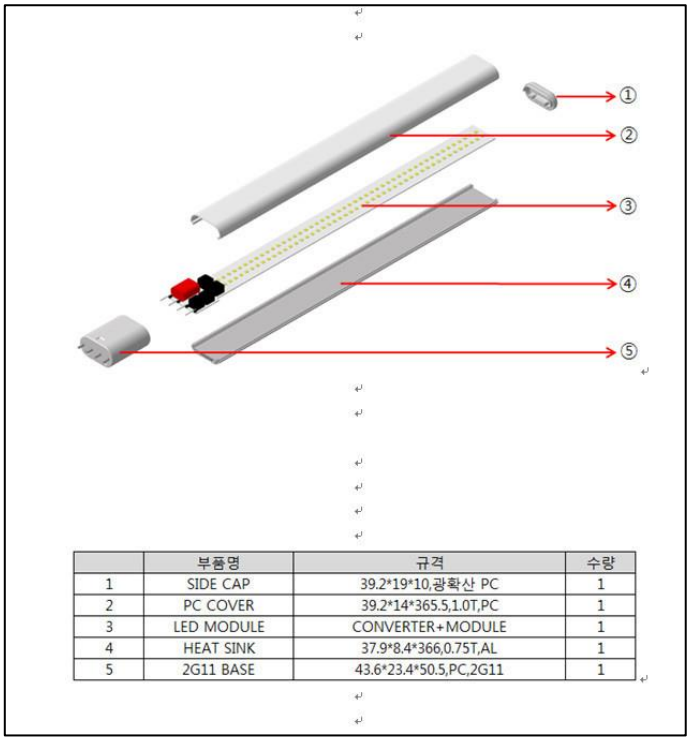

	부품명	규격	수량
1	SIDE CAP	39.2*19*10,광확산 PC	1
2	PC COVER	39.2*14*365.5,1.0T,PC	1
3	LED MODULE	CONVERTER+MODULE	1
4	HEAT SINK	37.9*8.4*366,0.75T,AL	1
5	2G11 BASE	43.6*23.4*50.5,PC,2G11	1

Figure 1-1: The illustration of the LED light

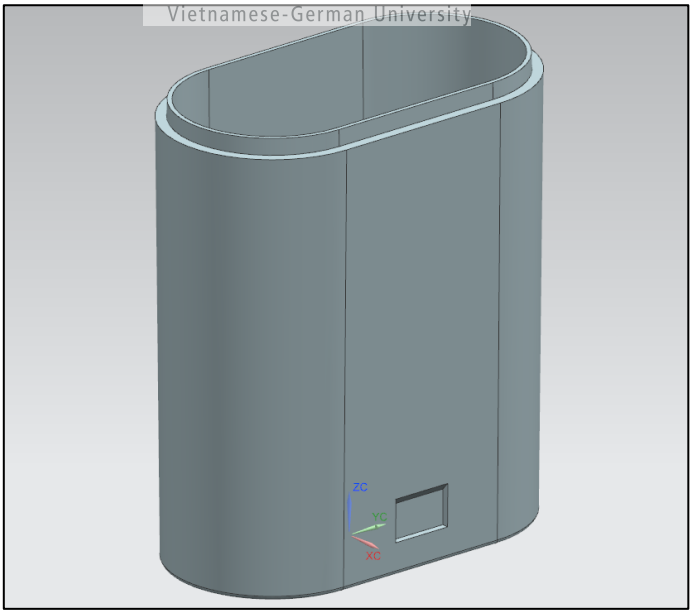

Figure 1-2: The isometric view of the targeted product model

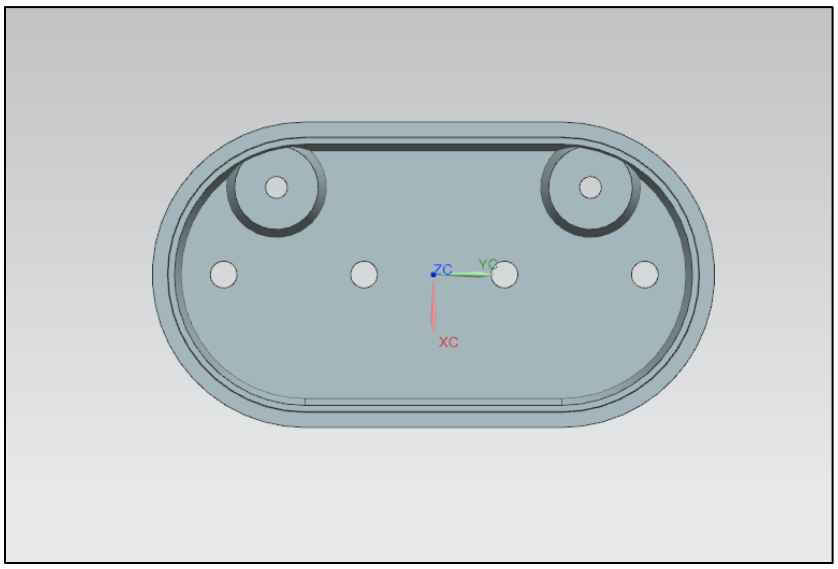

Figure 1-3: The top view of the targeted product model

Figure 1-4: The bottom view of the targeted product model

From the figures above, the targeted product is the 2G11 base. The purpose of this cover is to protect the electrical board and components that control the LED light. The base dimension is 50.5 mm in height and 43 mm in width. The base possesses a thin wall profile, and the wall thickness is 1.8 mm. The opening of the base is especially thin, whose thickness reaches only 0.8 mm. Inside the case consists of two cylindrical-shaped pillars to guide the direction of the screw to attach the cover to the LED light's heat sink. This thesis chooses this product for mold flow analysis and mold design due to the object's geometry. The thin wall geometry can produce various molding defects if the feed system is not suitably located and designed.

The chosen material for the LED light's base cover is Polycarbonate (PC). Polycarbonate is an engineering plastic classified as a non-crystalline material, which possesses high mechanical properties. This material is distinguished from other engineering materials, due to its capability of reaching compelling commercial success.

There are many manufacturers that can provide this material, in which LG chemical is selected for their high-quality PC material. The chosen PC material's trade name is LUPOY GN1008RF. The following table contains the relevant material properties, which are required for the mold flow analysis.

Properties	Values
Yield strength (MPa)	59.8
Mold shrinkage (%)	0.6
Melt temperature range (°C)	240-310
Mold temperature range (°C)	60-90
Mold surface temperature (°C)	75

Table 1-2: The material properties of LUPOY GN1008RF

1.3. Goal and scope

From the information of the injection molding process mentioned above, we perceive that to produce a plastic product with this process requires a product-shaped cavity and the feed system that acts as path for the molten plastic to flow. This thesis focuses in theoretically designing the feed system by applying a specialized mold flow analysis program, and the model of each mold component via the CAD/CAE programs. These components are then assembled to create the appropriate cavities and feed system to manufacture the desirable quality of the targeted product. Additionally, this study conducts the stress and deflection analysis to ensure the mold components can resist deformation caused by the acting clamp force and melt pressure. The stress analysis is conducted with the assistance of the CAD/CAE program's FEM analysis.

2. Mold flow analysis

2.1. Introduction of the feed system and the feed system analysis

The most important part of a plastic injection mold is the core insert and the cavity insert that form the product shaped mold cavity, in which the plastic flows into to duplicate the product. The feed/runner system acts as a pathway for the hot plastic melt to flow from the nozzle into the mold cavity. A sprue, runners, and gates are the three channels that make up the feed system in general.

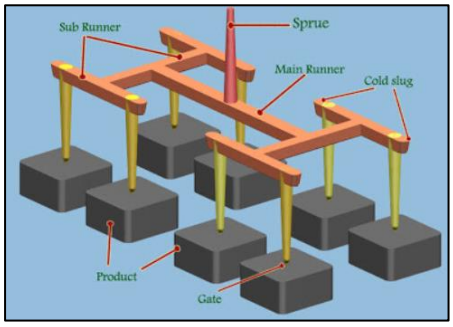

Figure 2-1: Illustration of the part cavities and feed system

The material flow must be analyzed to design the mold cavity and runner system. This analysis aids in determining if the material can completely fill all of the part's cavity with the specified process setting. Possible molding defects such as weld lines and volumetric shrinkage can be anticipated and avoided by altering the feed system design and the process condition.

2.2. Autodesk Moldflow Insight

Autodesk Moldflow Insight is a specialized program that focuses in conducting material flow simulation and analysis. The program uses the initially specified material's properties, process condition, and the product's meshed model to analyze and interpret the molding results. These results can be visualized as color-coded regions on the product model's surface, or the line graph based on the chosen parameter such as the pressure graph, shear stress graph, etc. Based on these results, the user determines the optimal molding condition and potential problems to adjusted for a suitable feed system. To achieve the aforementioned results, Autodesk Moldflow Insight provides a sequence of analyses. These analyses include: gate location analysis, molding window analysis, fill + pack analysis, runner balance analysis, etc.

2.3. Meshing

It is complicated to model and simulate the molten plastic (a non-Newtonian flow) flowing through the cavity to form the product's shape. Meshing is a process that simplifies the modeling process by transforming the product's shape into smaller elements that contains multiple nodes. On each individual element, variables such as temperature, pressure, and flow velocity are calculated. [1] Autodesk Moldflow Insight provides the user with three distinct meshing method:

- The midplane meshing
- The dual domain meshing
- The 3D meshing

The dual domain mesh model is suitable for analyzing the object with a thin-walled structure.

2.4. Meshing procedure

1. Import the CAD geometry of the product and choose the mesh type as dual domain.
2. Choose Create mesh to generate a mesh for the model
3. Click Mesh

2.5. Gate location analysis

A gate position is critical to the quality of the product. Its position directly influences the path that the plastic melt flows to the mold cavity, which determines the melt flow, the mold shrinkage, part dimension, warpage, and the weld lines. The gate should be located at the location where a balanced and unidirectional flow can be achieved. Additionally, situating the gate at the thickest area of a thin-walled object to ensure complete filling of the cavity. [2], [3]

Autodesk Moldflow insight indicates the area with the highest flow resistance with the red color, where as the lowest flow resistance area is indicated with the blue color. The analysis's process setting is as follows:

Mold temperature: 90 °C

Melt temperature: 300 °C

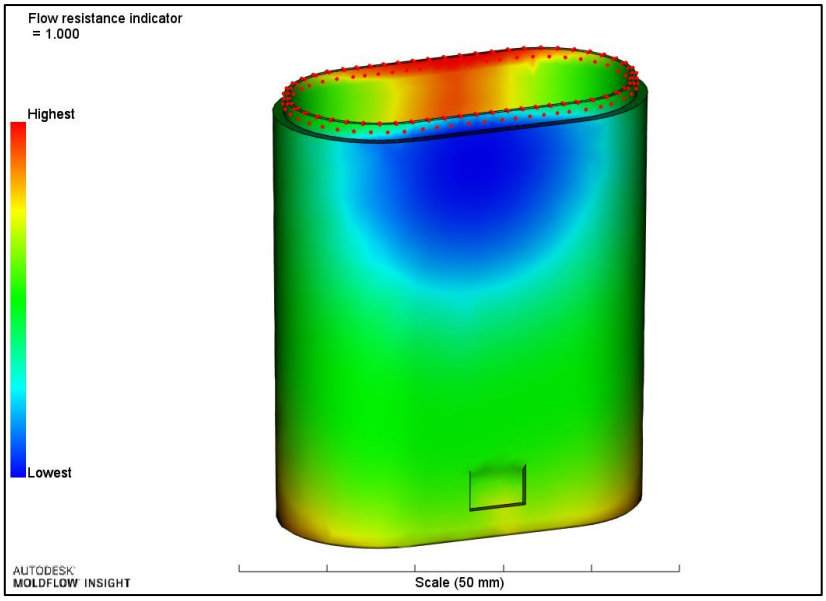

Figure 2-2: The flow resistance indicated on the LED model

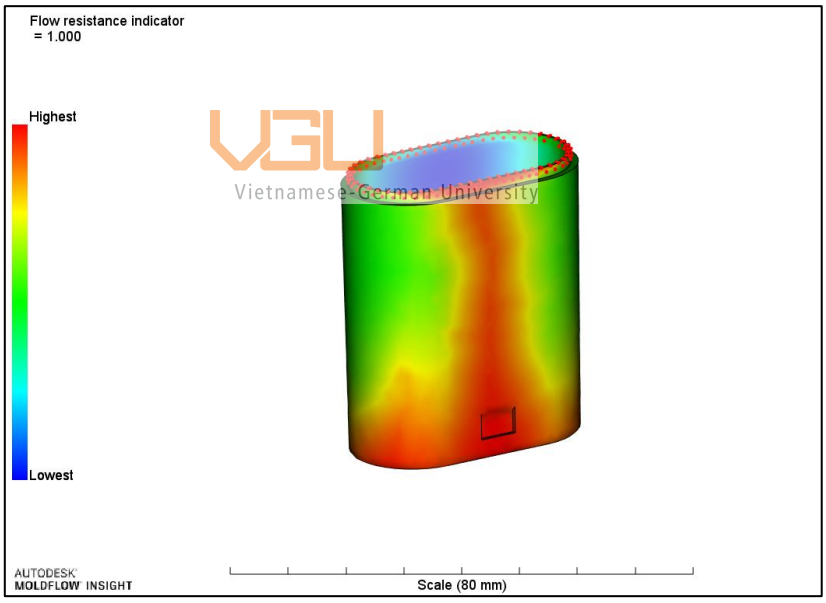

Figure 2-3: The flow resistance between the two screw pillars

There is a noticeable contrast in the flow resistance on both sides of LED base cover. Approaching the two screw guide pillars, the resistance value increases, where as the highest value is observed between the two screw guide pillars. This suggests that the screw guide pillars hinder the melt flow rate.

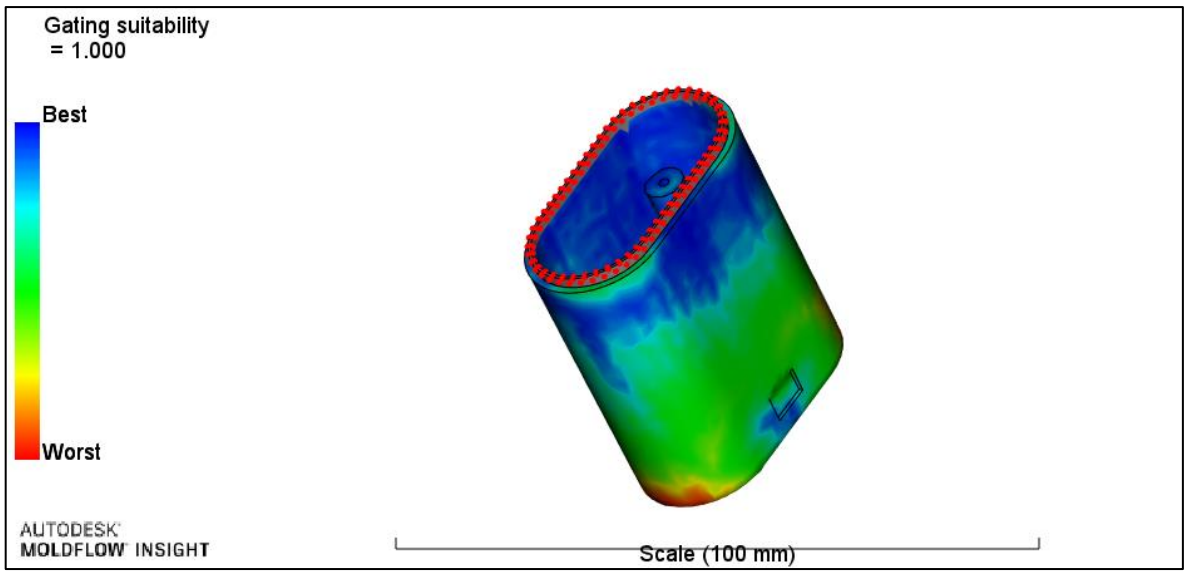

Figure 2-4: The gating suitability result

The gating suitability result suggests that the areas near the mouth of the LED base cover is the most suitable location for the injector.

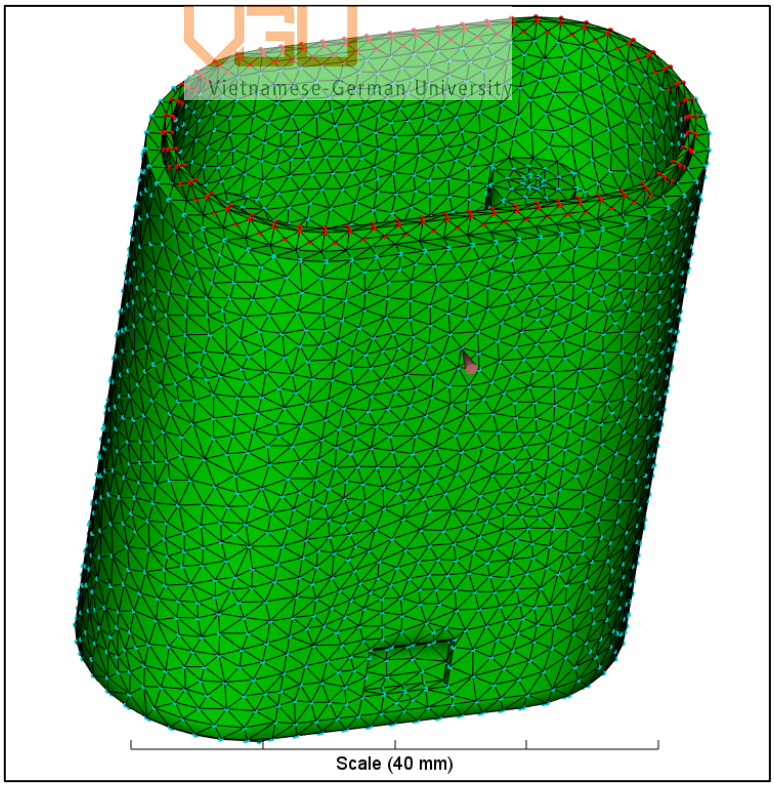

Figure 2-5: The pink cone indicates the gate location

2.6. Molding window analysis

Conducting a molding window analysis before designing the runner system and the mold cavities assists in determining the optimal molding conditions, including the injection time, mold temperature and melt temperature.

Autodesk Moldflow Insight uses the part geometry, the selected material, the gate location, and the process setting values as inputs to run a series of calculation. Each calculation is taken at a different process setting, whose results are compared to select the optimal molding conditions. Because of each molding cycle produces four LED base cover, the part cavity is duplicated by four. [4]

Prior to the analysis calculation, some default parameters of the process setting should be changed:

- Set the maximum injection machine pressure limit to 140 MPa for an undetermined machine capacity.
- In the molding windows advanced option, set the feasible injection limit factor from 1 (by default) to 0.8.
- In the molding windows advanced option, set the preferred injection limit factor from 0.8 (by default) to 0.5.
- Set the preferred flow front temp. drop limit to 20°C, set the preferred flow front temp. rise to 2°C.

Reducing the injection pressure limit factor implies that the hydraulic unit should not be working at its maximum capability, which increases the hydraulic unit lifetime.

The results calculated are represented as a color-coded graph, which is addressed as the zone (molding window) graph by the program. This graph represents the feasibility of the process conditions:

- The red color indicates the not feasible process conditions for a particular gate location and material, and should not be selected.
- The yellow color specifies the feasible process conditions, where the part can be molded but the quality may not be high.

- The green color implies that the process conditions are preferred for the particular gate location and material, which highly increases the chance that the part can be molded well.

From the zone (molding window) graph, the program provides the recommended process condition for the user in the analysis log window:

Recommended mold temperature: 83.33 °C

Recommended melt temperature: 310.00 °C

Recommended injection time: 0.3633 s

These values are located in the green region of the graph, where the process conditions are preferred.

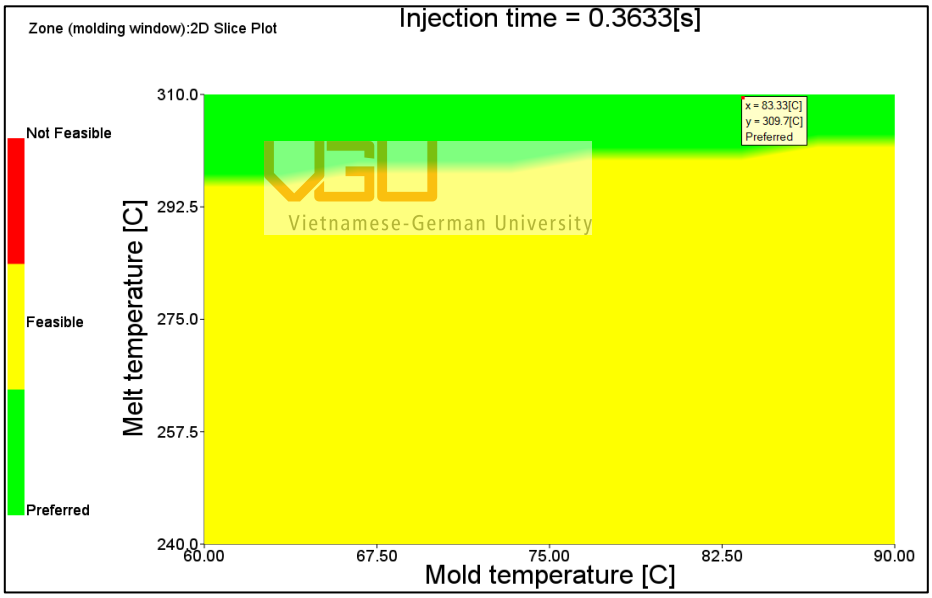

Figure 2-6: The zone (molding window) graph

The overall quality of the part at each particular melt temperature, mold temperature, and injection time is assessed by the quality (molding window): XY plot. The recommended process conditions provide the quality value reaching 0.85 according to the line graph.

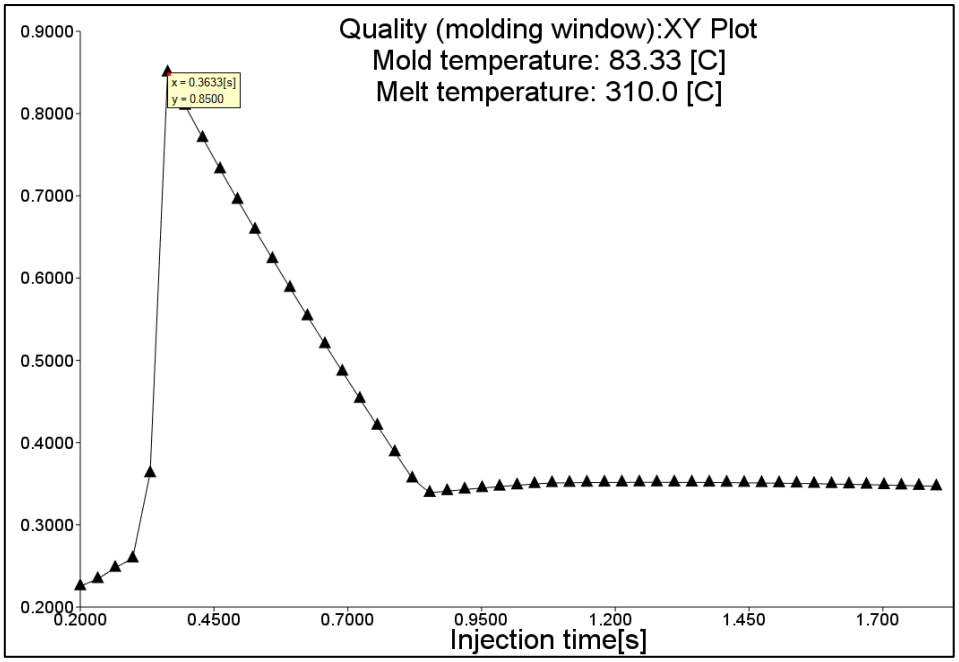

Figure 2-7: The quality (molding window): XY plot

The molding window analysis also provides the shear stress and shear rate plot in correspondence with each molding condition. To ensure the part's structural integrity is maintained, the shear stress value at the recommended process condition is compared to the material's permissible shear stress.

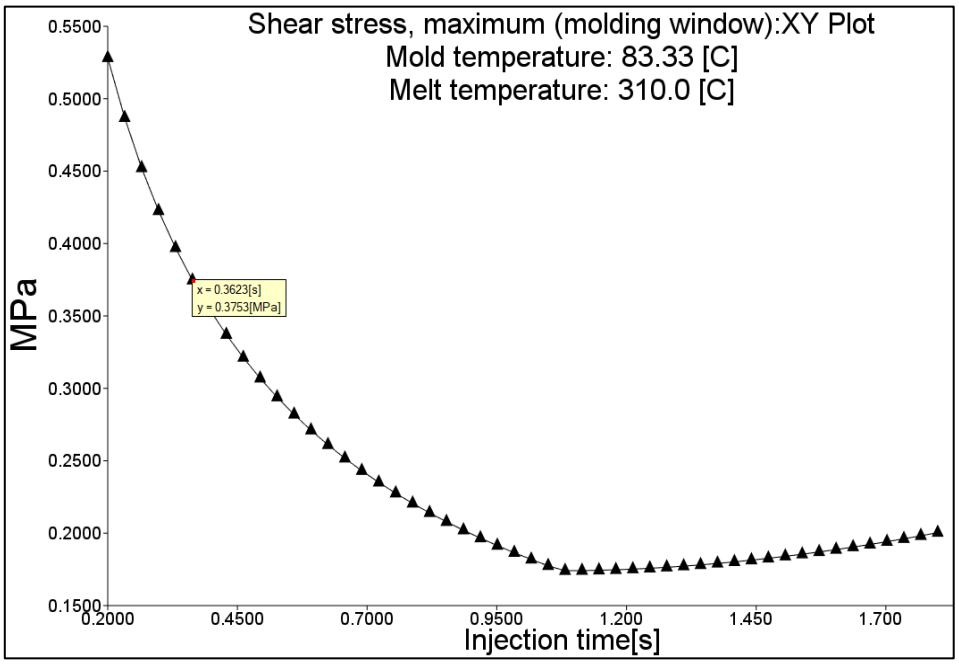

Figure 2-8: The shear stress at the recommended process conditions

With the recommended conditions, the shear stress generated by the melt reaches 0.37 MPa. The material's allowable shear stress is 0.5 MPa, which is higher comparing to the melt's shear stress. Therefore, the recommended conditions are accepted.

The shear rate value represents the speed of the plastic layers that slide past each other. This phenomenon occurs when polymer is forced to flow, which forces the molecules to parallelly align. As a result, the material's viscosity is reduced and the plastic flows more easily. However, a high shear rate breaks the molecular bonds and degrade the material. [5], [6]

Generally, the material's allowable shear rate is higher than the shear rate produced at the part's cavity. The material's shear rate can be obtained by:

- Right click on the material's name in the task window, and choose Edit
- Choose the recommended processing tab in the thermoplastic material window

The shear rate value of Polycarbonate provided by Autodesk Moldflow Insight reaches 40000 1/s. The melt's shear rate value can be observed in the shear rate plot below:

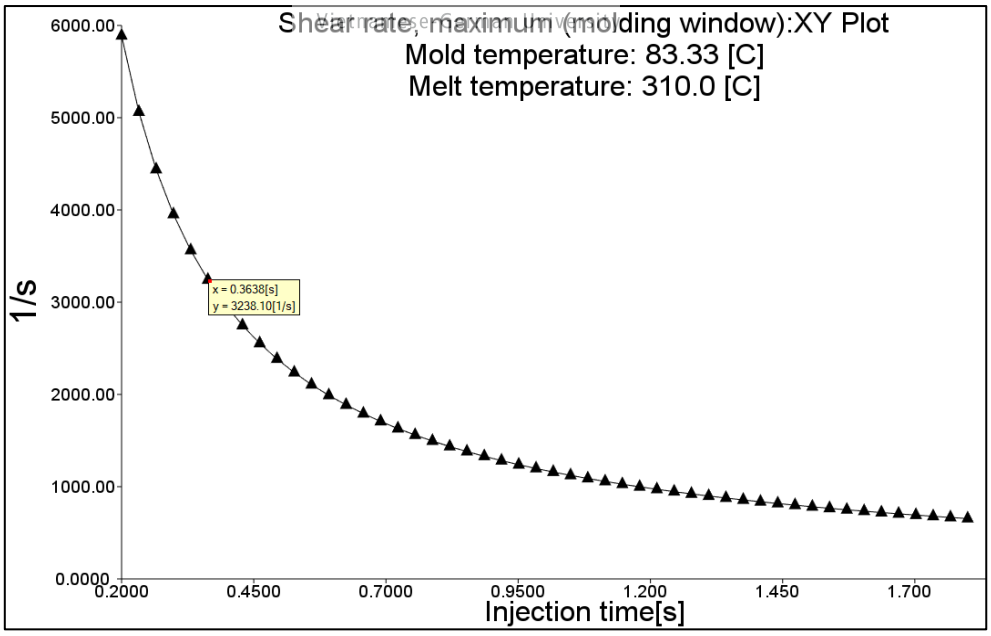

Figure 2-9: The shear rate at the recommended conditions

The melt shear rate at the cavity reaches 3238.10 1/s with the recommended process condition, which is much lower compared to the material's allowable shear rate. Therefore, the material's degradation should not occur at the cavity.

The maximum cooling time at the cavity is also calculated by the program. This value is directly proportional to the mold temperature. Since the recommended mold temperature is 83.3°C, the maximum cooling time reaches 17.4 seconds according to the plot. The actual cooling time can be decreased with the introduction of the cooling system.

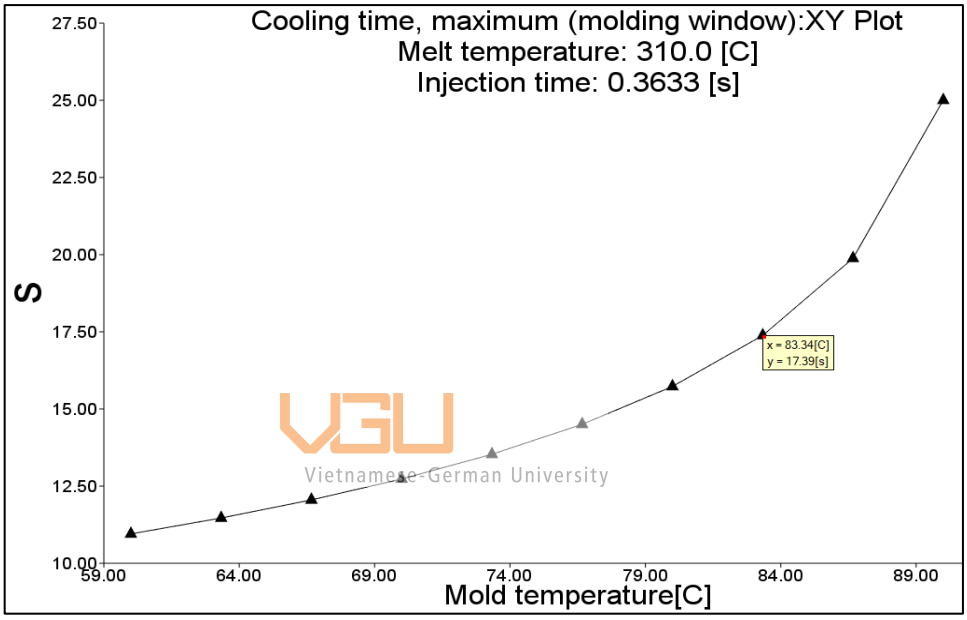

Figure 2-10: The maximum cooling time at the cavity

On summarizing, the molding window analysis is a preliminary selection step that provides the designer with the optimal molding condition to produce high-quality parts. With the predetermined conditions, the designer uses these values as inputs for the following analyses. The summary table consists of the recommended process conditions is given below:

Parameters	Results
Recommended mold temperature	86.67 °C
Recommended melt temperature	310 °C
Recommended injection time	0.37 seconds

Table 2-1: The recommended values from the molding window analysis

2.7. Fill + pack analysis

The fill + pack analysis, as its name suggests, predicts the material flow within the cavity during the filling and packing phase. Generally, this analysis verifies that the mold cavity can be filled using the melt pressure generated by the injection molding machine (IMM). An inadequate filling pressure reflects a poor molded part design or improper processing conditions. This analysis not only shows the filling pressure, but also the fill time, which implies the uniformity of the flow in the cavity.

2.8. Fill time analysis

One of the most important process parameters for any particular molded part is the fill time. This parameter suggests the time it takes for the melt to flow from the nozzle and spread throughout the entire cavity. Autodesk Moldflow Insight represents the fill time as the color-coded region, such that the fill time begins with the blue regions and concludes with the red regions. The highest value at the red region is 0.63 seconds, suggesting the four LED base covers require the same amount of time to be filled.

Generally, a balanced flow pattern is more preferred to achieve uniform filling and avoid overpacking. According to the illustration below, the wall on the same side of the gate consists of blue and green colors, while the opposite wall has yellow and red color. This indicates that current gate location may result in overpacking at the wall on the same side of the gate based on the gate location analysis.

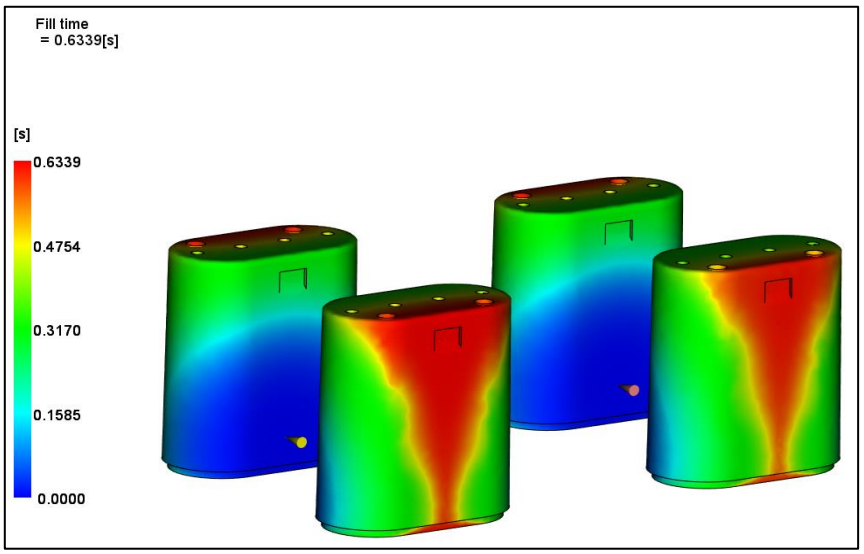

Figure 2-11: Visualization of the product's filling time

2.9. Pressure analysis

The fill + pack analysis generates two pressure parameters to be analyzed. The pressure result represents the pressure distribution along the flow path inside the cavity at the time the result was recorded. The application assigns the pressure result deviation into a spectrum of color. The absence of color indicates that there is no pressure in the cavity at the start of the filling. As the flow front reaches a particular position, the pressure develops, represented by the blue color. The yellow color suggests that the pressure further increases in porportion with the flow length between the flow front and the examined location.

The magnitude of the pressure is directly proportional to the resistance of plastic. It requires more pressure to fill the cavity because of the high material viscosity. The maximum pressure magnitude is always located at the injection location, and the minimum magnitude is at the melt flow front. Due to the polymer moves in the direction that has a negative pressure gradient, the aforementioned conditions ensure that the melt can flow inside the cavity. [7]

A pressure plot representing the pressure requirement at the gate location of each cavities is generated below:

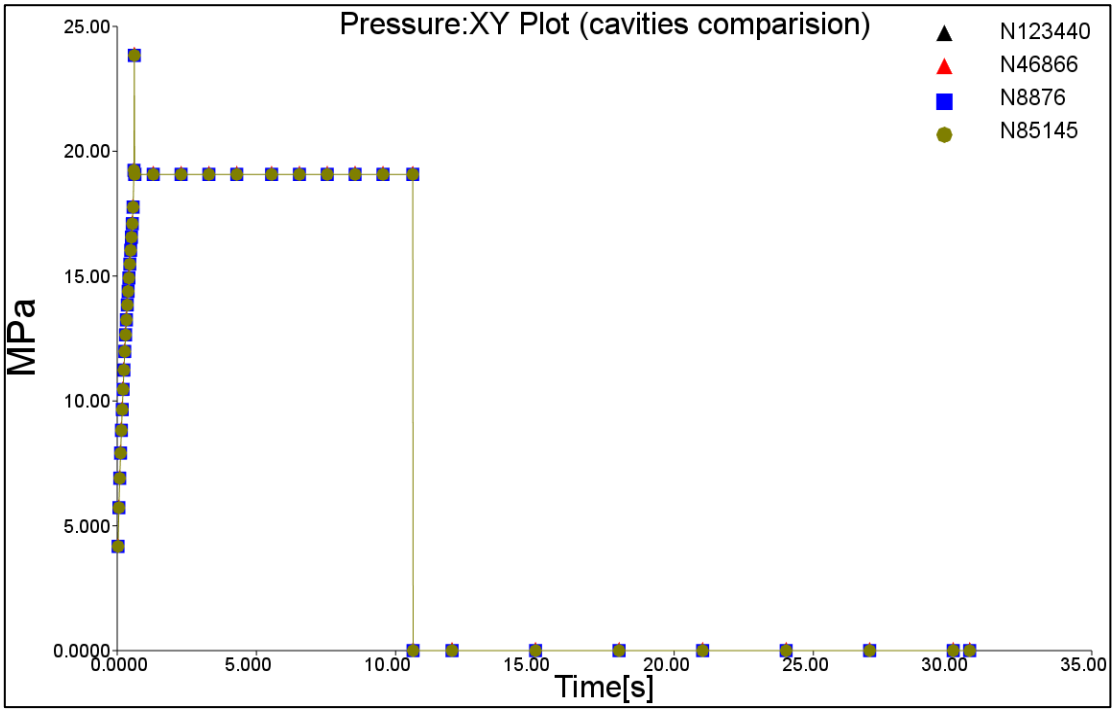

Figure 2-12: The pressure and time graph at the gate location

This suggests that under the current molding conditions, the Polycarbonates requires up to 23.8 MPa of pressure during the packing phase. The required highest pressure is substantially lower compared the IMM's capability of 140 MPa. It should be mentioned that the maximum pressure for parts with runners should not exceed 100 MPa, and for parts without runners, it should not exceed 70 MPa.

2.10. Volumetric shrinkage

Volumetric shrinkage is the decline of plastic's volume as a result of temperature change from melt temperature to ambient temperature. This phenomenon is caused by thermal contraction, which describes the extent that material's volume change as it transforms from liquid to solid. High volumetric shrinkage causes warpage and sink marks, which effects the aesthetic of the final product. A suggested solution to decrease the volumetric shrinkage is to increase the packing pressure.

The fill + pack analysis provides the volumetric shrinkage result, which suggests that the curved corners of the LED base cover experience shrinkage up to 10% with the current processing condition.

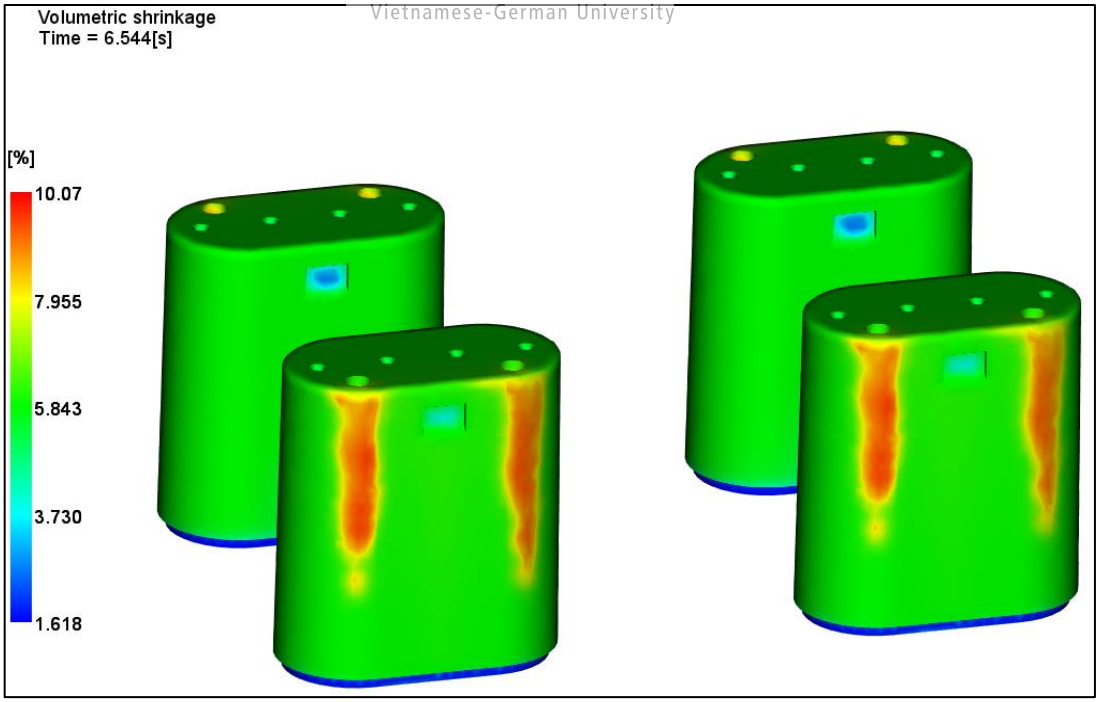

Figure 2-13: The volumetric shrinkage of the product

2.11. Weld lines

Weld line is the line where the flow fronts meet but they are not “knit” together, causing the surrounding area of the product to be weaken. Aesthetical defects, including lines, notches, and color change on the surface of the molded part, can be produced by weld lines. Weld lines are unavoidable for this product because of its geometry, which causes the flow front to split and fill the two sides of the cavity. The two flow fronts eventually meet at the opposite wall and form weld lines. [8]

According to the analyzing result, the weld lines are concentrated at the opposite wall to the gate location. This causes aesthetical defects and weakens the physical integrity of this area. The result implies that the designer should looks into other analyses to decide the most suitable gate location, even if the molding window analysis suggests a preferred gate location.

Figure 2-14: The weld lines develop on the product’s wall

2.12. Frozen layer fraction

The frozen layer can be interpreted as the frozen material layer due to its temperature falls below the transition temperature. This analysis value indicates the thickness of the frozen layer as the fraction of the part weight. A high frozen layer fraction value implies a high percentage of the material has been frozen in a particular area, increasing the flow resistance. Additional material to flow into the cavity is prevented by the high flow resistance, possibly causing an incomplete cavity fill during the packing phase. Thus, it is recommended to consider the packing time to be equal or less than the time that the frozen layer fraction reaches the value of one. [9], [10]

Autodesk Moldflow Insight provides a visualization of the frozen layer fraction that occurs at the product cavity. The value of the frozen layer fraction is color coded, with the blue color represents a low fraction value, whereas the red color indicates a fraction value of 1. The animated plot below shows the frozen layer fraction value taken at 10.63 seconds:

- The thin wall's frozen layer fraction value reaches 1
- The thick wall's frozen layer fraction value reaches around 0.35
- The thickest wall's frozen layer fraction value reaches up to 0.2

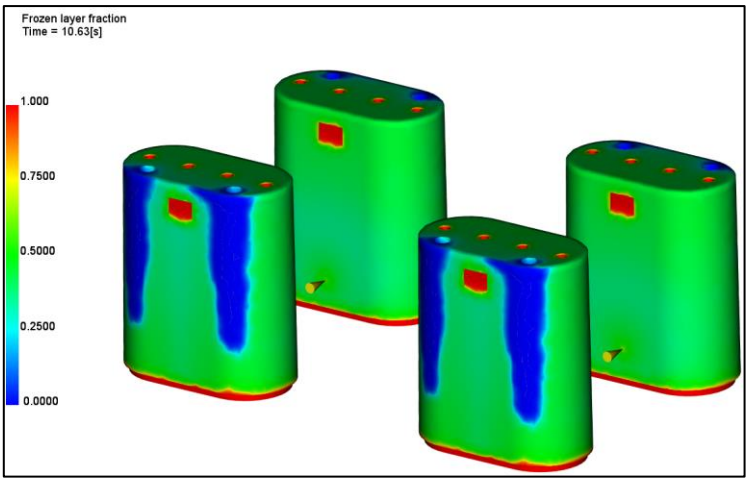

Figure 2-15: The frozen layer fraction plot

These results suggest that the increase rate of the frozen layer fraction is inversely proportional to the wall thickness. The thinner wall section freezes quicker than the thicker wall section. Hence, a frozen layer fraction: XY plot is generated to examine the time for the fraction to reach 1 at three locations.

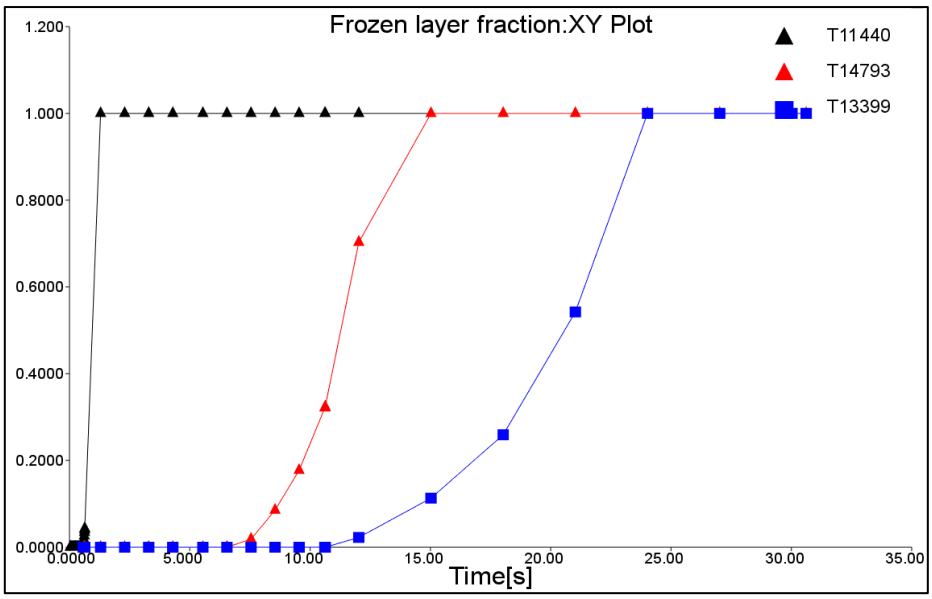

Figure 2-16: The frozen layer fraction: XY plot of a cavity

At the thin-walled section, the frozen layer fraction reaches 1 at 1.3 seconds. Since the thin wall area is frozen much earlier compared to the other areas, a pressure plot is created at this location to determine if the cavity is completely filled.

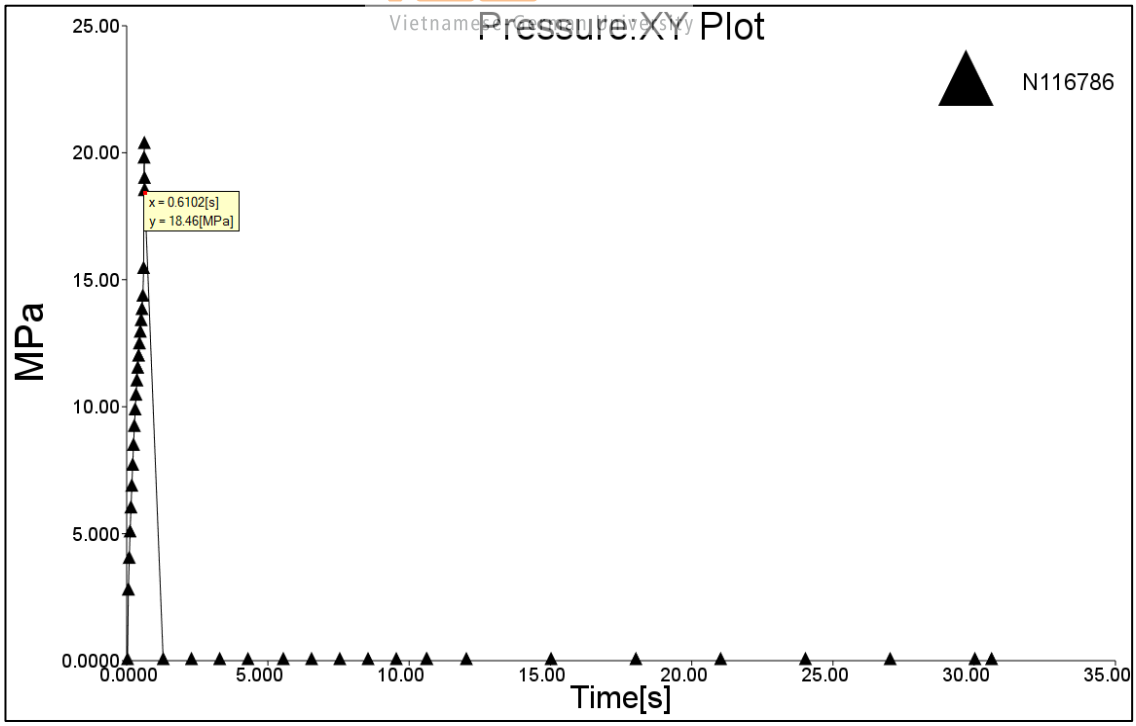

Figure 2-17: The pressure: XY plot taken at the thin-wall section

The plot above suggests that the packing time is 0.61 seconds, which is earlier than the time for the frozen layer fraction takes to reach 1. Therefore, the plastic can certainly fill the cavities without being completely prevented by the frozen layer.

2.13. Process optimization

After conducting the molding window and the fill + pack analysis for the part cavities, adjustment to the gate location is implemented to achieve balanced filling and reduce the weld lines. The new gate location is placed at the bottom of the LED cover. With this approach, the plastic will flow downward and the flow fronts won't collide at the product wall. Thus, reducing the number of weld lines.

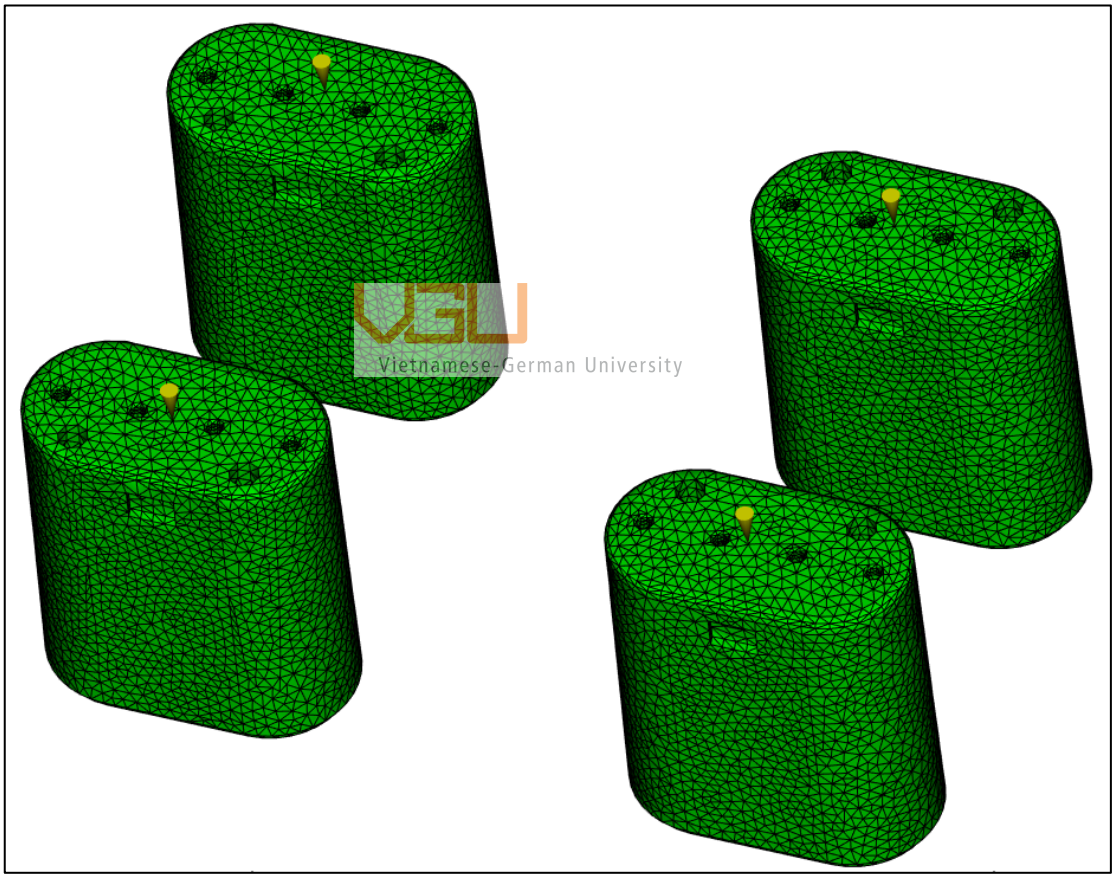

Figure 2-18: The new gate location

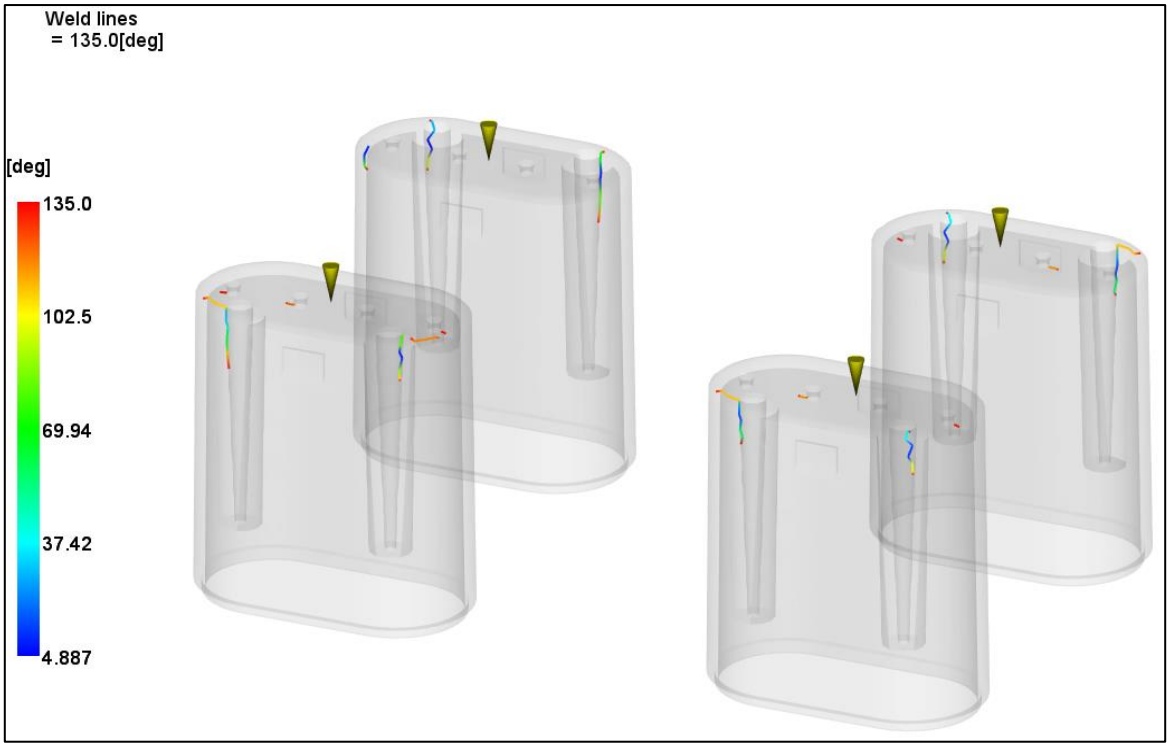

Figure 2-19: The reduced number of weld lines

The optimal process conditions have altered as a result of the injector's change in location. Therefore, the same sequences of analyses and analyzing results are conducted and evaluated respectively to detect any new problems.

The analyzing result of the molding window analysis are:

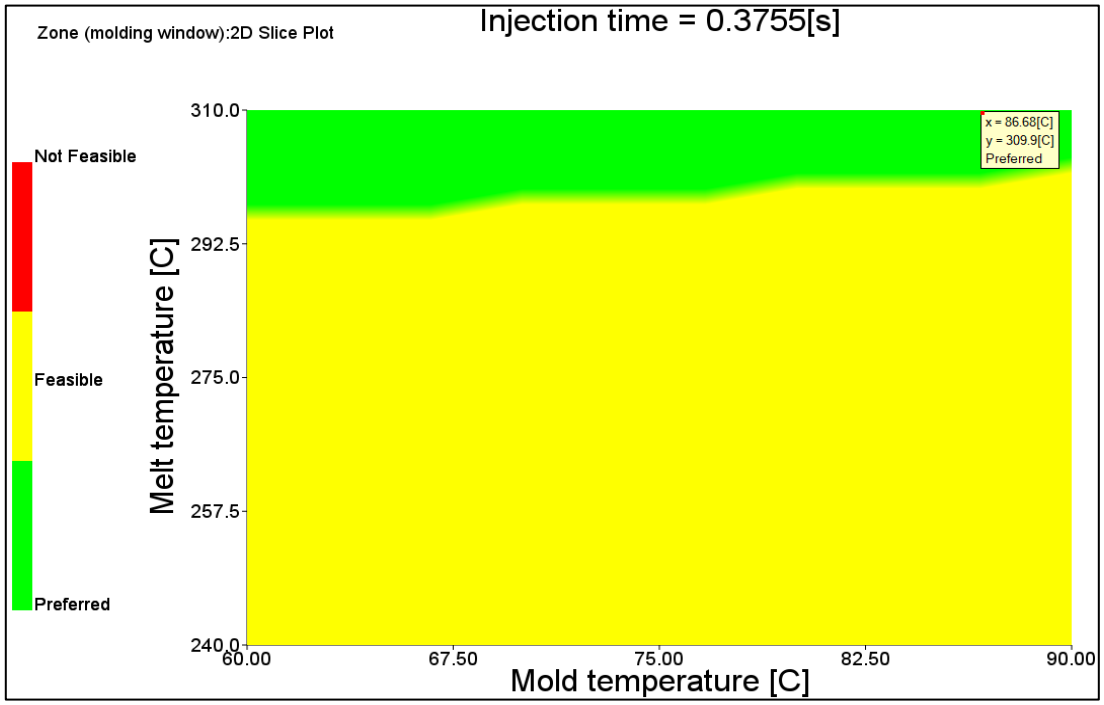

Figure 2-20: The new recommended molding conditions

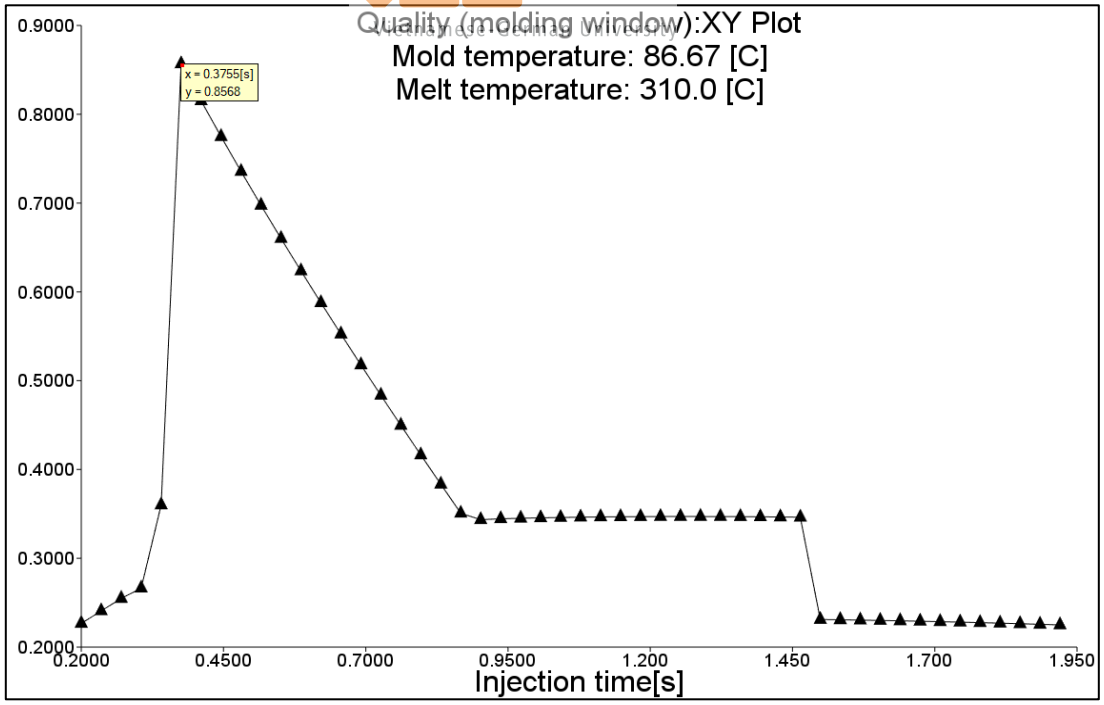

Figure 2-21: The quality: XY plot for the new gate location

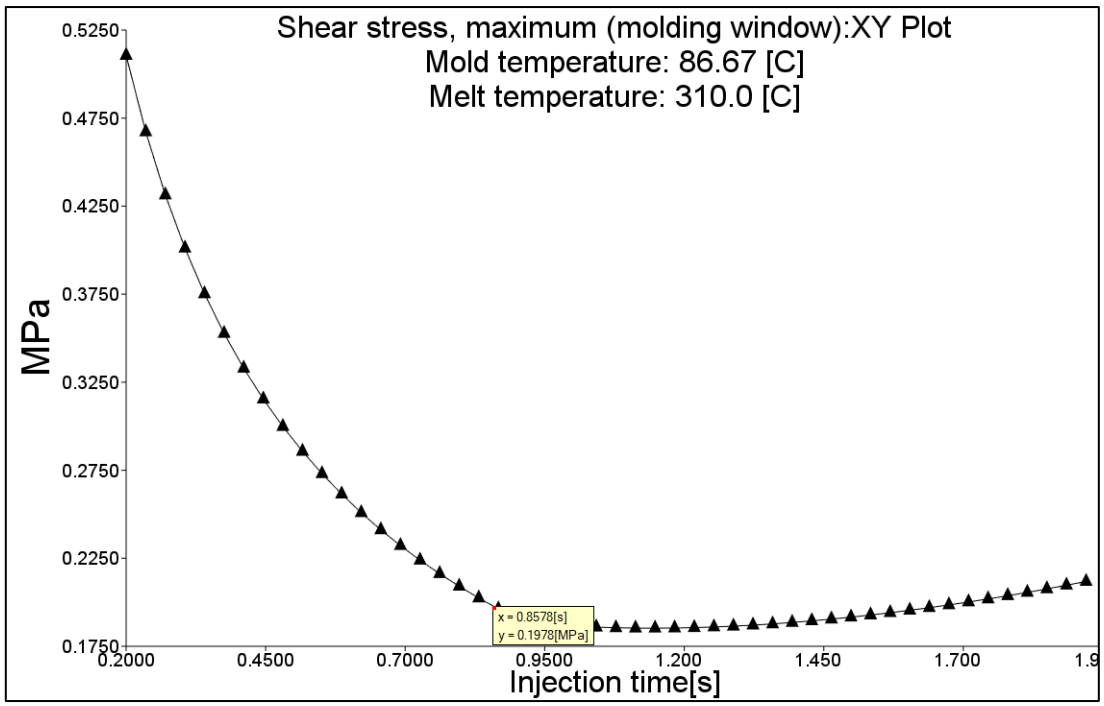

Figure 2-22: The new shear stress value

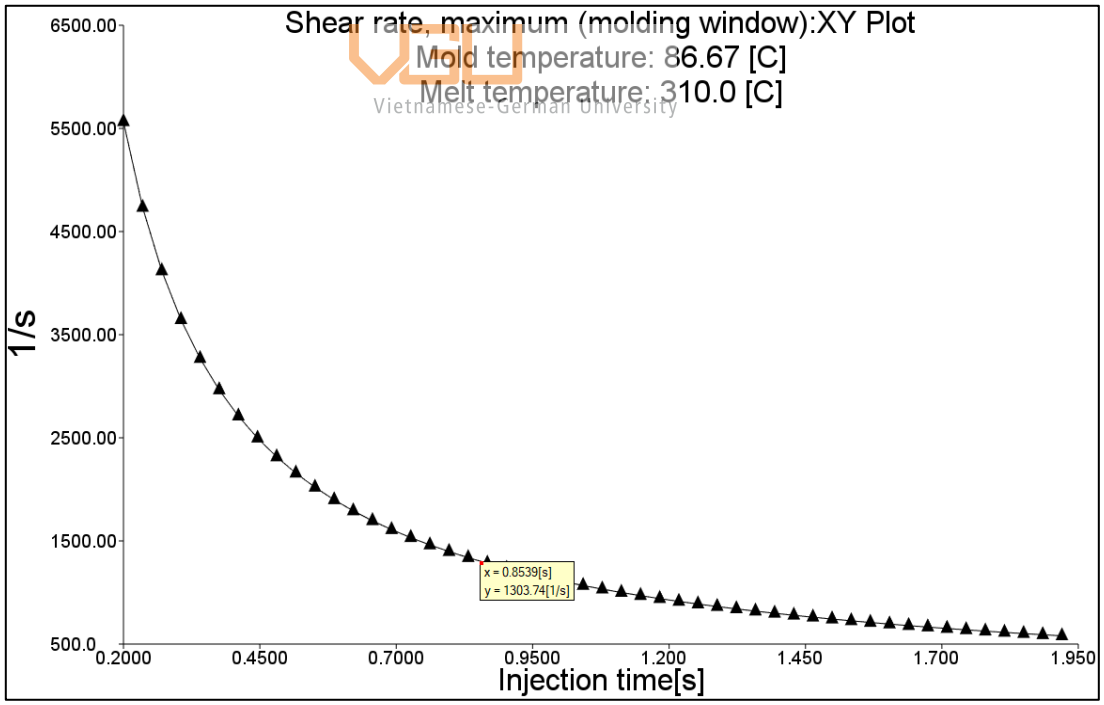

Figure 2-23: The new shear rate value

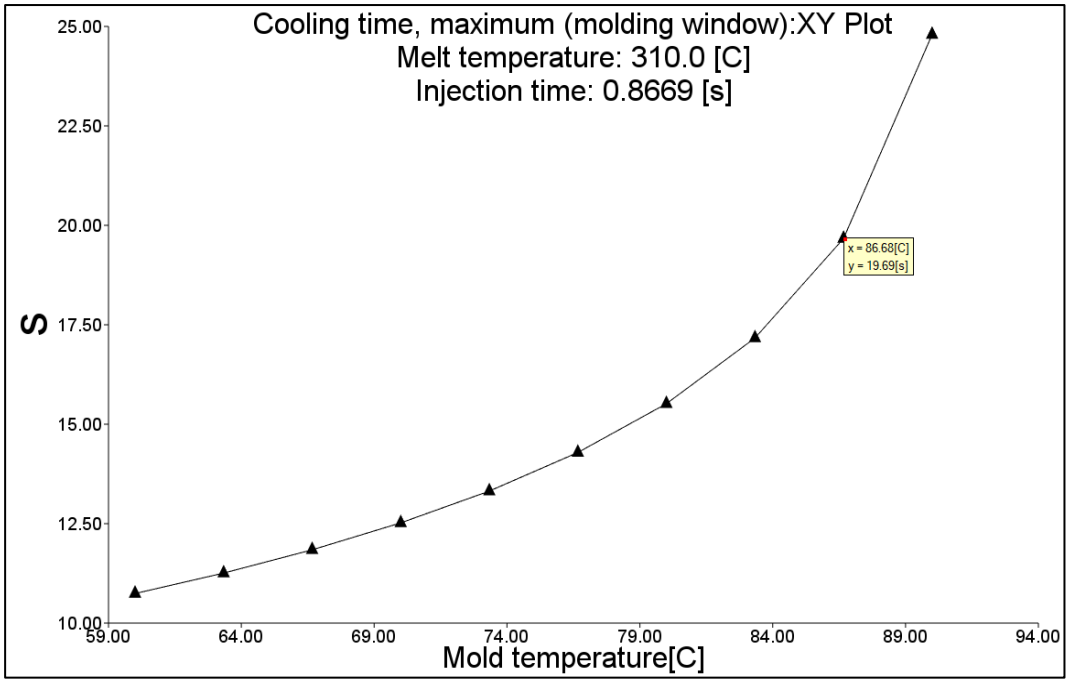

Figure 2-24: The new maximum cooling time

The above results are summarized into the following table:

Parameters	Results
Maximum design clamp force	212464 N
Maximum design injection pressure	140 MPa
Recommended mold temperature	86.67 °C
Recommended melt temperature	310 °C
Recommended injection time	0.86 seconds
Shear stress at the recommended molding conditions	0.20 MPa
Shear rate at the recommended molding conditions	1303.7 1/s
Maximum cooling time corresponds to the new molding conditions	19.69 seconds

Table 2-2: The molding window analysis results with the new gate location

The results from the table above suggests that some results have been slightly differ. The sum of injection time and the maximum cooling time have increased by 2.6 seconds. This result in a slight increase in the total molding cycle time. The new gate location decreases the new shear stress and shear rate, respectively by 0.20 MPa and 1303.7 1/s.

The following results are taken from the fill + pack analysis of the cavities with the new gate locations.

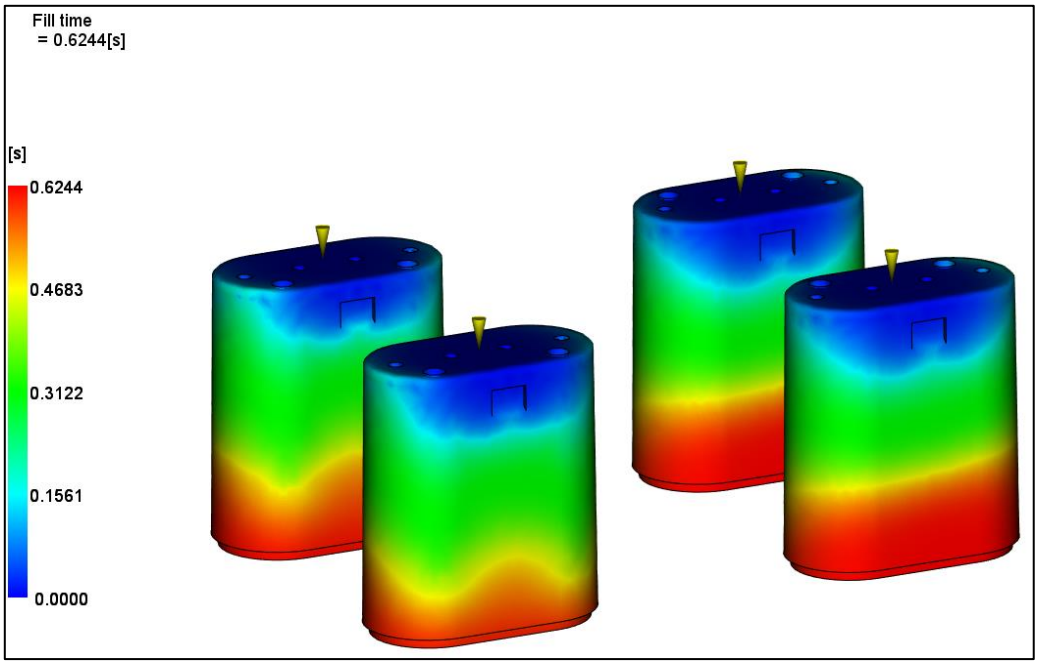

Figure 2-25: The new fill time of the cavities

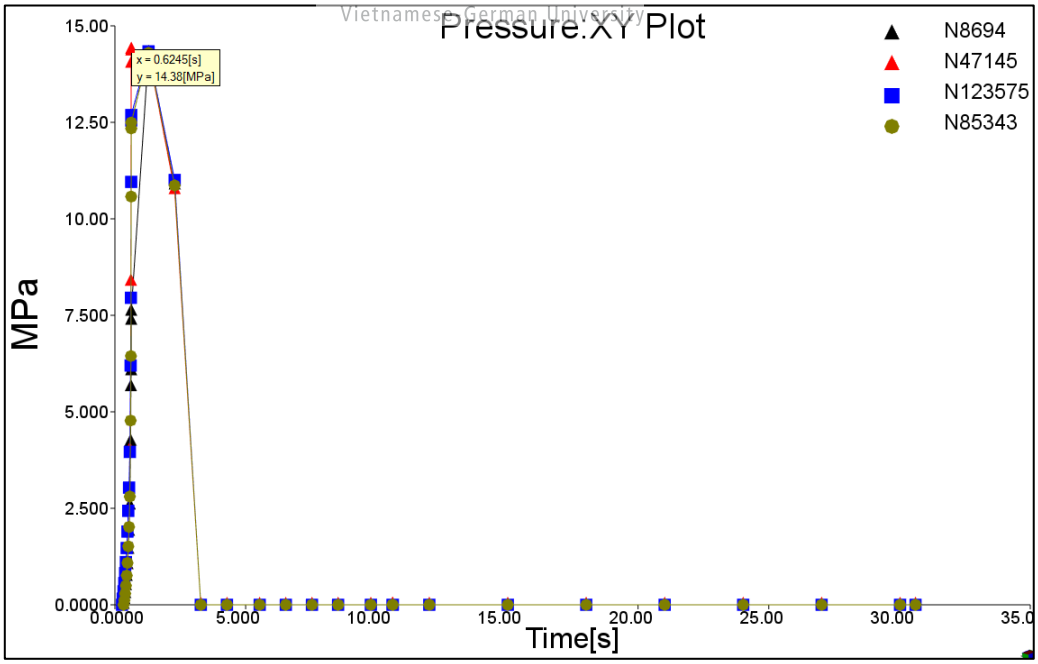

Figure 2-26: The pressure plot taken at the similar position of each cavity

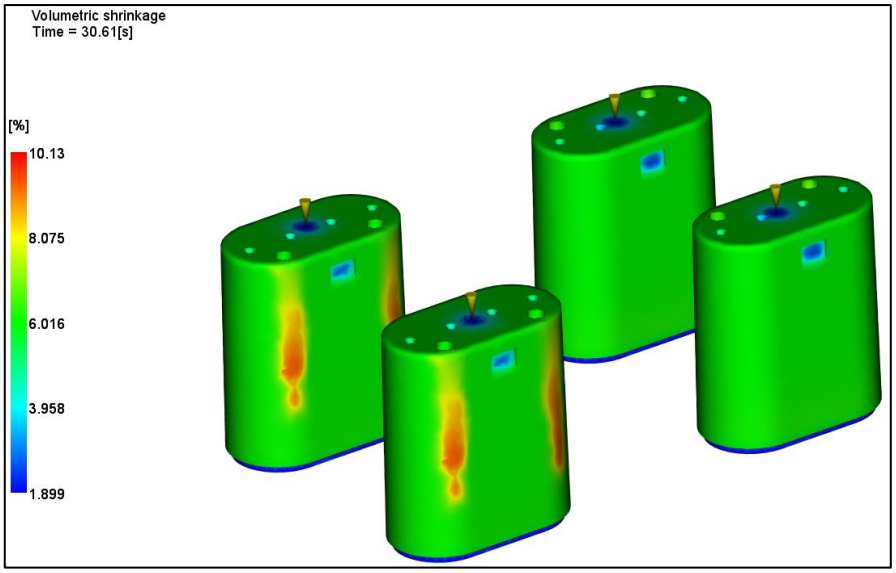

Figure 2-27: The new volumetric shrinkage of the products

Figure 2-28: The reduced number of weld lines

The volumetric shrinkage area has shrunk, while the value of the volumetric shrinkage only increases slightly. This result implies that volumetric shrinkage is highly influenced by the geometry of the part cavity, not by the injector location.

The new fill + pack analysis's weld lines result shows that there are much less weld lines on the wall. The weld lines only occur near the edge where the screw locations are positioned. The length of the weld lines is also greatly reduced, improving the quality of the products.

The frozen layer fraction result is re-evaluated to determine the possible problems regards to the cavity filling capability. These results are obtained from the fill + pack analysis with the new molding conditions.

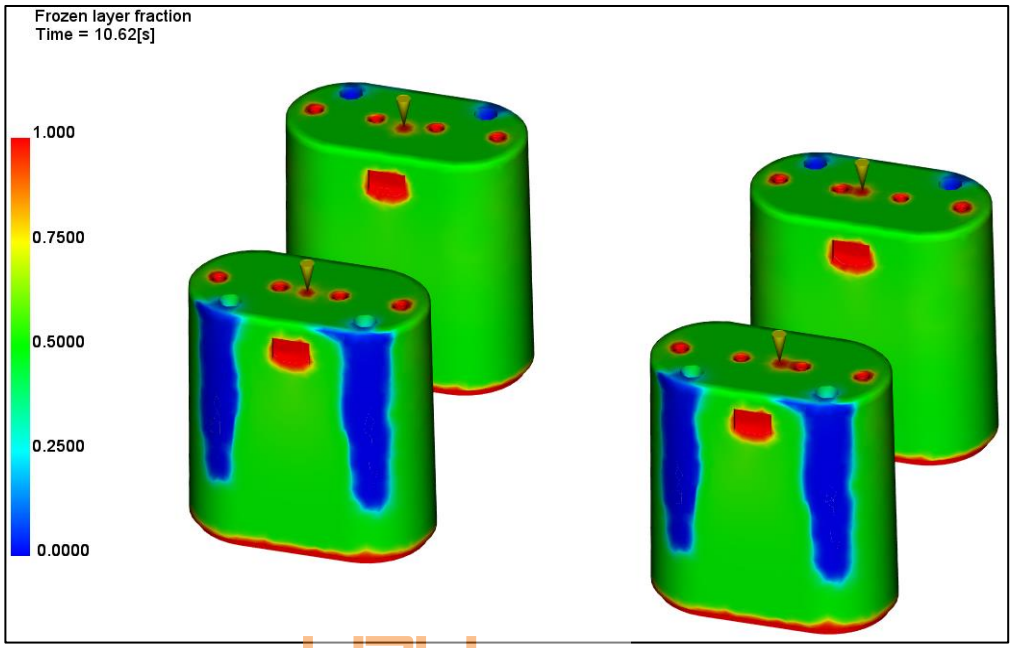

Figure 2-29: The frozen layer fraction visualization at different areas

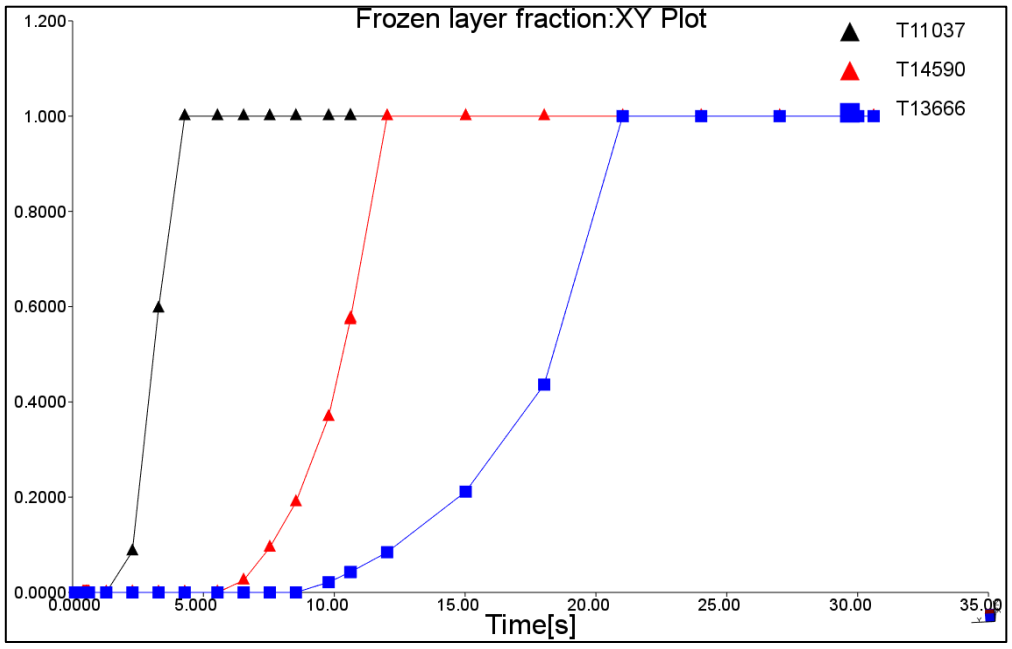

Figure 2-30: The frozen layer fraction: XY plot taken at the analyzing positions

According to the frozen layer fraction: XY plot, the thin-walled area's frozen layer fraction reaches 1 at 4.3 seconds. The packing time is 1.28 seconds, which is shorter than the freezing time, according to the pressure plot at the same location. These findings imply that the material can be adequately fill every area of the cavity. By comparing the result between the new and the old frozen layer fraction: XY plot, the time difference between the packing time and the freezing time at the thin-walled area has extended. The increase in time difference suggests that the material can be conveniently move to the cavity without being obstructed by the high frozen layer fraction.

In conclusion, shifting the gate location is necessary to achieve a better product quality. The final gate has less weld lines development, achieve more balanced fill, and improves the material flow within the thin-walled portion, even if the previous gate location has a lower flow resistance according to the molding window study. These improvements directly influence the product's structural integrity and aesthetic.

3. Designing the feed system

3.1. Feed system definition

The feed system's function is to transfer the plastic melt from the molding machine into the mold cavities. A suitable feed system reduces the cycle time and generate less material waste for each molding cycle. Generally, each feed system consists of 3 sections:

1. Runners, shown in red
2. Sprue, shown in green
3. Gates, shown in yellow

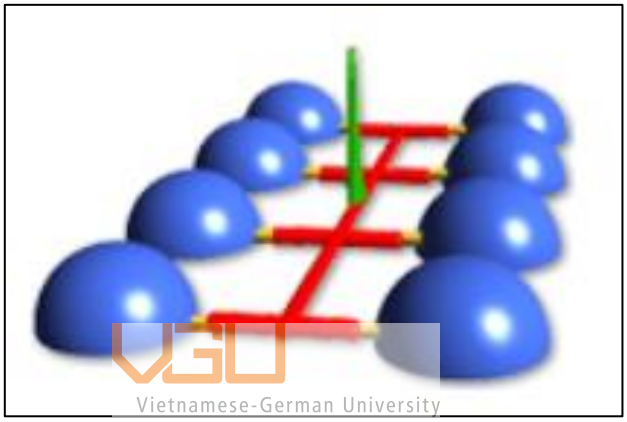

Figure 3-1: A general feed system

There are three steps to design a feed system: selection of the feed system type, the routing of the feed system in the mold, and the selection of each segment diameter. [10]

The feed system has a large variety of designs, which are classified into 3 categories:

1. Cold runner mold
2. Hot runner mold
3. Insulated runner mold

The cold runner mold can be divided into two subcategories, consisting of the two-plate cold runner and the three-plate cold runner.

The two-plate cold runner mold generally has the simplest, which provides the lowest design cost compared to the other cold runner system. Because of this, it also provides a lower lead time and molding cycle time. A distinguishable design trait of this type of mold

is the position of the whole feed system. The sprue, runners, gates, and cavities are all located on the same side of the mold. [10], [11]

A major disadvantage of the two-plate mold is the inability to automatically separate the sprue and runner system from the product. An additional separation step is required to achieve the final product, which demands either manual labor or separating machine [12].

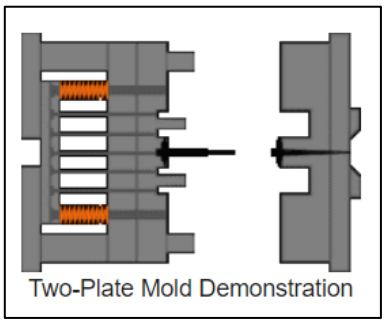

Figure 3-2: Demonstration of a two-plate mold

The three-plate mold is similar to the two-plate mold, with the stripe plate being an additional layer. This type of feed system possesses 2 parting planes, and the mold is split into 3 sections. The three-plate mold gives the designer more freedom to decide the gate's location, while the two-plate mold requires the parting plane to align with the gate. The additional stripe plate allows the runner to be ejected separately, which achieve the automatic de-gating requirement. The drawbacks of this mold type include longer cycle time, more complicated design, higher injection pressure and material waste. [10], [11], [13]

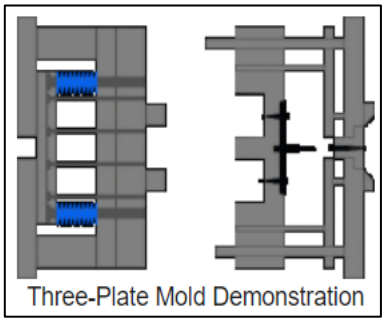

Figure 3-3: Demonstration of a three-plate mold

This thesis focuses in designing the three-plate mold for the automatic de-gating capability, reducing the demand for manual labor.

3.2. Feed system analysis

The pressure drops, the consumed material forming the feed system (waste), and the mold cooling time are the factors that should be taken into account when designing a functioning feed system. [10]

Autodesk Moldflow Insight provides the user with the runner system wizard tool, and it automatically creates the feed/runner system. The tool requires the user to provide each segment's diameter. Hence, the designer must estimate each segment's diameter as input for the program.

A sufficient melt pressure can comfortably push the material into the cavity. As the melt travel through feed system into the cavity, the pressure starts dropping, decreasing the material flow rate. Short shots or other defects are likely to develop if the flow rate significantly drops before the flow completely fill the cavities. To prevent this, the pressure drop typically should not exceed 50% of the pressure required to fill the mold cavities. Minimizing the pressure drop requires the sprue's diameter to be the largest, and the following segments have their diameter decrease gradually. Generally, a smaller runner system volume of less than 30% of the cavities' volume is desired to reduce the material waste. [10]

The runner system's cooling time is another factor to take into account. The melt inside the cavities and the runner must cool and solidify before the ejection phase. A larger feed system requires a longer cooling time, which increases the total process cycle time, and reducing the process productivity. Adjusting for a smaller runner system reduce the cooling time and the waste material, but increases the required pressure of the feed system.

3.2.1. Pressure drop analysis

The pressure drop can be estimated with the following equations, given the layout and length of the feed system:

$$\Delta P = \frac{2kL}{R}\left(\frac{\left(3+\frac{1}{n}\right)V_{melt}}{\pi R^3}\right)^n \qquad (3-1)$$

Where:

K: flow consistency index (= 17,000 Pa s^n)

n = 0.35

R: radius of the section (m)

L: length of the section (m)

The pressure drops at each segment, including the sprue, primary runner, secondary runner, and gate can be estimated, if the inlet volumetric flow rate is 100 cc/s (1 cc/s = 10^{-6} m^3/s). The sprue dimension relates to the standardized sprue bushing provided by MISUMI.

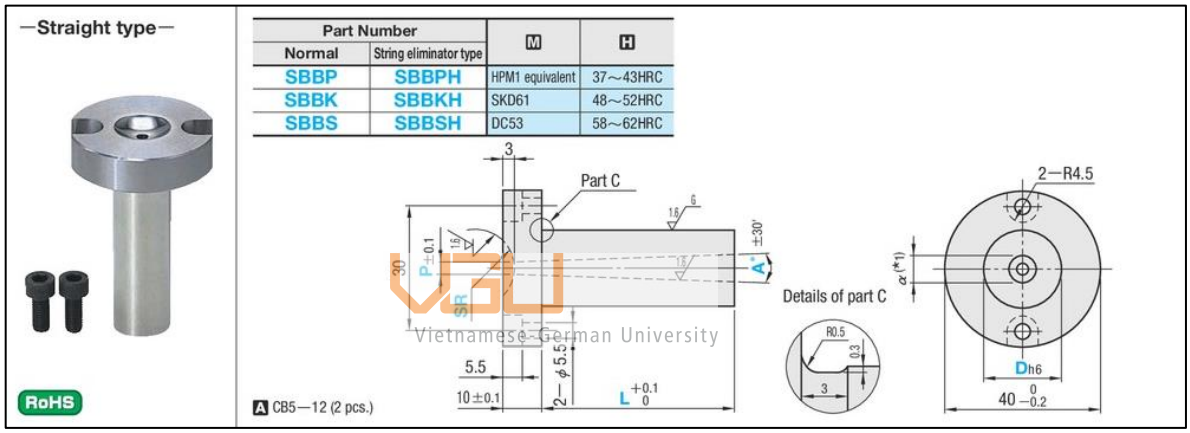

Figure 3-4: The sprue bushing provided by MISUMI

The straight type sprue bushing is 50 mm in length, 8 mm in diameter at the orifice, and 1.5° at the included angle. A reasonable estimation for the pressure drop is derived by modeling the sprue's cone-shaped profile into a cylinder with a constant radius of 4.65 mm. The predicted pressure drop is:

$$\Delta P_{sprue} = \frac{2 \times 17000 \times 50 \times 10^{-3}}{4.65 \times 10^{-3}} \left(\frac{\left(3 + \frac{1}{0.35}\right) \times 100 \times 10^{-6}}{\pi (4.65 \times 10^{-3})^3}\right)^{0.35} = 5.09\ MPa$$

Each primary runner's length is 42 mm, and the assumed diameter is 4 mm. Since the feed system is symmetrical, the flow rate of each primary runner is half of the sprue's flow rate. Applying the equation, the pressure drop is:

$$\Delta P_{primary\ runner} = \frac{2 \times 17000 \times 44 \times 10^{-3}}{2 \times 10^{-3}} \left(\frac{\left(3 + \frac{1}{0.35}\right) \times 50 \times 10^{-6}}{\pi (2 \times 10^{-3})^3}\right)^{0.35} = 19.82\ MPa$$

Each primary runner is then separated into two identical secondary runners. Therefore, the flow rate of each secondary runner is half of the primary runner. The secondary runner is 34 mm, and its diameter is identical to the primary runner. The calculated pressure drop is:

$$\Delta P_{secondary\ runner} = \frac{2 \times 17000 \times 0.034}{2 \times 10^{-3}} \left(\frac{\left(3 + \frac{1}{0.35}\right) \times 25 \times 10^{-6}}{\pi (2 \times 10^{-3})^3}\right)^{0.35} = 12.02\ MPa$$

From the calculated values above, the total pressure drop from the inlet to the outlet is:

$$\Delta P_{total} = \Delta P_{sprue} + \Delta P_{primary\ runner} + \Delta P_{secondary\ runner} \quad (3-2)$$

$$\Delta P_{total} = 5.09 + 19.82 + 12.02 = 36.93\ MPa$$

The total pressure drop is within the injection pressure limit of 140 MPa, which fulfills the mentioned criteria.

The program provides the runner system wizard tool, which automatically creates a runner system using the provided parameters. These parameters are:

Parameter	Value
Sprue's orifice diameter	8 mm
Sprue's length	50 mm
Runner's diameter	4 mm
Side gate's orifice diameter	1 mm
Side gate's length	2 mm

Table 3-1: The required input for runner system wizard

At each segment, the estimated pressure drop is compared to the calculated pressure drop. By subtracting the pressure value of a point at the start of the segment to a point at the end of the segment, the calculated pressure drop is obtained.

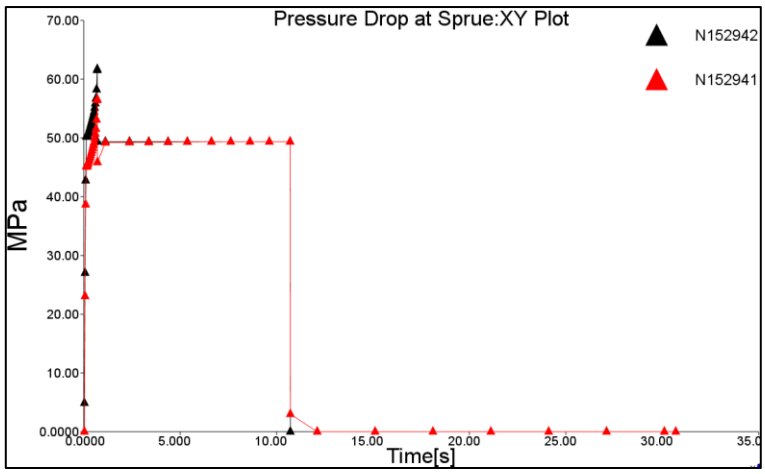

Figure 3-5: The pressure drop at the sprue

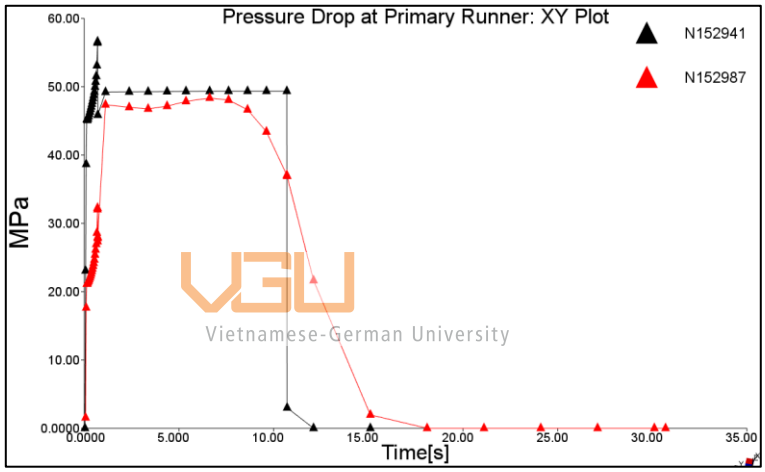

Figure 3-6: The pressure drop at the primary runner

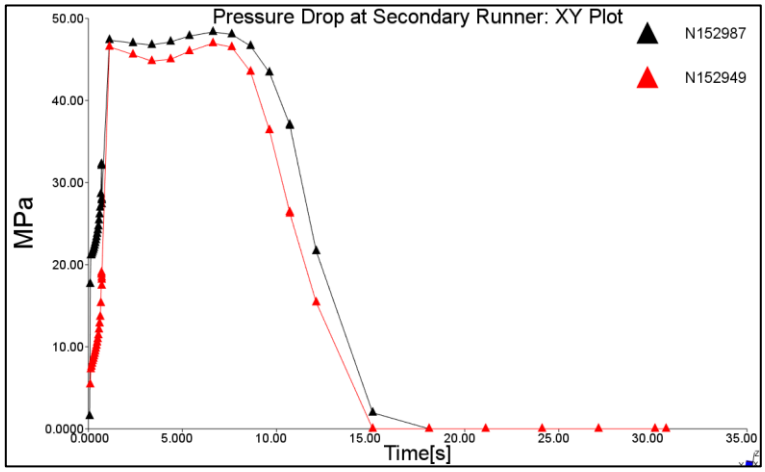

Figure 3-7: The pressure drop at the secondary runner

	Estimated values	Calculated values
Sprue	5.09 MPa	5.2 MPa
Primary runner	18.92 MPa	24.19 MPa
Secondary runner	12.02 MPa	12.94 MPa
Total pressure drops	36.03 MPa	42.33 MPa

Table 3-2: Comparison between the estimated and calculated pressure drop values

The difference in the pressure drop value is caused by the program's different calculating model. Both results fall within the pressure limit of 50 MPa, which implies that the pressure drop requirement of the current feed system is acceptable.

3.2.2. Feed system's material consumption

The feed system should be narrow and compact to reduce the amount of waste of each molding cycle. The recommended material consumption limit is 30% of the cavities volume. The total cavities volume is 55 cm^3, and the volume of the feed system is 5.15 cm^3, which is equivalent to 9.36% of the total cavities volume. Hence, the material consumption criteria are fulfilled with the current feed system. [10]

3.2.3. Runner balance analysis

To optimize the current feed system, the runner balance analysis is conducted. This analysis modifies the feed system's dimension to avoid overpacking, achieve balanced filling at each cavity, and minimized the feed system. To run the program's runner balance analysis, the target pressure is a required input. The target pressure range for the runner balance analysis is the spike in the pressure: XY plot. [15]

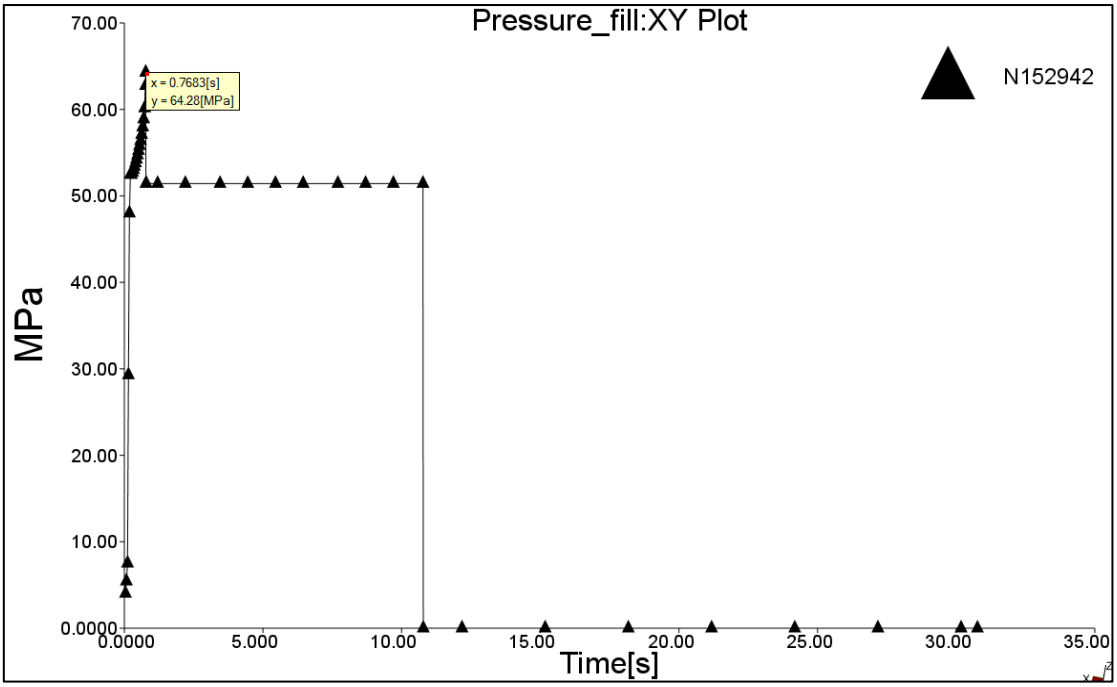

Figure 3-8: The target pressure for the runner balance analysis

The runner balance analysis suggests a decrease in the feed system volume. The amount of volume decreased is color-coded, in which the lower value is indicated by the red color, and the higher value is represented by the blue color. The primary runner's volume drops by approximately 2%, whereas the secondary runner's volume roughly reduces by 7%.

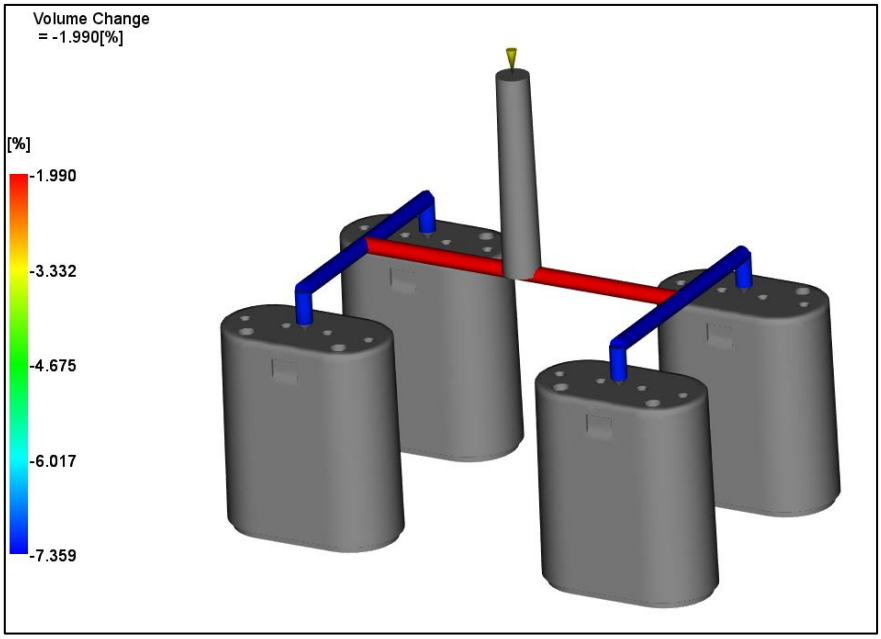

Figure 3-9: The modified feed system

Since a runner has a cylindrical shape, the modified volume can be calculated, and the modified diameter can be derived from, the volume.

$$V_{modified\ primary\ runner} = \frac{\pi \times 4^2}{4} \times 88 \times \frac{(100-2)}{100} = 1084\ mm^3$$

$$R_{modified\ primary\ runner,} = \sqrt{\frac{1084 \times 4}{88 \times \pi}} = 3.96\ mm$$

$$V_{modified\ secondary\ runner} = \frac{\pi \times 4^2}{4} \times (105.5) \times \frac{(100-7)}{100} = 1233\ mm^3$$

$$R_{modified\ secondary\ runner} = \sqrt{\frac{1233 \times 4}{105.5 \times \pi}} = 3.85\ mm$$

	Primary runner diameter	Secondary runner diameter
Before runner balance	4 mm	4 mm
After runner balance	3.96 mm	3.85 mm

Table 3-3: The balanced runner's diameter

By conducting the fill + pack analysis on the modified runner system, it shows that the processing results such as the pressure, the fill time, volumetric shrinkage, temperature, experience an insignificant change. These changes only apply to the magnitude of the considered parameter, but the color distribution representing the melt flow remains the same. Because the feed system is symmetrical and the cavities are identical, a balanced fill is achieved. Hence, this analysis only slightly decreases the runner's diameter to reduce the material used by the feed system. The alteration is only recognizable if the applied feed system connects to differently shaped cavities in the case of a family mold. In conclusion, the modification is unnecessary because it increases the manufacturing procedure 's accuracy requirement but provides no apparent improvement on the current feed system.

3.2.4. Runner cooling time analysis

The runner cooling time is defined as the time to reach ejection temperature results, provided by the fill + pack analysis. The time to reach ejection pressure is color-coded, with blue denoting a shorter time and red denoting a longer time.

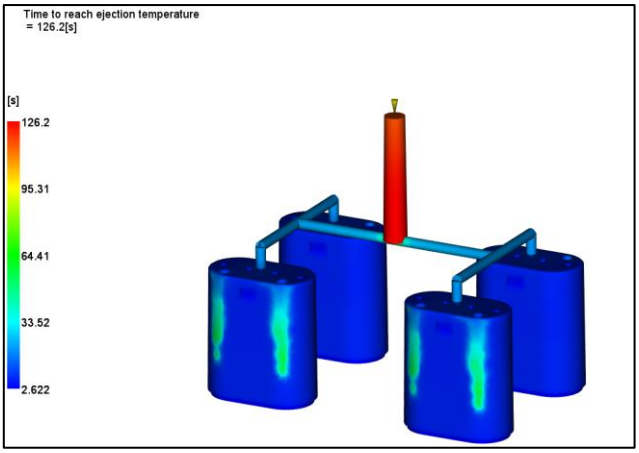

Figure 3-10: The visualization of the time to reach ejection temperature

The part cavities require up to 43 seconds, and the thickest section of the sprue reaches 126.2 seconds. Because of the sprue's thickness, it takes the most time to cool, which prolongs the total molding cycle time. Unlike the products, the sprue does not need to be as rigid, and can be ejected when solidifies enough to not stuck to the mold. However, it is difficult to precisely predict when the sprue solidifies sufficiently for ejection and requires actual experimentation. Another method to avoid this problem is to decrease the sprue volume, resulting in a higher pressure drop. [10]

Therefore, to reduce the diameter of the sprue, an additional fill + pack analysis is performed to ensure the pressure drop does not exceed the recommended pressure drop limit of 50 MPa. Assuming the sprue diameter reduces from 8 mm to 6 mm, the following table is obtained:

	Old pressure drop value	New pressure drop value
Sprue	5.2 MPa	8.1 MPa
Primary runner	8.6 MPa	22.8 MPa
Secondary runner	13.2 MPa	13.1 MPa
Total pressure drops	27 MPa	44 MPa

Table 3-4: The old and new pressure drop values of the adjusted feed system

The new total pressure drop rises significantly in accordance with the aforementioned pressure drop values, but remains below the recommended pressure drop limit by 50 MPa. The new time to reach ejection temperature can be seen below.

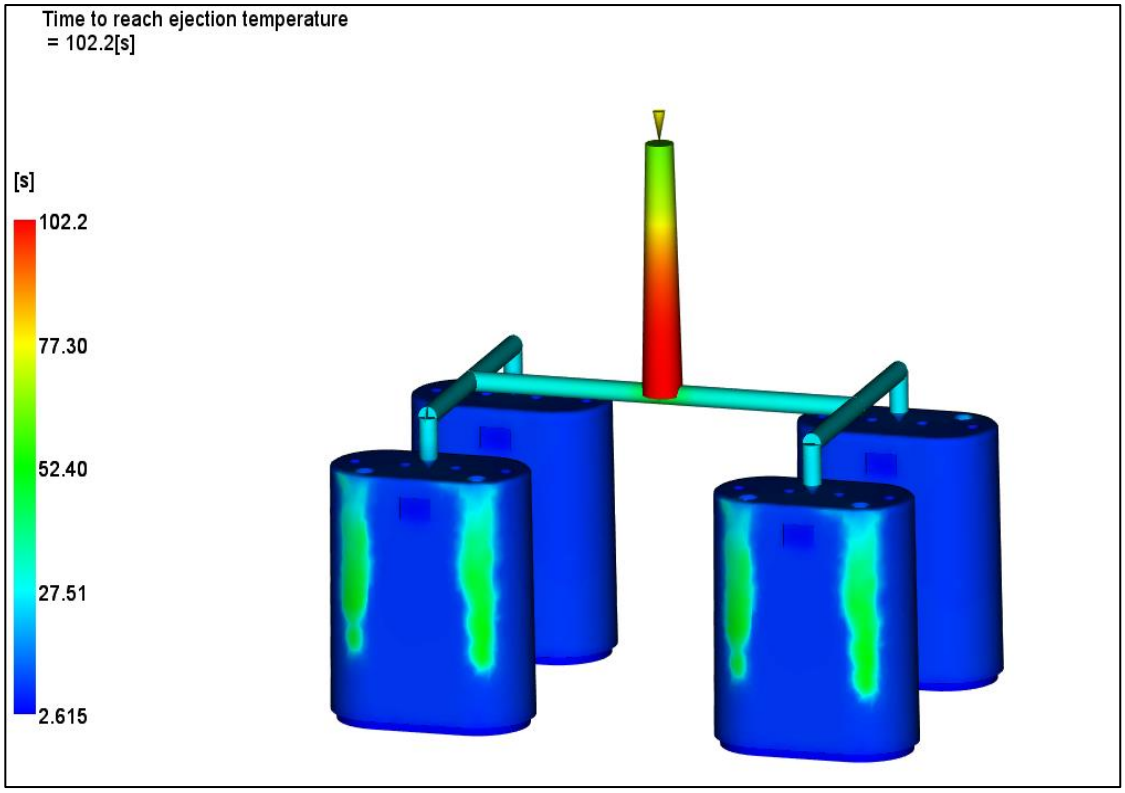

Figure 3-11: The new time to reach ejection temperature

The new time to reach ejection temperature decreases by 24 seconds to 102.2 seconds. Further decrease in the sprue volume possibly cause the total pressure drop to exceed the recommended limit. Therefore, the current change is feasible and is implemented for the feed system.

The feed system layout and dimension are shown below:

Parameter	Value
Sprue's orifice diameter	6 mm
Sprue's length	50 mm
Primary Runner's diameter	4 mm
Primary Runner's length	73 mm
Secondary Runner's diameter	4 mm
Secondary Runner's length	146 mm

Table 3-5: The dimension of the feed system

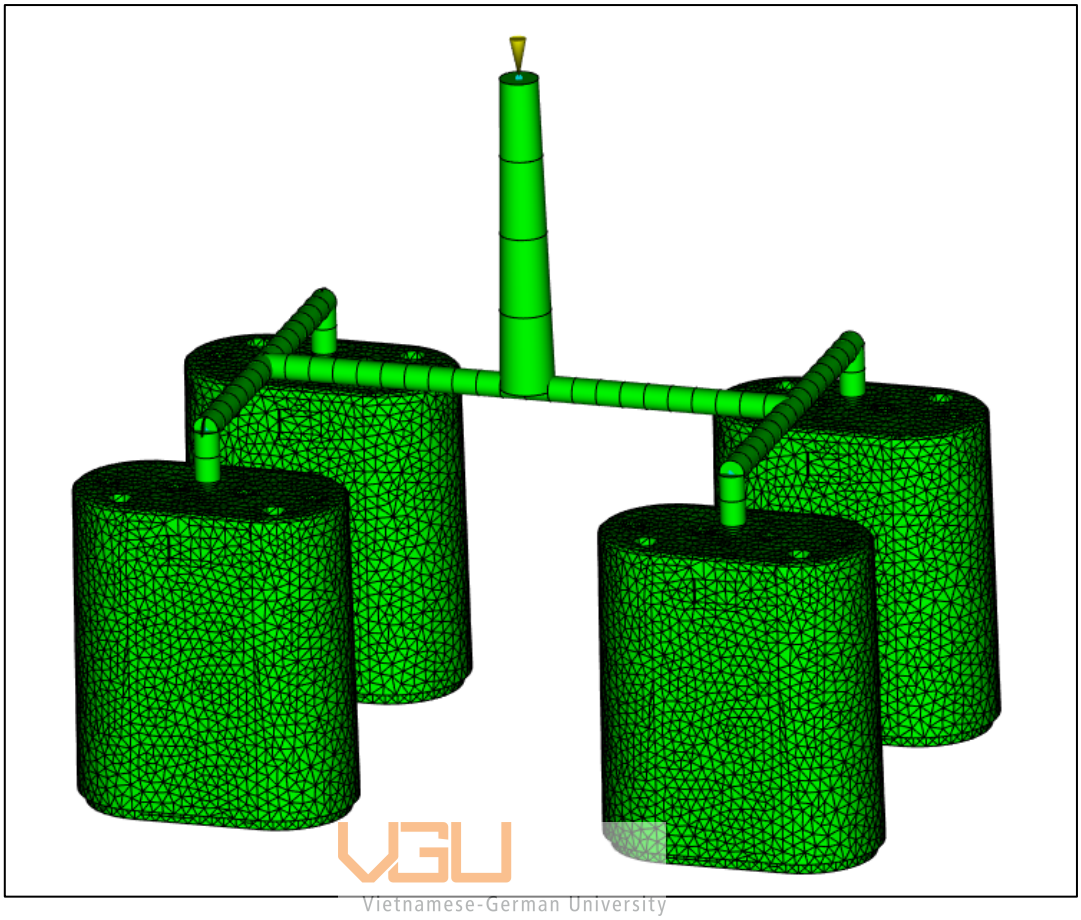

Figure 3-12: The finalized model of the feed system and part cavities

3.3. Designing the feed system's gate

A gate is a connection between the runner and the mold cavity to lead the plastic melt from the runner into the cavity to form the molding products. The gate's location and design decide the melt flow properties and the product's appearance. [10]

The current gate location has been determined from the gate location analysis. This section selects the type of gate and design it for the feed system. There are several commonly used gate designs, which includes the sprue gate, the pin-point gate, and the edge gate. Each gate is suitable for different mold types, and it also depends on the shape of the cavity.

In single cavity mold where the sprue directly connects to the cavity surface, the sprue gate is suitable, and frequently used. The lack of gate length provides no pressure drops. However, a major disadvantage is the de-gating process is more challenging for this type of gate, due to its diameter. [10]

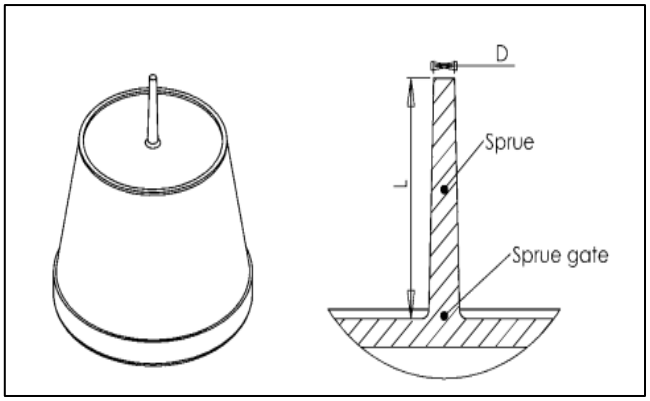

Figure 3-13: The sprue gate design

The pin-point gate is a common type of gate that connects the runner system to the part cavity via a small cylindrical opening. Simpler de-gating and minimal gate vestige can be achieved with the pin-point gate due to its small size. The three-plate molds often employ this type of gate. However, due to its small size, high pressure drops and shear rates could happen. [10]

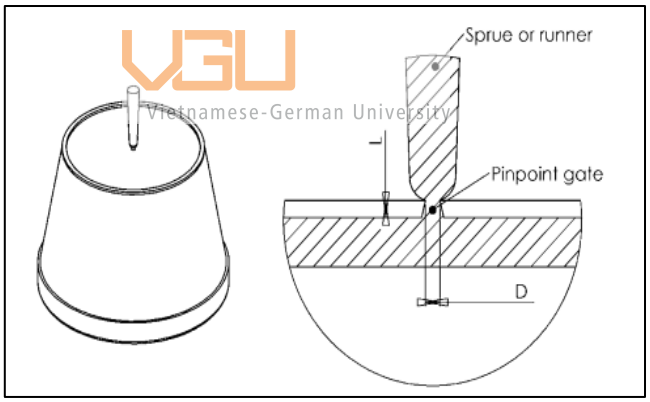

Figure 3-14: The pin-point gate design

The edge gate is commonly used to connect a cold runner to the edge of the mold cavity. This type of gate provides greatly reduced shear rates and pressure drop comparing to the pin-point gate. More material is allowed to flow because of the larger cross-sectional area, but the packing time can be longer due to the extended gate freeze time. Consequently, the larger gate size implies that the edge gate is preferably located inside to avoid being observed by the-end user. Due to the design of the LED casing, a gate placed inside the case leads to difficulty in the de-gating process. [10], [14]

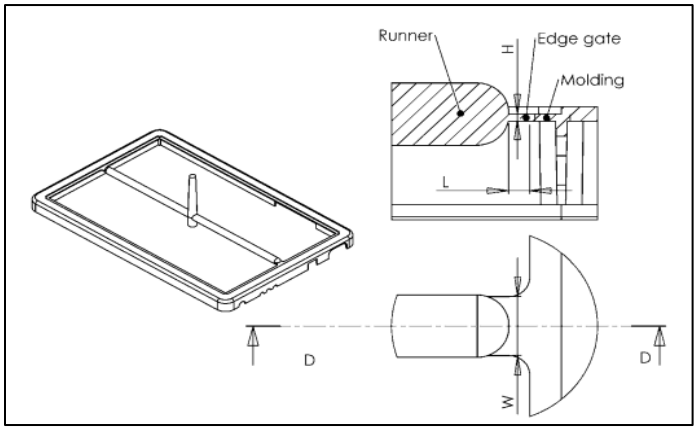

Figure 3-15: The edge gate design

From the three aforementioned gates, the most suitable gate for the LED base cover is the pin-point gate for its small size, resulting in simpler de-gating. The shear rates and pressure drop of the pin-point gate is then calculated to ensure these values do not exceed the allowable limit.

3.3.1. Calculate the gate shear rate

The gate shear rate of the pin-point gate is considerably high and must be calculated and compared to the material's permissible shear rate value. The gate dimension is then adjusted to suit this requirement.

Shear rate in gates and runners are typically calculated as a function of the volumetric flow rate. For a cylindrical-shaped gate, the shear rate is calculated as follow:

$$\dot{\gamma} = \frac{4 \times \dot{V}}{\pi r^3} \qquad (3-3)$$

Where:

$\dot{V}$: volumetric flow rate of the melt (m^3/s)

r: radius of the gate (m^3)

To initially specify the shear gate dimension, it is recommended for thicker gates with low and moderate shear rates (sprue and edge gate) have their initial thickness equals so the wall thickness at the gate location. For thinner gates that possess a moderate to high shear

rates (pin-point gate, tunnel gate, and submarine gate), the thickness equals to half of the wall thickness should be chosen as the initial gate dimension. [10]

Since the product's wall surface thickness at the injector location is 1.7 mm, the initial radius for the pin-point gate is 0.5 mm. The theoretical volumetric flow rate at the inlet is $25 \times 10^{-6}\ m^3/s$.

$$\dot{\gamma} = \frac{4 \times 25 \times 10^{-6}}{\pi \times (0.5 \times 10^{-3})^3} = 254{,}648\ 1/s$$

The calculated shear rate far exceeds the allowable shear rate of the material of 40,000 1/s.

The shear rate of the gate can also be assessed from the shear rate result provided by the program. Because the flow rate can fluctuate throughout the molding process, the program's result is different from the theoretically calculated result. However, the shear rate at the gate can reach up to 85,190 1/s, which also tops the material's allowable limit.

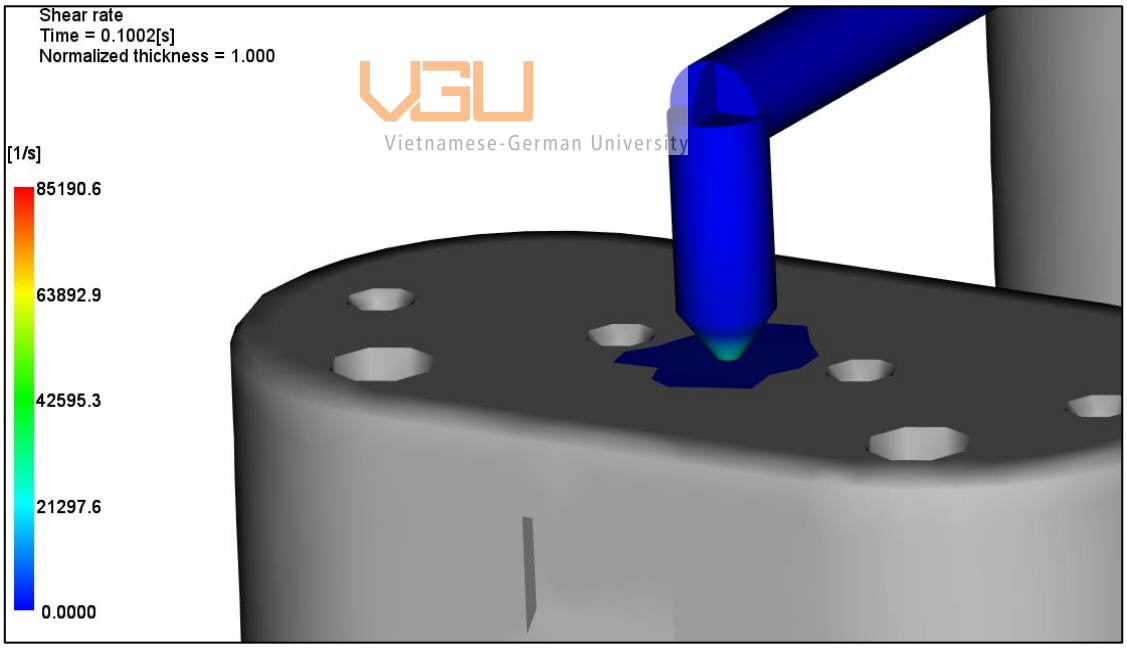

Figure 3-16: The shear rate result of the 1 mm gate

Increasing the gate size significantly reduces the melt shear rate at the gate to ensure that the material does not degrade. However, a larger gate size leads to more noticeable gate vestige and difficulty in the de-gating process. By applying the same calculation to each increasing diameter value, the following table is obtained:

Gate's diameter (mm)	Shear rate value (1/s)
1	254648
1.5	75451
1.8	43664
2	31831
2.5	16297

Table 3-6: The shear rate in correspondence with the increasing gate's diameter

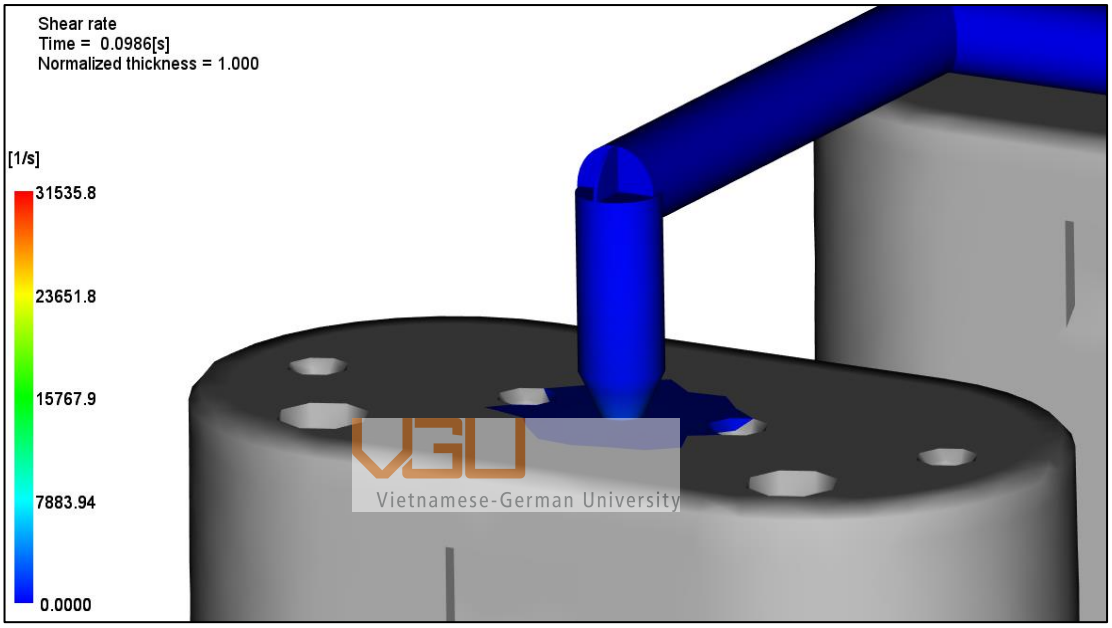

Figure 3-17: The shear rate result of the 2 mm gate

The program's maximum shear rate value at the 2 mm gate has reduced to 31,535 1/s, which is within the permissible shear rate value. From the table 3-6, the 2 mm gate diameter is the most suitable because it does not exceed the permissible value, while the gate vestige is relatively small.

3.3.2. Calculate the gate pressure drop

For a cylindrical gate, the pressure drop can be estimated with the pressure drop formula:

$$\Delta P_{gate} = \frac{2 \times 17000 \times 0.002}{0.001} \left(\frac{\left(3 + \frac{1}{0.35}\right) \times 25 \times 10^{-6}}{\pi (0.001)^3}\right)^{0.35} = 2.9\ MPa$$

This result can also be obtained by subtracting the program's pressure result conducted at the gate's end from the gate's start. The considered pressure points are at the end of the filling phase. Hence, the pressure drop is 2.7 MPa.

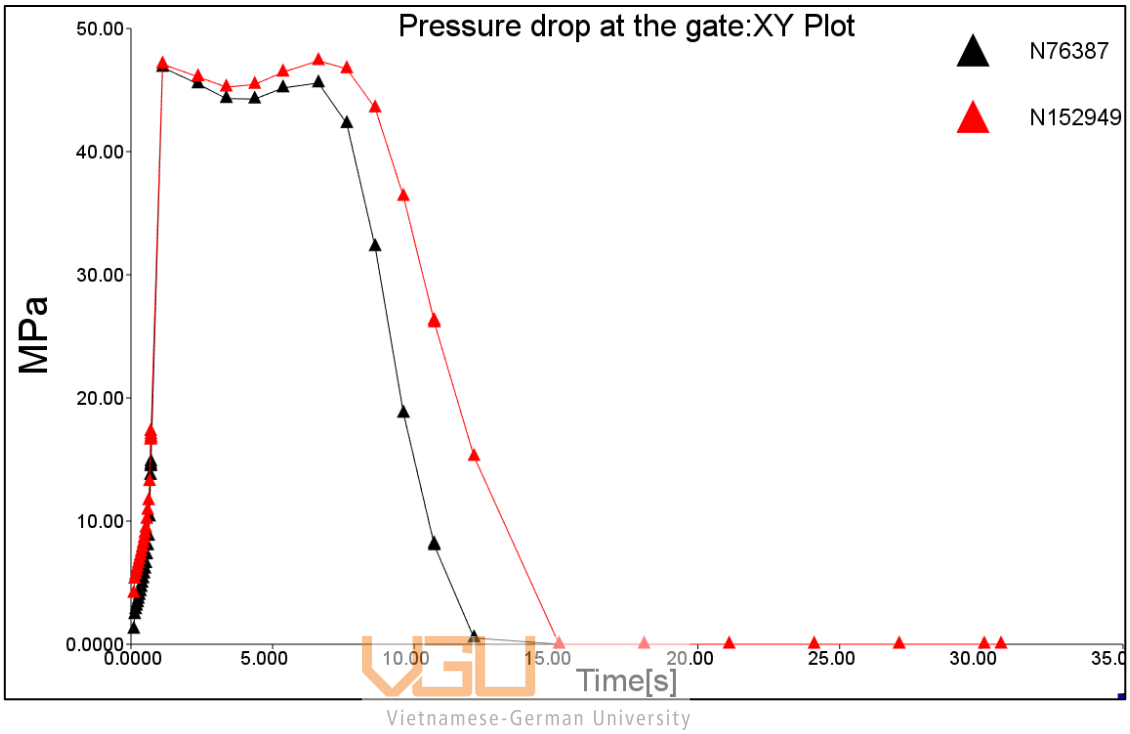

Figure 3-18: The pressure drop at the gate: XY plot

The pressure drop at the gate should not be larger than 10 MPa, exceeding this value suggests an inappropriate gate design. The current gate diameter provides a proper pressure drop for the feed system. [10]

3.3.3. Calculate the gate freeze time

When the material inside the cavity cools, the melt inside the gate also tends to cool. When the gate is frozen, the additional material is prevented from entering the cavity, and the volumetric shrinkage will not be compensated. Hence, the final product will not have the desirable dimension and quality.

The gate freeze time is estimated with the following equation. Noted that the actual freeze time is typically longer due to the equation does not take into account the convection of heat that prevents the freezing of the gate. [10]

$$t_s = \frac{D^2}{23.1 \times \alpha} \ln\left(0.692 \frac{T_{melt} - T_{coolant}}{T_{no_{flow}} - T_{coolant}}\right) \quad (3-4)$$

Where:

D: diameter of the gate

$\alpha = 8.69 \times 10^{-8}\ m^2/s$

T_{melt}: melt temperature

$T_{no_{flow}}$: no flow melt temperature

$T_{coolant}$: coolant temperature

The estimated gate freeze time is:

$$t_s = \frac{(0.002)^2}{23.1 \times 8.69 \times 10^{-8}} \ln\left(0.692 \frac{310 - 60}{143 - 60}\right) = 1.46\ (s)$$

The cooling time of the cavity can be estimated using the following equation:

$$t_s = \frac{h^2}{23.1 \times \alpha} \ln\left(\frac{4}{\pi} \times \frac{T_{melt} - T_{coolant}}{T_{no_{flow}} - T_{coolant}}\right) \quad (3-5)$$

Where:

h: wall thickness of the part ($h = 1.7\ mm$)

The estimated cooling time of the part is:

$$t_s = \frac{(0.0017)^2}{23.1 \times 8.69 \times 10^{-8}} \ln\left(\frac{4}{\pi} \times \frac{310 - 60}{143 - 60}\right) = 1.9\ (s)$$

Comparing the two results, the gate will freeze prematurely and the product can not be adequately packed. An under-packed product can experience poor surface finish, sinks, voids, uncontrolled shrinkage, and warpage. In conclusion, the current gate provides an acceptable pressure drop, shear rate, and relatively small gate mark, but the gate freeze time might not be sufficient to properly pack the product. [16]

Parameter	Value
Gate's start dimension	4 mm
Gate's end dimension	2 mm
Taper angle	26.5
Gate's length	2 mm

Table 3-7: The gate's dimension

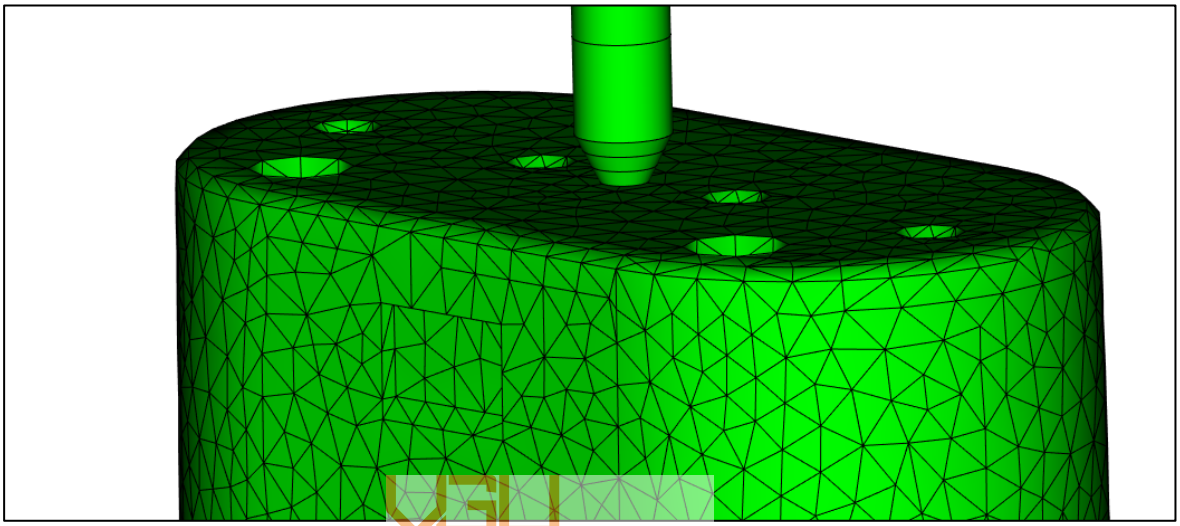

Figure 3-19: The gate design of the feed system

The finalized runner system and gate dimensions are mention in the table below:

Parameter	Value
Sprue's orifice diameter	8 mm
Sprue's length	50 mm
Primary Runner's diameter	4 mm
Primary Runner's length	42 mm
Secondary Runner's diameter	4 mm
Secondary Runner's length	34 mm
Type of gate	Pin-point gate
Gate's start diameter	4 mm
Gate's end diameter	2 mm
Gate's length	2 mm

Table 3-8: The finalized dimension of the feed system

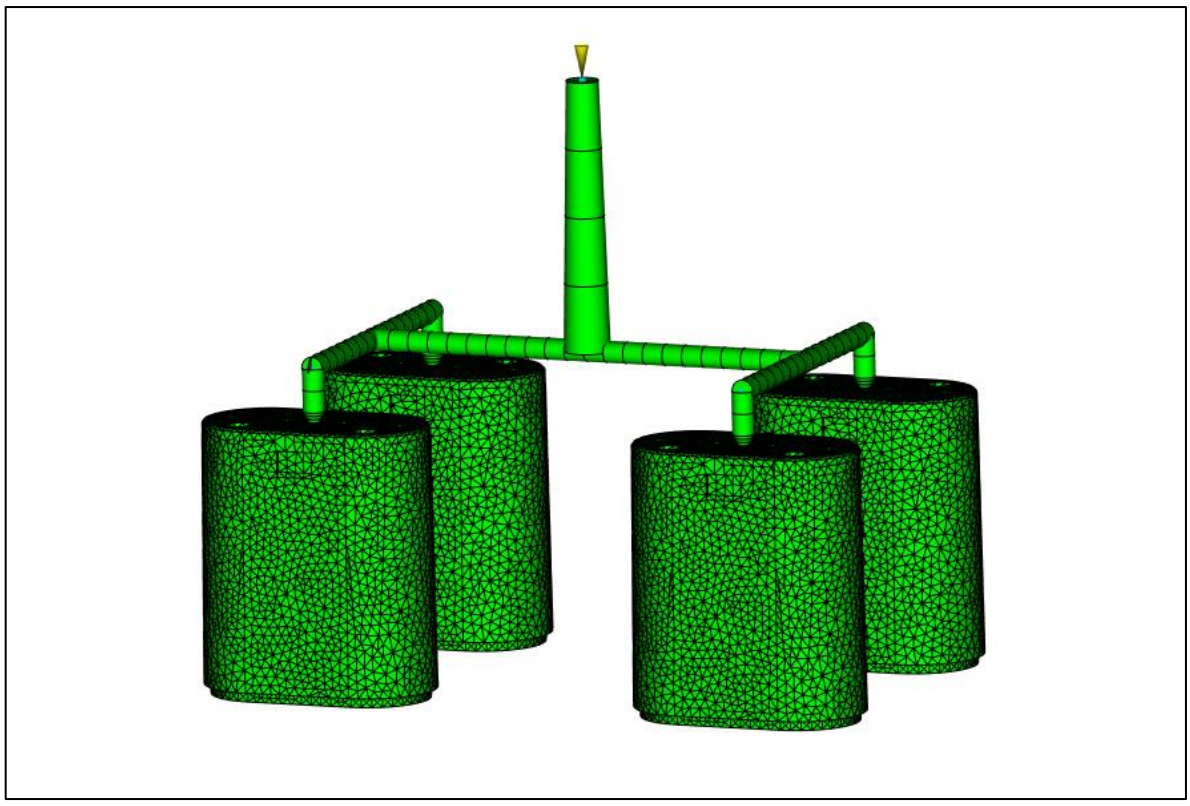

Figure 3-20: Visualization of the finalized feed system

4. Selection of the cooling system

The cooling system of the injection mold is designed to provide uniform cooling for the mold cavities. A proper cooling line design potentially reduces the cooling and cycle times of the process. Additionally, a suitably designed cooling system prevents a significant rise of the temperature gradient, which causes differential shrinkage and warpage of the moldings. [10]

A cooling system has various designs, but it is advised to avoid continuously loop the cooling lines. Such design creates a low coolant flow rate due to the high flow resistance, which is generated by the combined length of the cooling lines.

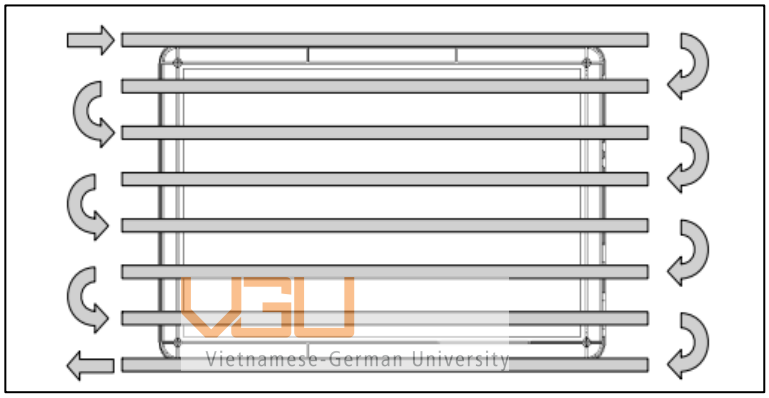

Figure 4-6: The cooling system with the continuously looped cooling lines

A more preferred design is to connect two sets of cooling lines with a short return loop at the other side of the mold. This reduces the flow resistance due to the reduced length of the loop, while maintaining uniform cooling and high cooling rates.

Figure 4-7: The cooling system with short return loop

However, the downside of this cooling system design is the increase in number of inlets and outlets leads to difficulty in the set-up procedure of the mold and the IMM. This problem can be solved by adding the main lines that distribute coolant at the beginning of the cooling lines and accumulate the coolant at the end of the cooling lines. The addition of the main lines reduces the number of inlet and outlet, which make the connection procedure of the mold to the IMM much simpler. [10]

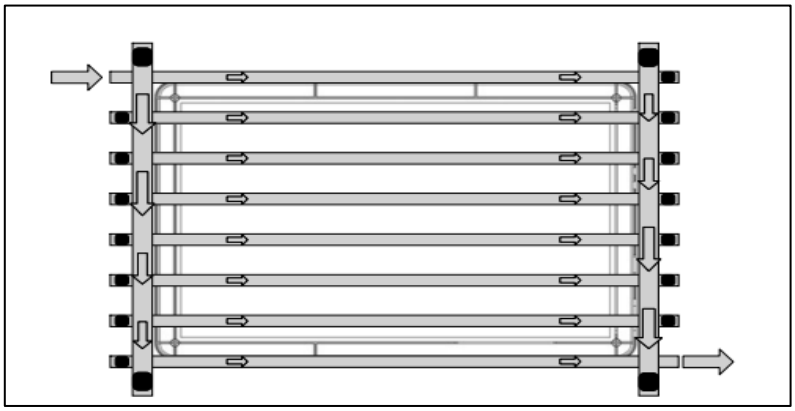

Figure 4-8: The main distribution and accumulation line cooling layout

Another design that provides the best space usage is to place the cooling lines around the periphery of the part. This design is suitable for smaller mold to produce small objects. For a three-plate mold, there is no heat being generated in the central area of the mold. Hence, this design provides cooling for the outside of the cavity, and reduce the mold making cost [4].

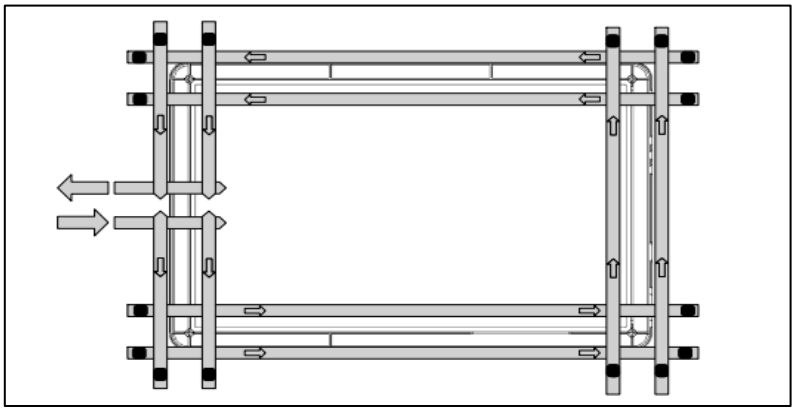

Figure 4-9: The peripheral cooling line layout

4.1. Calculation of the estimated cooling time

The cooling time is defined as the time required for the plastic to solidify after filling the cavities, and becomes sufficiently rigid to be ejected. The estimated cooling time of the product can be calculated with the following equation as a function of melt temperature, eject temperature and coolant temperature [17]:

$$t_c = \frac{h^2}{\pi^2 \times \alpha} \ln\left(\frac{4}{\pi}\frac{T_{melt} - T_{coolant}}{T_{eject} - T_{coolant}}\right) \quad (4-1)$$

Where:

h: product's wall thickness

α: thermal diffusivity of the melt material

T_{melt}: melt temperature

$T_{coolant}$: coolant temperature

T_{eject}: ejection temperature

Since the nominal thickness of the LED base cover is 1.7 mm, the thermal diffusivity of PC is 1.89 × 10^{-7} m^2/s, the melt, eject and coolant temperature is 310°C, 80°C, and 60°C respectively, the estimated cooling time is:

$$t_c = \frac{0.0017^2}{\pi^2 \times 1.89 \times 10^{-7}} \ln\left(\frac{4}{\pi}\frac{310 - 60}{80 - 60}\right) = 4.29\ (s)$$

The runner's theoretical minimum cooling time can be calculated with the following equation:

$$t_c = \frac{D^2}{\pi^2 \times \alpha} \ln\left(\frac{4}{\pi}\frac{T_{melt} - T_{coolant}}{T_{eject} - T_{coolant}}\right) \quad (4-2)$$

With D is the diameter of the runner (D = 4 mm), the theoretical minimum cooling time of the runner is equal to:

$$t_c = \frac{0.004^2}{\pi^2 \times 1.89 \times 10^{-7}} \ln\left(\frac{4}{\pi}\frac{310 - 60}{80 - 60}\right) = 23.7\ (s)$$

4.2. Calculation of the cooling line diameter

The heat transfer rate, also known as the "cooling power" of the feed system is defined as the amount of energy to be removed per second of the cooling time. This energy is the total amount of heat produced by the molded parts and the associated cold runners, which can be calculated as:

$$Q_{moldings} = m_{moldings} \times C_p \times (T_{melt} - T_{eject}) \quad (4-3)$$

Where:

$Q_{moldings}$: the heat produced by the molded parts

$m_{moldings}$: the total mass of the molded parts and the associated cold runners

C_p: specific heat capacity of the PC material

The total mass of the molded parts can be calculated by multiplying the material's density (ρ_{PC} = 1.18 g/cm^3) with the molded parts volume, which are obtained from the CAD program. Hence, the energy to be removed is:

$$V_{molded\ parts} = 4 \times 12.5 = 50\ cm^3$$

$$m_{molded\ parts} = 50\ cm^3 \times 1.18\ g/cm^3 = 59\ g$$

$$Q_{molded\ parts} = 59 \times 10^{-3} \times 2160 \left(\frac{J}{kg.°C}\right) \times (310 - 80) = 29311\ J$$

The cooling power is calculated as:

$$\dot{Q}_{cooling} = \frac{Q_{moldings}}{t_c} = \frac{29311(J)}{23.7\ (s)} \approx 1237\ W$$

Assuming that there are three cooling lines positioned around the periphery of the cavities, the cooling power of each cooling line is:

$$\dot{Q}_{line} = \frac{\dot{Q}_{cooling}}{3} = \frac{1237\ W}{3} \approx 412\ W$$

The temperature of the coolant increases as it travels through the cooling lines because the heat is transferred from the plastic melt to the coolant. As a result, the coolant is unable to provide sufficient cooling at the end of the cooling lines. High thermal gradient causes differential shrinkage and warpage if the coolant's temperature increases exponentially. The increase in coolant temperature can be controlled by adjusting the coolant's volumetric flow rate according to the following equation:

$$\Delta T_{coolant} = \frac{\dot{Q}_{line}}{\dot{V}_{coolant} \times \rho_{coolant} \times C_{P,coolant}} \quad (4-4)$$

Where:

$\dot{V}_{coolant}$: volumetric flow rate of coolant

$\rho_{coolant}$: coolant density

$C_{P,coolant}$: coolant specific heat capacity

In order to determine the sufficient volumetric flow rate of the coolant, the value range of the temperature increase is initially specified. A typically allowable increase of the coolant temperature is 1°C. Assuming that the chosen coolant is water for its lower price comparing to Ethylene glycol and Oil. The density of water is 1000 kg/m^3 and its specific heat capacity is 4187 J/kg°C. Therefore, the coolant volumetric flow rate is calculated as:

$$\dot{V}_{coolant} = \frac{\dot{Q}_{line}}{\Delta T_{coolant} \times \rho_{coolant} \times C_{P,coolant}} = \frac{412}{1°C \times 1000 \frac{kg}{m^3} \times 4187 \frac{J}{kg°C}}$$

$$= 9.8 \times 10^{-5} \frac{m^3}{s}$$

From the required value of the volumetric flow rate, the diameter of each cooling line can be decided according to the heat transfer and fluid flow constraints. A turbulent flow is desired in each cooling line to provide adequate heat transfer. The Reynolds number determines if the flow is a turbulent flow or a laminar flow. To achieve a turbulent flow, the Reynold number must be:

$$Re = \frac{4 \times \rho_{coolant} \times \dot{V}_{coolant}}{\pi \times \mu_{coolant} \times D} > 4000 \quad (4-5)$$

Where:

D: the cooling line's diameter

$\mu_{coolant}$: the coolant viscosity

The viscosity of water is 0.001 PaS. Hence, the maximum value of the cooling line's diameter is:

$$D_{max} = \frac{4 \times 1000 \times 9.8 \times 10^{-5}}{\pi \times 0.001 \times 4000} = 0.031m = 31\ mm$$

This value suggests that any value of the cooling line's diameter that is below 31 mm can provide turbulent flow.

The minimum constraint of the diameter relates to the required pressure drop to push the coolant at a certain volumetric flow rate. The pressure drop through the cooling line can be calculated with the following equation:

$$\Delta P_{line} = \frac{\rho_{coolant} \times L_{line} \times (\dot{V}_{coolant})^2}{10\pi \times D^5} \quad (4-6)$$

Assuming that the allowable pressure drop of the coolant is 100 kPa. The length of the cooling line is obtained by sketching the layout of the cooling line on paper. The estimated total length of the cooling lines is 3000 mm. The minimum diameter of the cooling line is:

$$D_{min} = \sqrt[5]{\frac{1000 \times 3 \times (12.2 \times 10^{-5})^2}{10\pi \times 100 \times 10^3}} = 0.007\ m = 7\ mm$$

The minimum value of the cooling line is 7 mm to provide a suitable pressure drop for the cooling line. Combining the turbulence and pressure drop requirement, the value range of the cooling line's diameter is:

$$7\ mm < D_{line,molded\ parts} < 31\ mm$$

The cooling lines are manufactured by drilling multiple intersecting holes to the plate. To prevent the coolant from flowing out of the system, one end of the drill hole is plugged with a cooling plug. In accordance to the cooling line diameter requirement, the chosen diameter is 8 mm.

DME plug	Normal pipe thread	Cooling line diameter
JP-250	1/16	4.76 mm
JP-251	1/8	6.35 mm
JP-352	1/4	9.53 mm
JP-553	3/8	11.1 mm
JP-554	1/2	15.9 mm

Table 4-1: Specifications of Typical Cooling Plugs

From the table above, the suitable DME plug for the current line is the JP-352. A drill bit with a diameter of 3/8 inches is used to drill a concentric hole with the current drill hole. The drill depth is deep enough to fully insert all of the plug's thread.

4.3. Selection of the cooling line depth

The cooling line depth is defined as the distance between the cooling line and the surface of the mold cavity. The closer the cooling line is placed near the mold cavity surface, the higher the stress concentration occurs around the cooling line. The commonly used range in mold design is:

$$2D_{line,molded\ parts} < H_{line,molded\ parts} < 5D_{line,molded\ parts}$$

Therefore, the value range of the cooling line depth is equal to:

$$16\ mm < H_{line,molded\ parts} < 40\ mm$$

The value range above acts as a constraint in conjunction with the mold dimensions and layout to determine the appropriate cooling line depth for the mold.

4.4. Selection of the cooling line pitch

The cooling line pitch represents the distance between each cooling line. A smaller pitch value provides faster and more uniform cooling. However, more cooling lines require more space on the mold plate, and increases the chance to conflict with other mold components.

It is recommended to choose the cooling pitch in the following range to avoid high temperature gradient between cooling lines:

$$H_{line,molded\ parts} < W_{line,molded\ parts} < 2H_{line,molded\ parts}$$

Assuming that the cooling line depth chosen from the value range above is 17 mm. The cooling line pitch can be any values between the range of:

$17\ mm < W_{line,molded\ parts} < 34\ mm$

The value ranges above suggest an appropriate cooling line dimension and layout for the molded products. It is noted that the cooling line must avoid intersecting with the cavities or plate's guide holes to prevent insufficient cooling due to coolant leakage.

Parameter	Value (mm)
Cooling line diameter	8
Cooling line depth	17
Cooling line pitch	20

Table 4-2: The cooling line's parameter

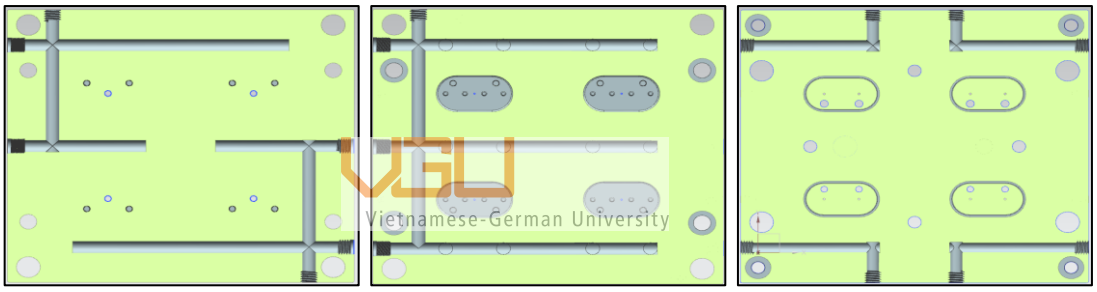

Figure 4-10,6,7: The cooling system of the plate A and plate B

5. Designing the mold components with NX

This part of the thesis focuses in the introduction of the computer aided designing program, and the designing method of the injection mold's components. The designing procedure of the injection mold is based on the flow analysis results and the cooling system calculation results, which are acquired from the previous chapters. Since each mold component is required to be calculated to estimate the sufficient strength to prevent potential failure. Hence, this chapter also covers the calculation of force applied to some mold components.

5.1. Introduction of the computer aided designing program

To meet the precision requirement in designing and manufacturing, along with the increase in the complexity of the product, computer aided designing (CAD), is created to assist in the development, modification, and optimization of the design. The chosen CAD software for this thesis is Siemens NX 12. This program provides the necessary tools and easy to use environment to create, modify the 2D layout and 3D model of each mold component. These components are assembled to create the injection mold. Furthermore, the program can conduct the FEM analysis to determine the deformation caused by the acting stress on each mold component.

5.2. Designing the mold plates

The plate in mold design implies a rectangular structure, whose length and width are greater than the thickness. The majority of the injection mold consists of multiple plates, including the top clamp plate, stripe plate, A plate, B plate, stripe plate, ejector plate, ejector support plate, space block, and bottom clamp plate. The aforementioned plates are organized and assembled to create two separable sides of the injection mold: the stationary side and the movable side. For the three-plate mold, the stationary side includes the top clamp plate, the stripe plate, the runner plate and the A plate. The movable side consists of the B plate, the support plate, the ejector plate, ejector support plate, the spacer blocks and the bottom clamp plate. [10], [19]

During the molding cycle phases, the plastic melt exerts pressure on the surfaces of the cores and cavities on plates A and B, the stripe plate's runner cavity, and the sprue bushing's cavity. Additionally, the compressive forces due to mold clamping cause uniform

compressive stresses throughout the mold plates. Therefore, the mold plates are designed to be sufficiently robust to withstand the following stress, bending, and defect [10]:

- The stress on the cores, cavities, feed system's cavity caused by the melt pressure
- The uniform compressive stresses due to mold clamping
- The excessively defect under load due to fatigue from many molding cycles [18]
- Plate bending during the molding cycle caused by the stacking of plates [10]
- Avoid overly heavy and high production cost [10]

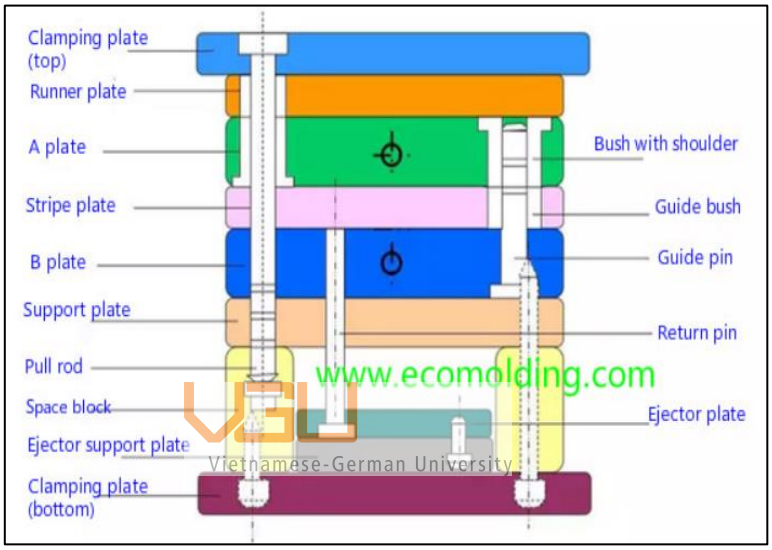

Figure 5-1: The mold plates of the injection mold

5.2.1. Mold plates modeling process

The model of each plate is designed using siemens NX 12 program. Most mold plates have similar dimensions, but some mold plates are smaller or wider depending on their function. For example, the ejection plate and the ejector support plate are smaller to be placed between the spacer blocks. The top and bottom clamp plate are a slightly wider to leave space for the clamping unit. In order for the plates to be aligned with leader/guide pins during operation, each plate must have at least four drill holes, one at each corner of the plate.

The plate is created by:

- Draw a 200 x 180 mm rectangle on a 2D sketch environment provided by NX. For the ejector plates, the rectangle is 140 x 120 mm. For the top and bottom clamp plate, draws a rectangle of 240 x 180 mm.
- Extrude a 3D body from the 2D sketch with thickness from 10 to 51 mm depending on the plate.
- Draw circles with varying diameters and locations on the face of the plate.
- Use the extrude tool, select the circles and choose the subtract option in the Boolean operator selection box to create circular holes. The depth of the hole is equal to the extrude distance.
- Use the thread tool to create threaded holes. The tool is located in the design feature option, which creates a predetermined thread based on the size of the circular hole. For example, an M6 thread is created from a M5 circular hole, since the M6 threaded hole has 1 mm pitch.
- The cooling system is created by forming multiple intersecting tunnels. Each tunnel is created by revolving a rectangle along an axis. The rectangles and axes are sketched on a plane positioned between the two faces of the plate. The cooling time, cooling power, cooling line diameter, cooling line depth and pitch of the system is calculated in the design of cooling system section.

5.2.2. Mold plates stress analysis using NX

To prevent the deformation of the plates throughout the molding cycle, a stress comparison is conducted after the creation of each plate's model. The von Mises stress, σ_{Mises}, is generally used to predict the failure of a structure [10]. The von Mises stress is calculated with the following equation:

$$\sigma_{limit} = \frac{\sigma_{yield}}{f} \quad (5-1)$$

Where:

σ_{limit}: limit stress

σ_{yield}: yield stress (For SKD61, σ_{yield} = 1000 ÷ 1380 MPa)

f: safety factor (f = 1.5)

$$\sigma_{limit} = \frac{1000 \div 1380}{1.5} = 666.7 \div 920\ MPa$$

Comparing this value range to the von Mises stress occurs on each mold plate to determine if the plate is capable of resisting the plastic deformation.

Calculating the von Mises stress and deformation on each plate by hand can be very time consuming and tedious. However, this task can be simplified using the program's finite element analysis (FEM analysis). Conducting the FEM analysis requires the user to conduct the following procedure:

- Assign the material
- Select the 3D tetrahedral mesh
- Assign the fixed constraints to the guide holes and threaded holes for the bolts
- Apply the melt pressure to the cavities and the clamp force on each plate's face

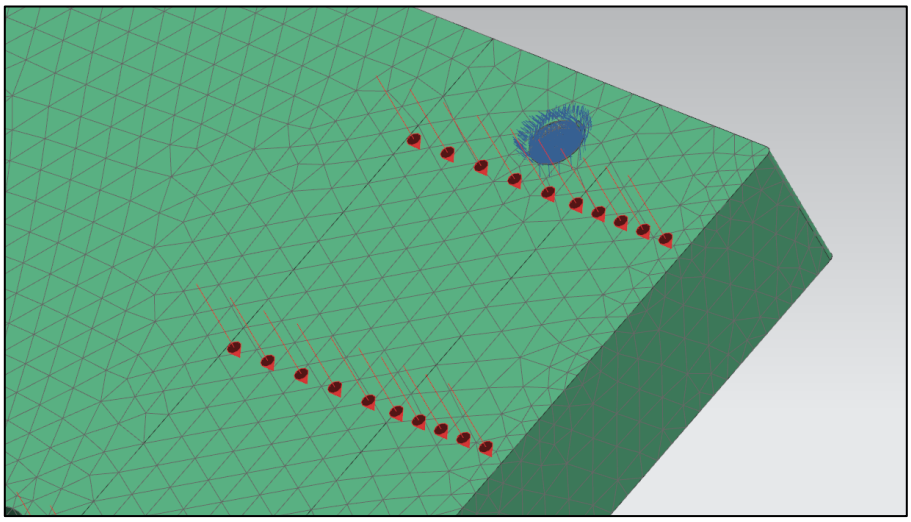

Figure 5-2: The applied force and the fixed constraint for the FEM analysis

According to the analysis result calculated by Autodesk Moldflow Insight, the maximum clamp force required is 212.46 kN during the packing phase. The acting melt pressure varies through the feed system, and the maximum value of the pressure is considered:

The maximum melt pressure at the sprue: 61.7 MPa

The maximum melt pressure at the primary runner: 49 MPa

The maximum melt pressure at the secondary runner: 47.6 MPa

The maximum melt pressure at the gate: 46.5 MPa

The maximum melt pressure at the mold cavities: 45.4 MPa

From the parameters above, the program calculates and visualize the von Mises stress occurs on each mold plate. The stress result suggests that the value range of the von Mises stress on each plate does not exceed the limit stress's value range. Higher value of stress occurs around the constrained areas at the guide holes. These results suggest that no structural failure should occurs on the mold plate throughout the molding cycle.

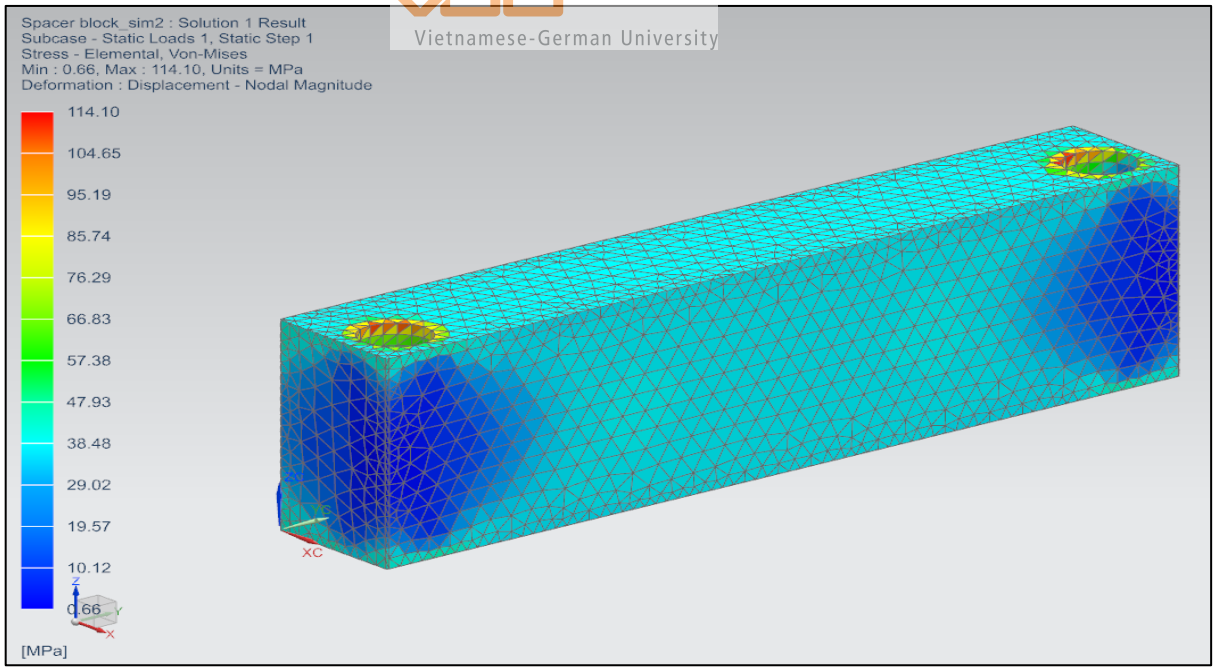

Figure 5-3: The von Mises stress on the spacer block

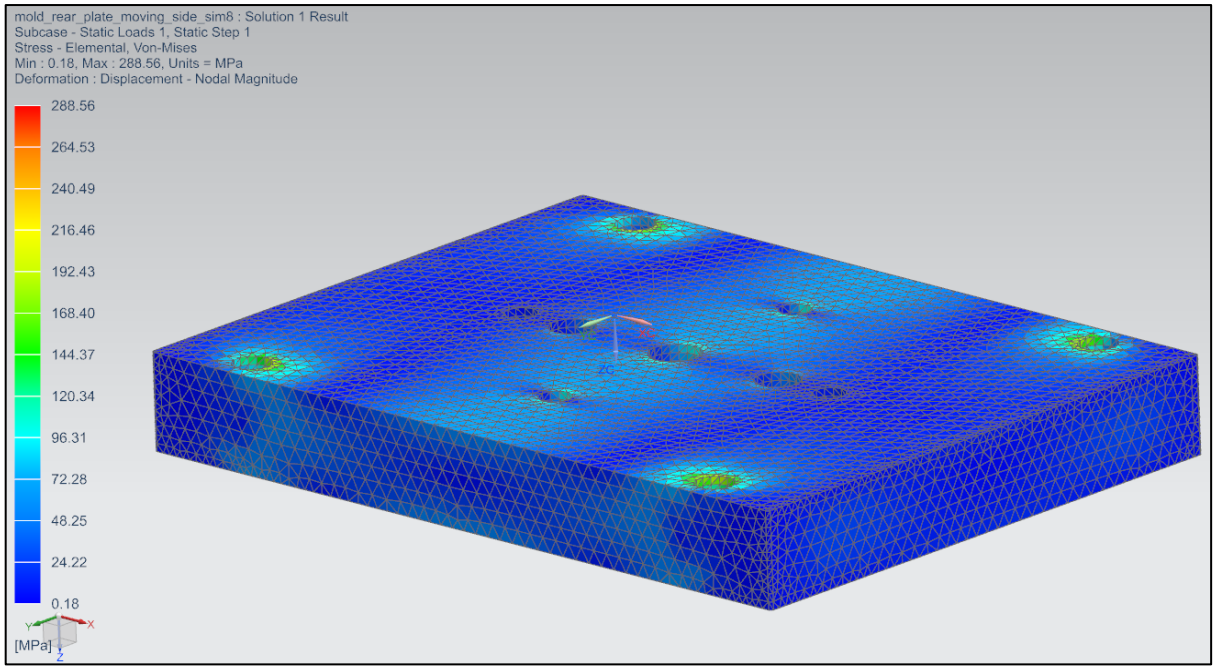

Figure 5-4: The von Mises stress on the bottom clamp plate

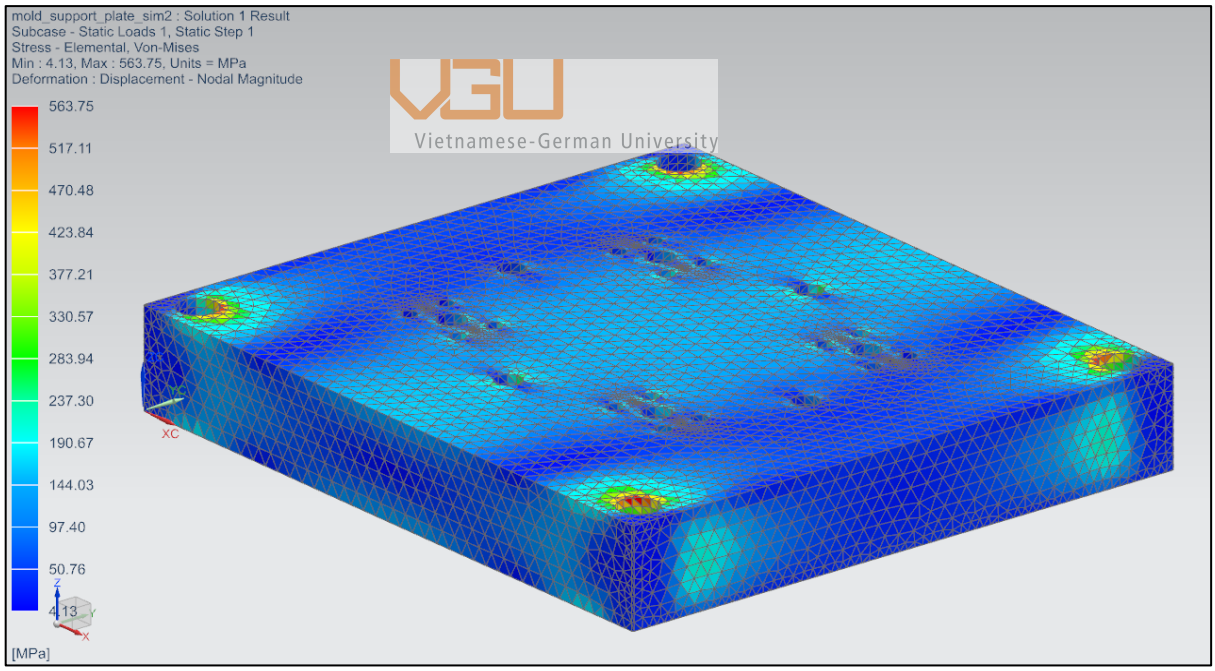

Figure 5-5: The von Mises stress on the support plate

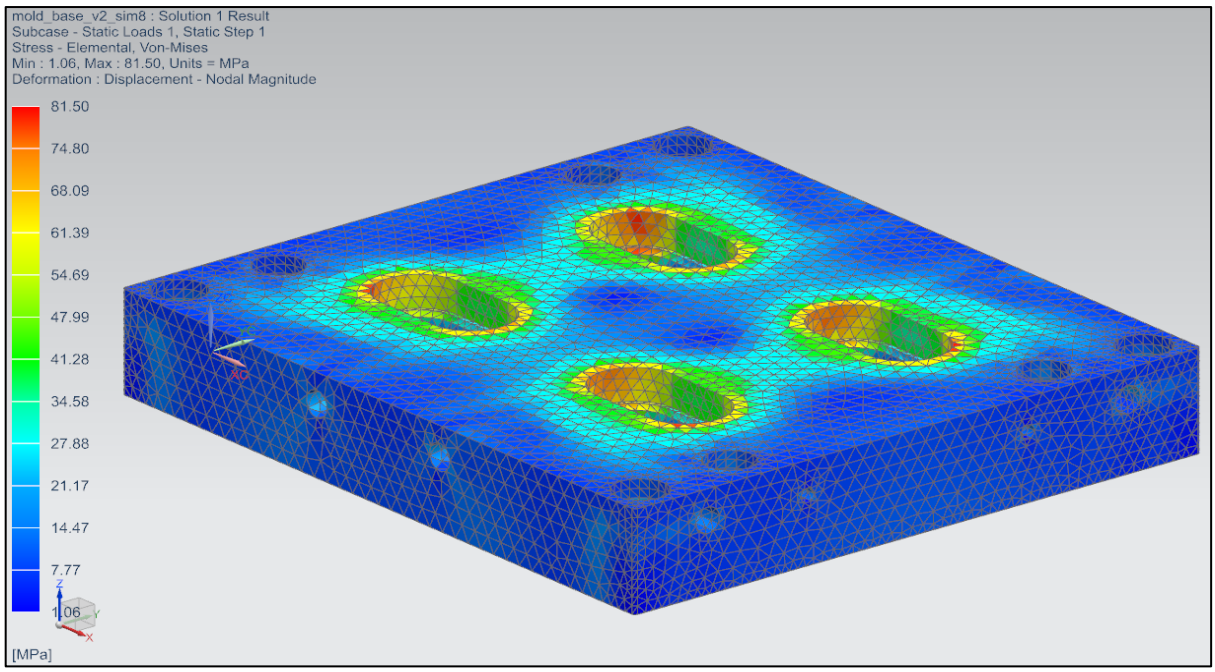

Figure 5-6: The von Mises stress on the B plate

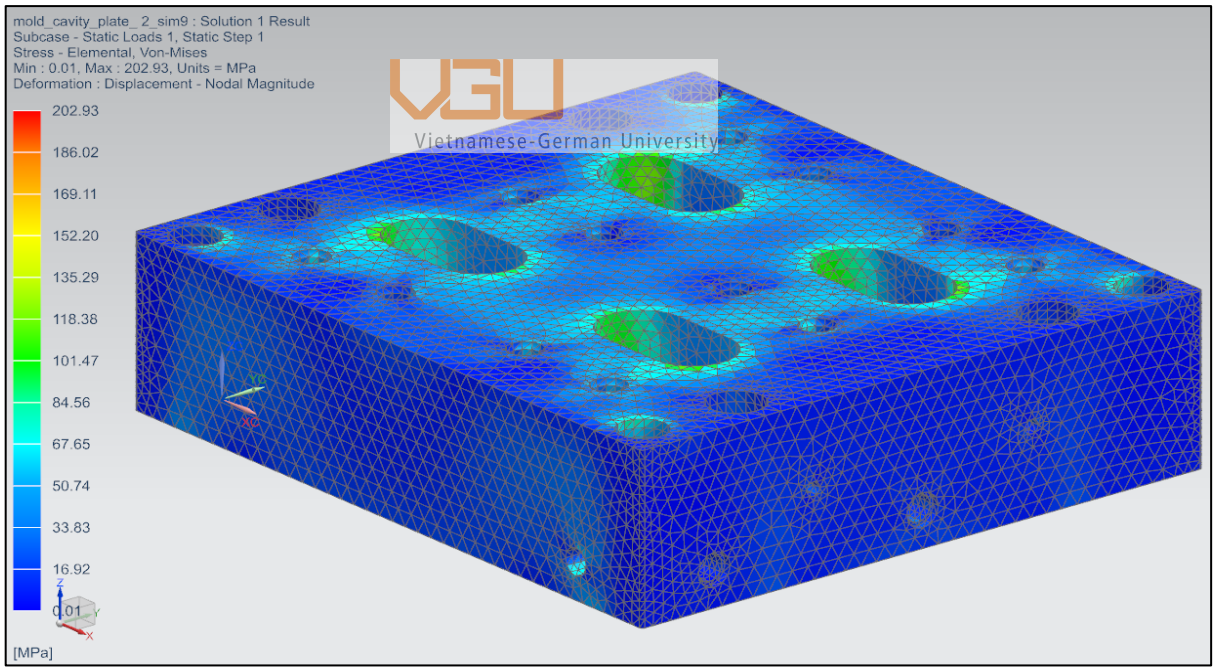

Figure 5-7: The von Mises stress on the A plate

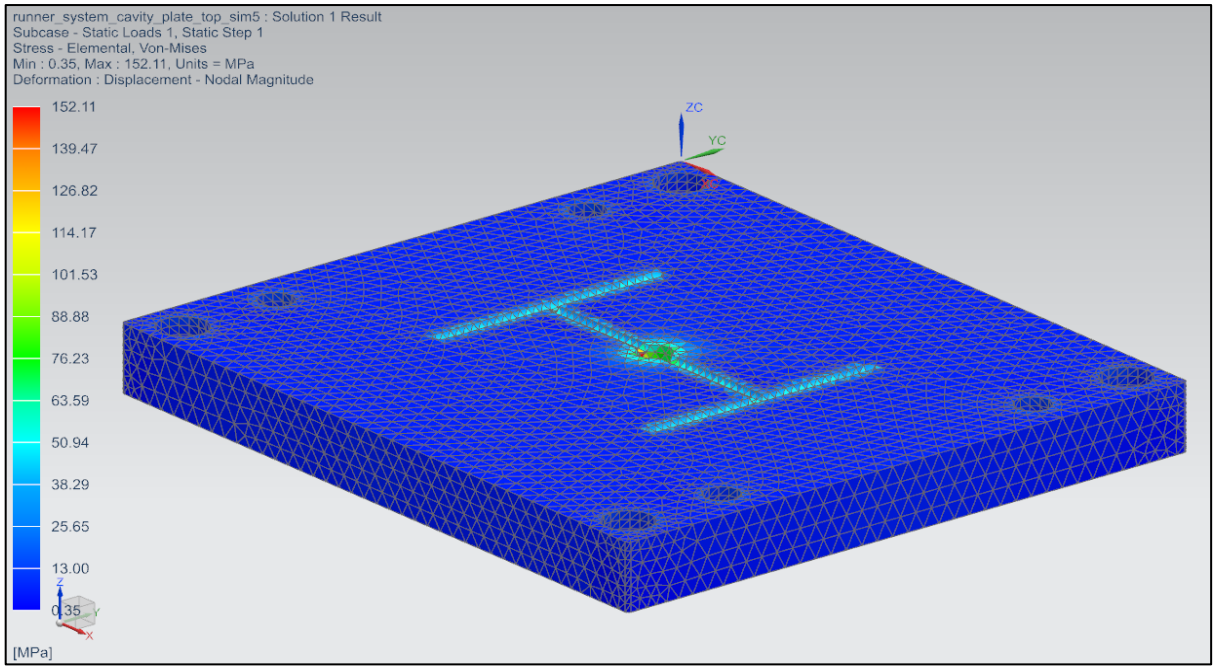

Figure 5-8: The von Mises stress on the stripe plate

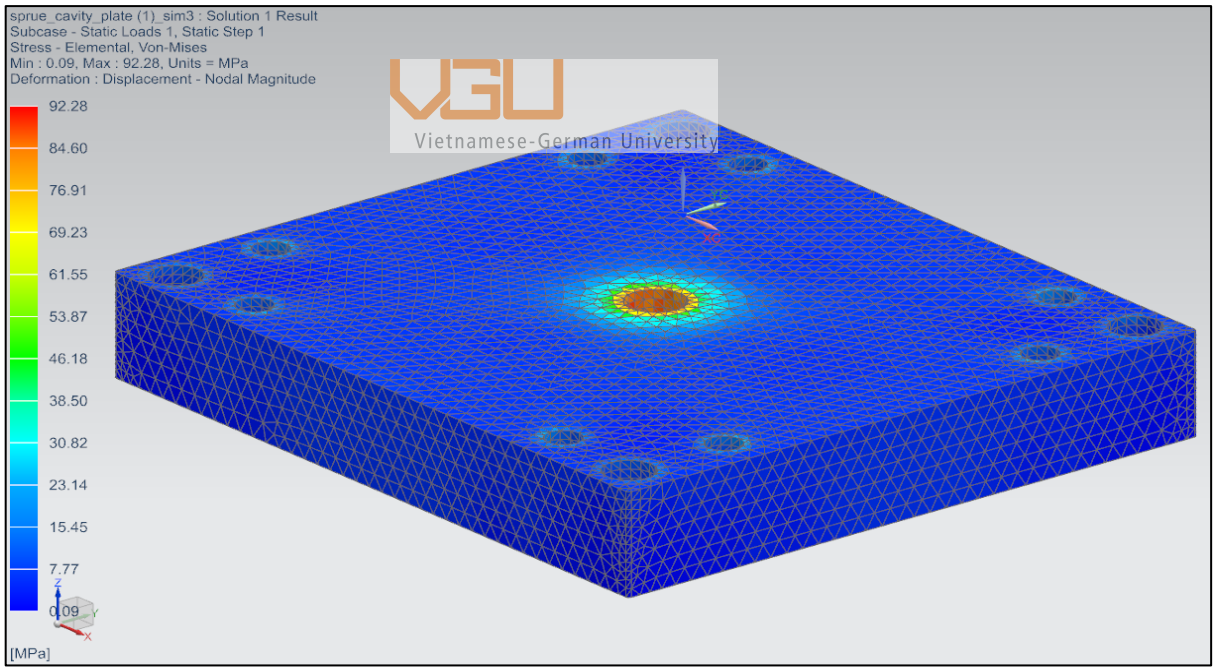

Figure 5-9: The von Mises stress on the runner plate

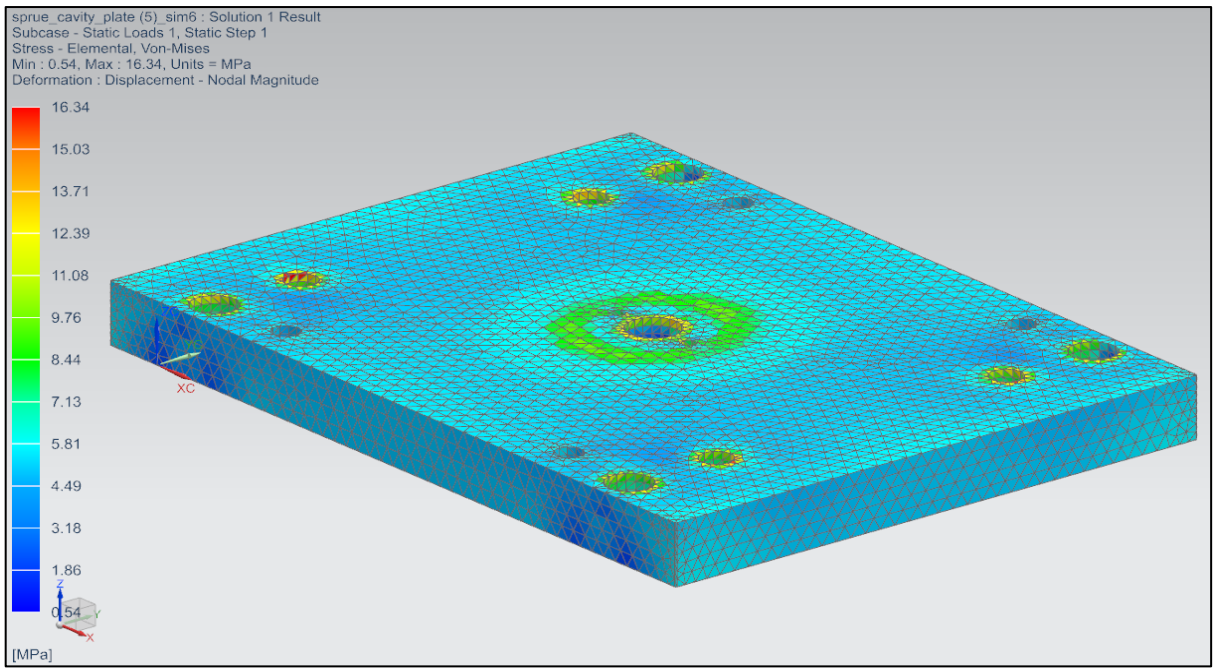

Figure 5-10: The von Mises stress on the top clamp plate

5.2.3. Plate bending analysis

Plate bending is a phenomenon that occurs when the plate is subjected to the load created by the clamping unit and/or the melt pressure acting on the mold cavities. Plate bending can generate the misalignment of the parting line, causing the excess plastic to form on the product at this location. This defect is called a "flash" of the injection molding process.

When a mold plate is fully supported by the plates underneath, the plates are uniformly compressed and plate bending is relatively small [10]. The bending value of each fully supported plate can be estimated with the following equations:

$$\sigma = \frac{F}{A_{compression}} \quad (5-2)$$

$$\varepsilon = \frac{\sigma}{E} \quad (5-3)$$

$$\delta = \varepsilon L \quad (5-4)$$

Where:

σ : compressive stress (MPa)

F : compression/clamp force (F = 212464 N)

$A_{compression}$: compressed area (m^2)

ε : the strain develops

E : the elastic modulus of the plate's modulus (GPa)

δ : amount of deflection

L : the height of the plate (mm)

The top and bottom clamp plate is mostly compressed by the clamping unit, where as the plates containing the mold cavity are also affected by the force generated by the melt pressure. This force varies dependedably on the area of each plate's cavity. Using the equations above, the estimated deflection result on each fully supported plate is recorded in the following table:

	Bottom clamp plate	Plate B	Plate A	Stripe plate	Runner plate	Top clamp plate
F (N)	424928	248118	386008	275121	212464	212464
$A_{compression}$ (mm^2)	52730	31732	33714	34132	34554	41766
σ (MPa)	8.05	7.82	11.4	8.06	6.15	5.09
E (GPa)	219	193	193	193	193	219
ε	3.68×10^{-5}	4.05×10^{-5}	5.93×10^{-5}	4.18×10^{-5}	3.18×10^{-5}	2.32×10^{-5}
L (mm)	30	30	51	20	30	20
δ (mm)	1.10×10^{-3}	1.21×10^{-3}	3.02×10^{-3}	8.35×10^{-4}	9.56×10^{-4}	4.65×10^{-4}

Table 5-1: The estimated deflection value of the fully supported plates

The plate bending values calculated by the program's FEM analysis are shown below:

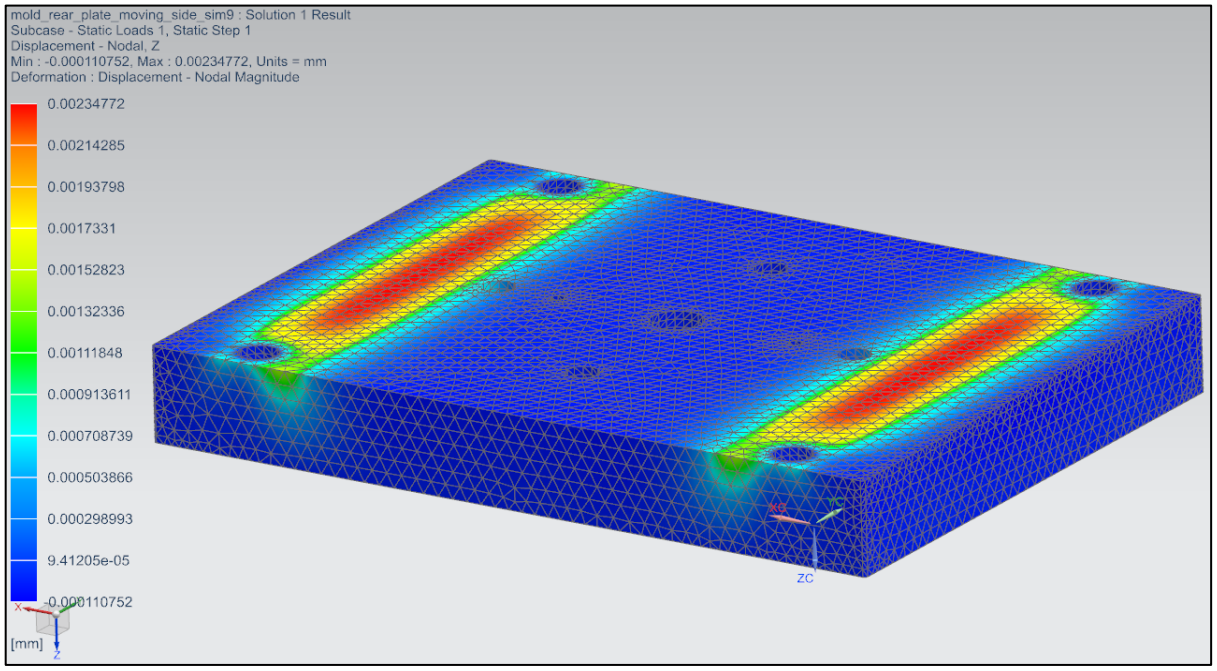

Figure 5-11: The bottom clamp plate's bending by compression

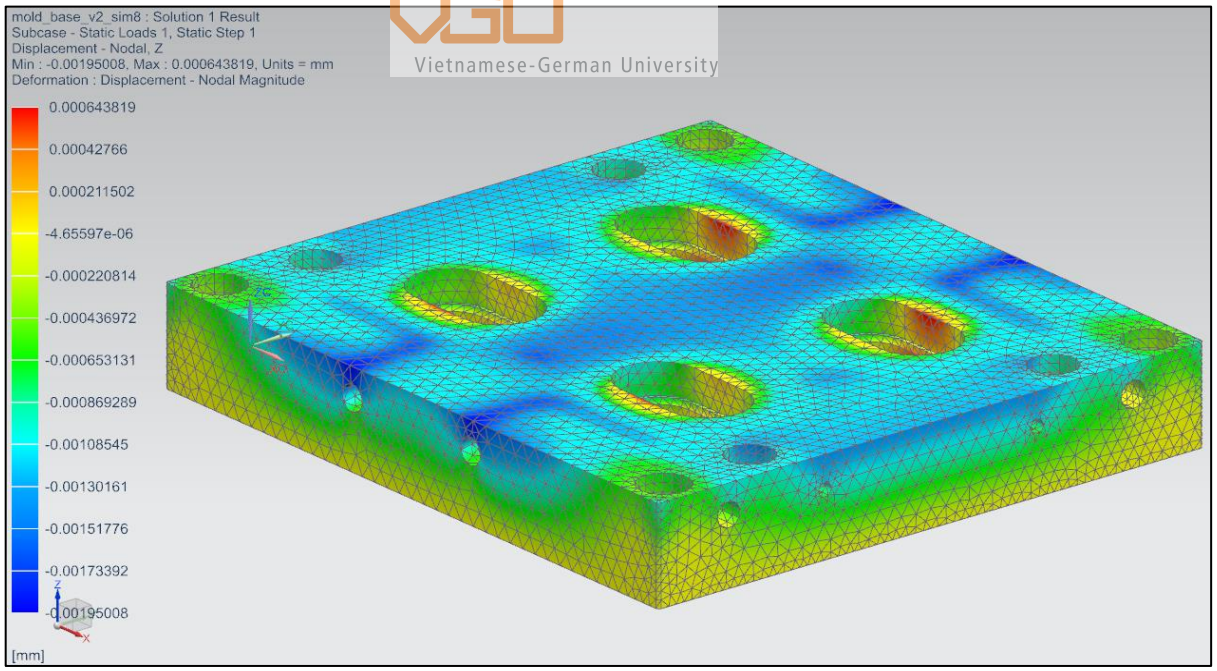

Figure 5-12: The plate B's bending by compression

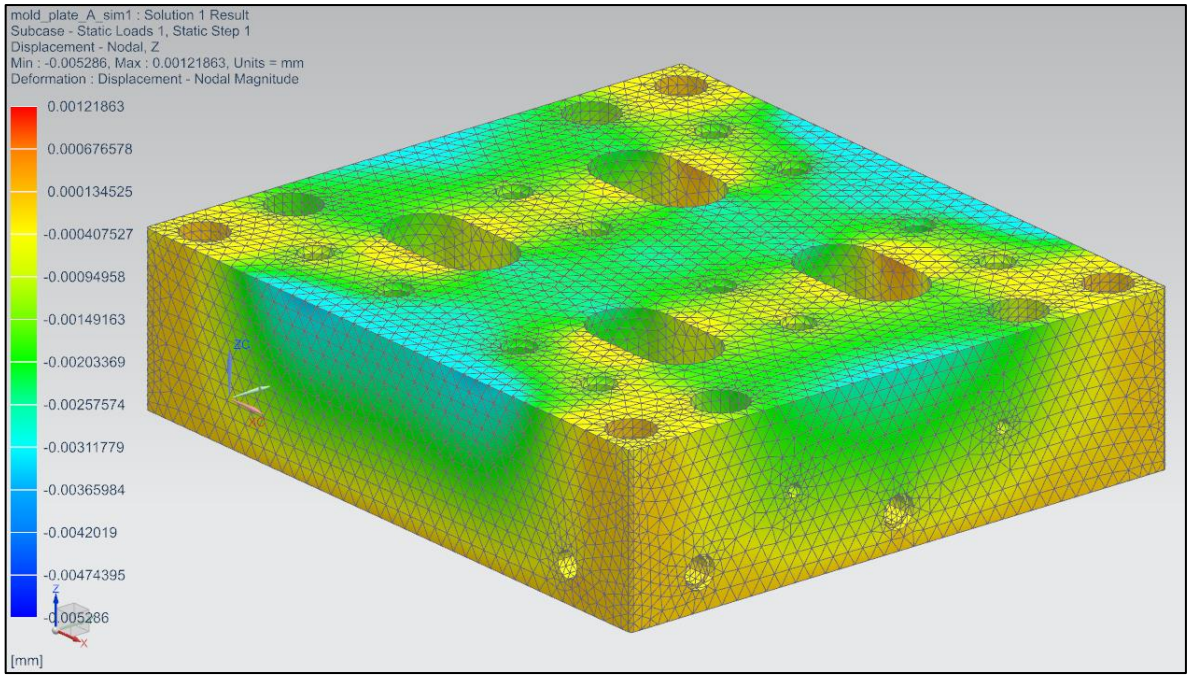

Figure 5-13: The plate bending by compression on the plate A

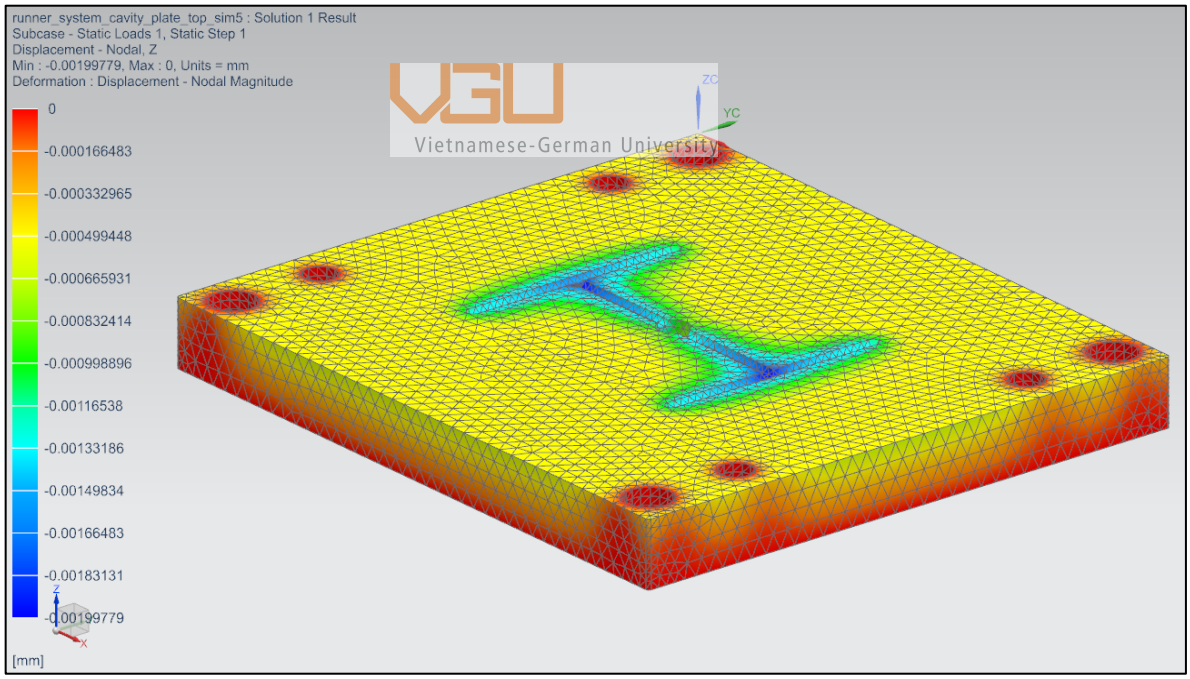

Figure 5-14: The plate bending by compression on the stripe plate

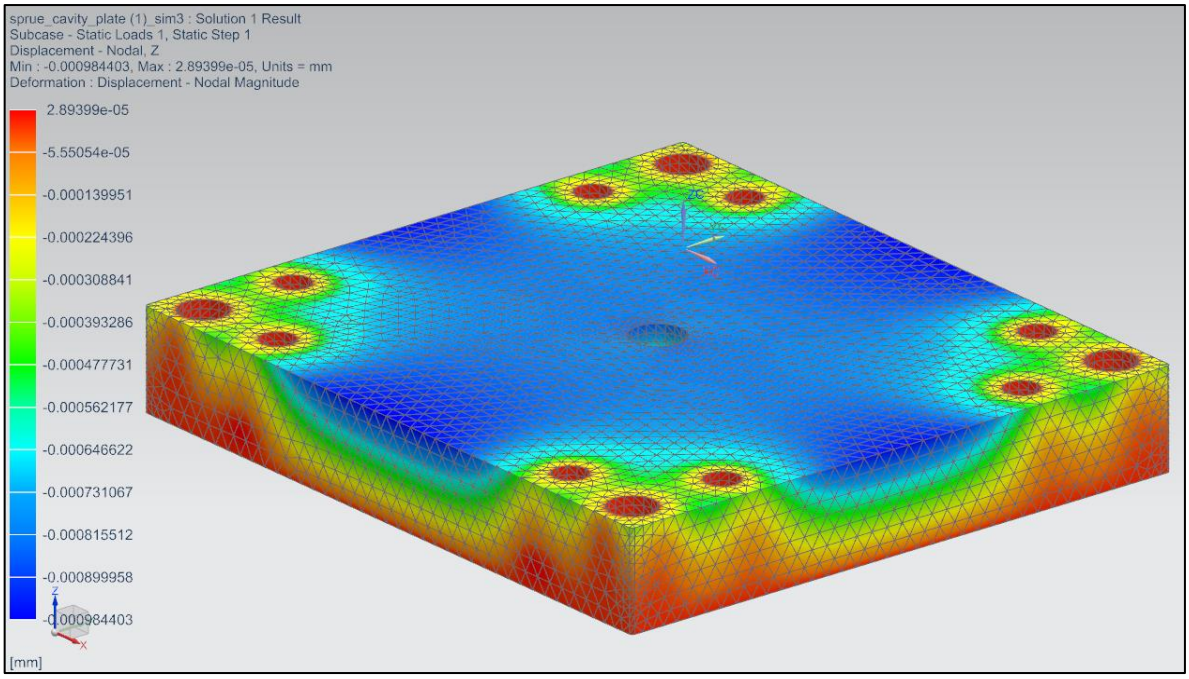

Figure 5-15: The plate bending by compression on the runner plate

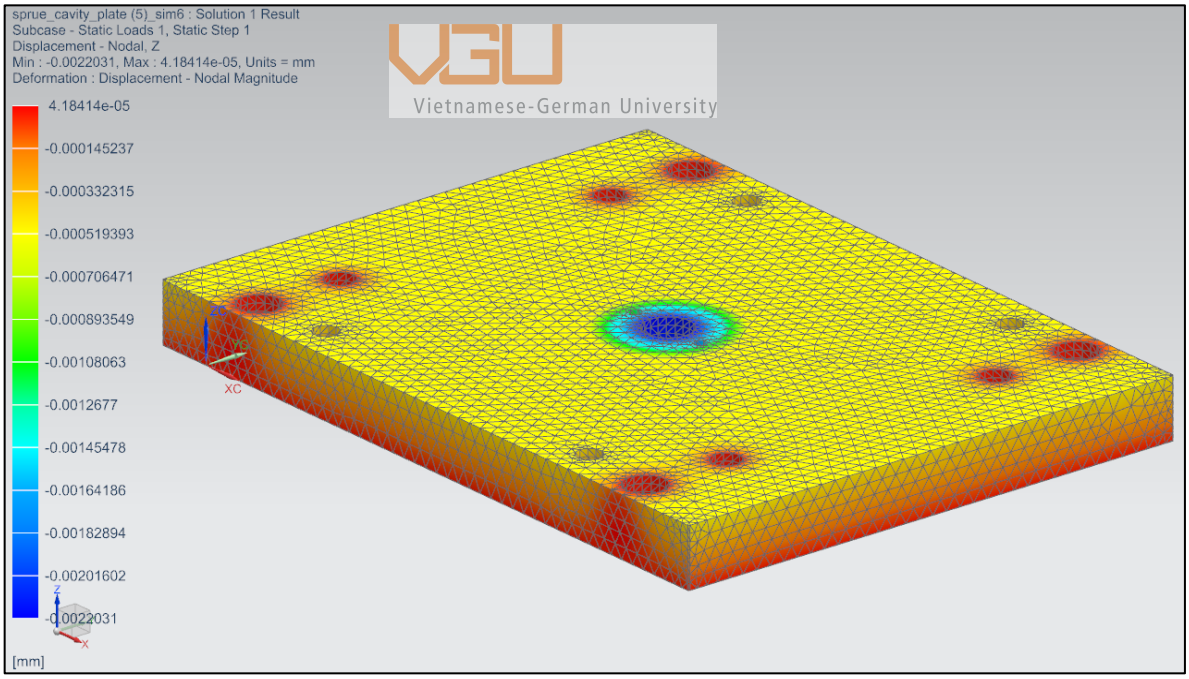

Figure 5-16: The plate bending by compression on the top clamp plate

The estimated and calculated values are different, but the former value correctly assesses the later value's order of magnitude. Both results suggest that the bending by compression is very small. For the not fully supported plates, the bending estimation is differently applied. In this case, the plate behaves like a beam, where large deflection develops across the long unsupported spans. The load is assumed to be applied to the center of the mold cross section to give a conservative estimate of the maximum deflection. [10]

The total deflection of the support plate is estimated using the beam bending equation with a central load:

$$\delta_{bending} = \frac{FL^3}{48EI} \quad (5-5)$$

Where:

L : the length of the unsupported span (L = 140 mm)

I : the moment of inertia

The central load applied on the support plate is the sum perpendicular forces acting on the support plate's face. These forces consists of the clamping force and the force generated by the melt pressure acting on the core inserts:

$$F = F_{clamp} + F_{melt\ pressure} = 212464 + 183960 = 396606\ N$$

The moment of inertia for the rectangular section is:

$$I = \frac{1}{12} WH^3 \quad (5-6)$$

Where:

W : the width of the mold section in bending (W = 180×10^{-3} m)

H : the thickness of the not fully supported plate (H = 36×10^{-3} m)

Hence, the bending of plate A is calculated as:

$$I = \frac{1}{12} \times 180 \times 10^{-3} \times (36 \times 10^{-3})^3 = 7 \times 10^{-7}\, m^4$$

$$\delta_{bending} = \frac{396606 \times (140 \times 10^{-3})^3}{48 \times (219 \times 10^9) \times 7 \times 10^{-7}} = 1.48 \times 10^{-4}\, m = 0.148\, mm$$

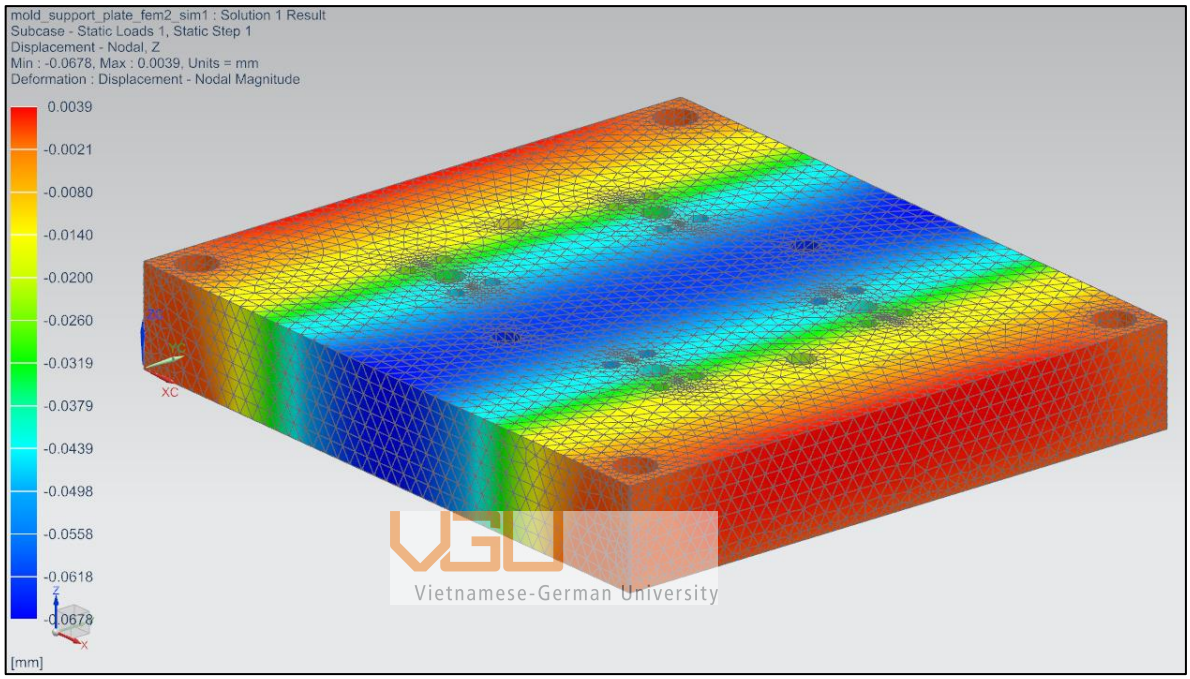

Figure 5-17: The bending value of the support plate

The estimated and calculated result implies that the former result is more than twice the later result. Due to the estimated result is calculated by assuming the total load to be a single load located at the center of the plate, rather than being a uniformly distributed load. Therefore, the estimated result is an over-predicted result which provides a robust plate design. The program calculated result indicates that the support plate deflects by 0.0678 mm downward at the middle of the plate. However, this value is too small to effect core inserts situated on top of the plate. [10]

The detailed 2D drawing of the mold plates are as follows:

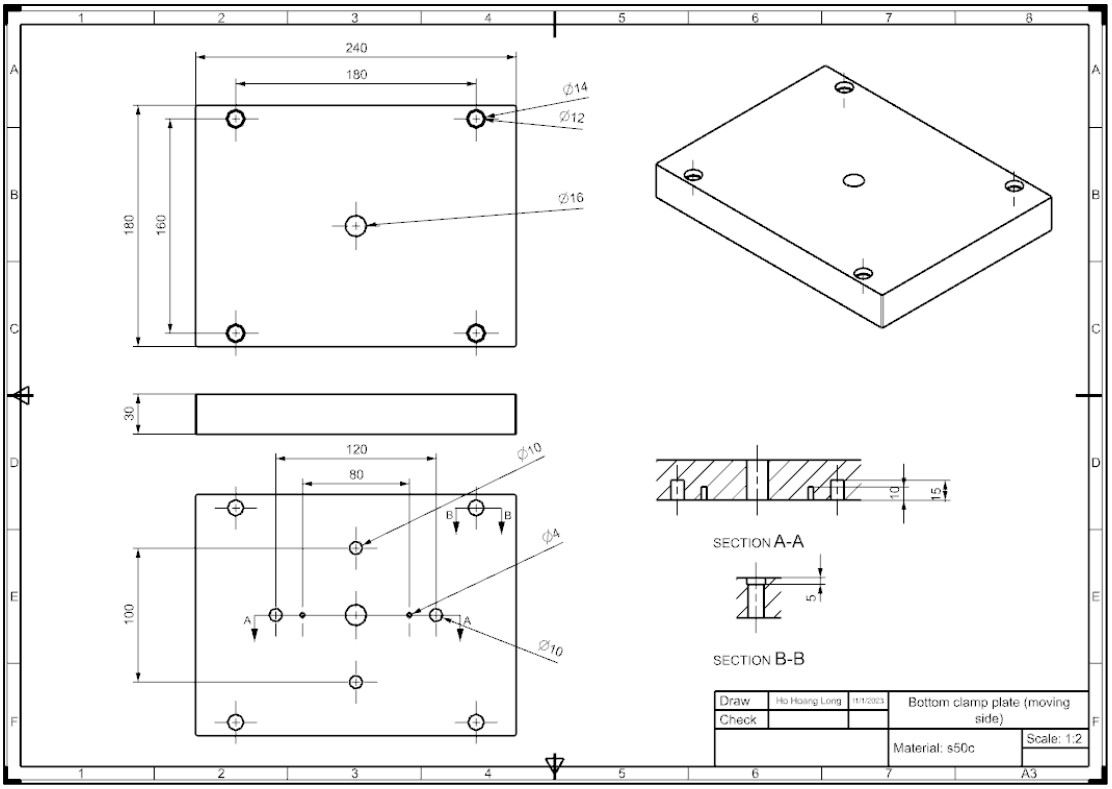

Figure 5-18: The bottom clamp plate

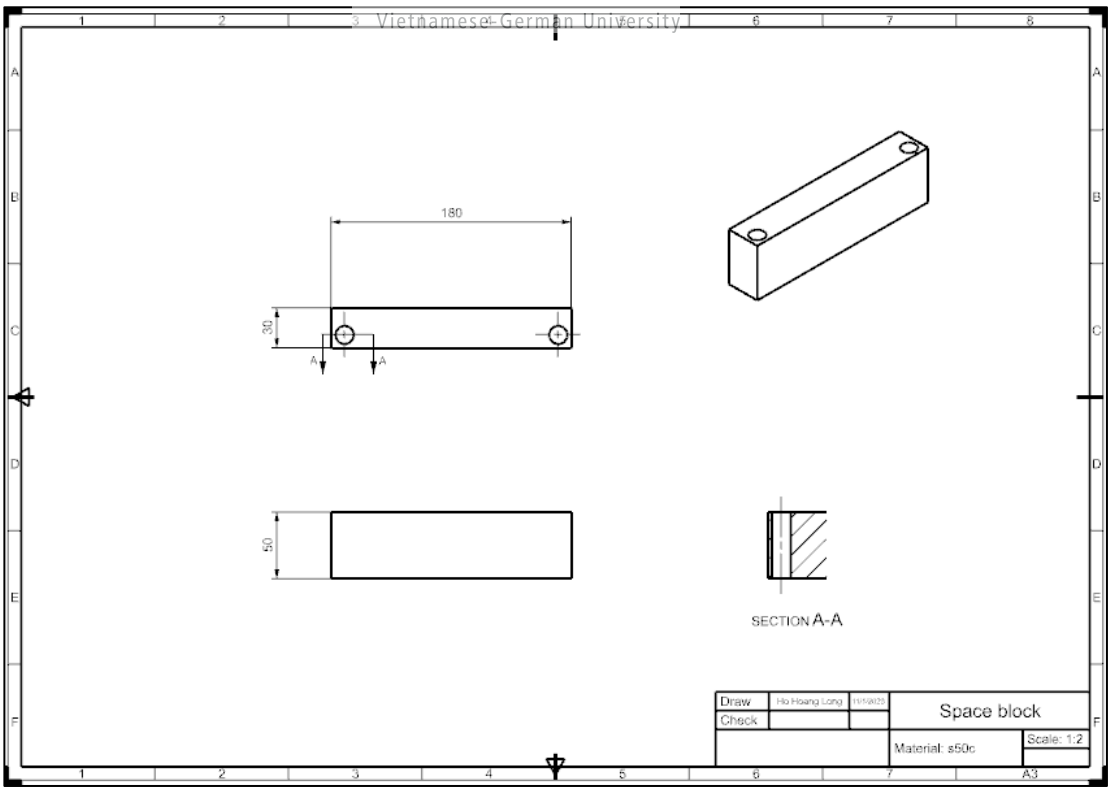

Figure 5-19: The space block

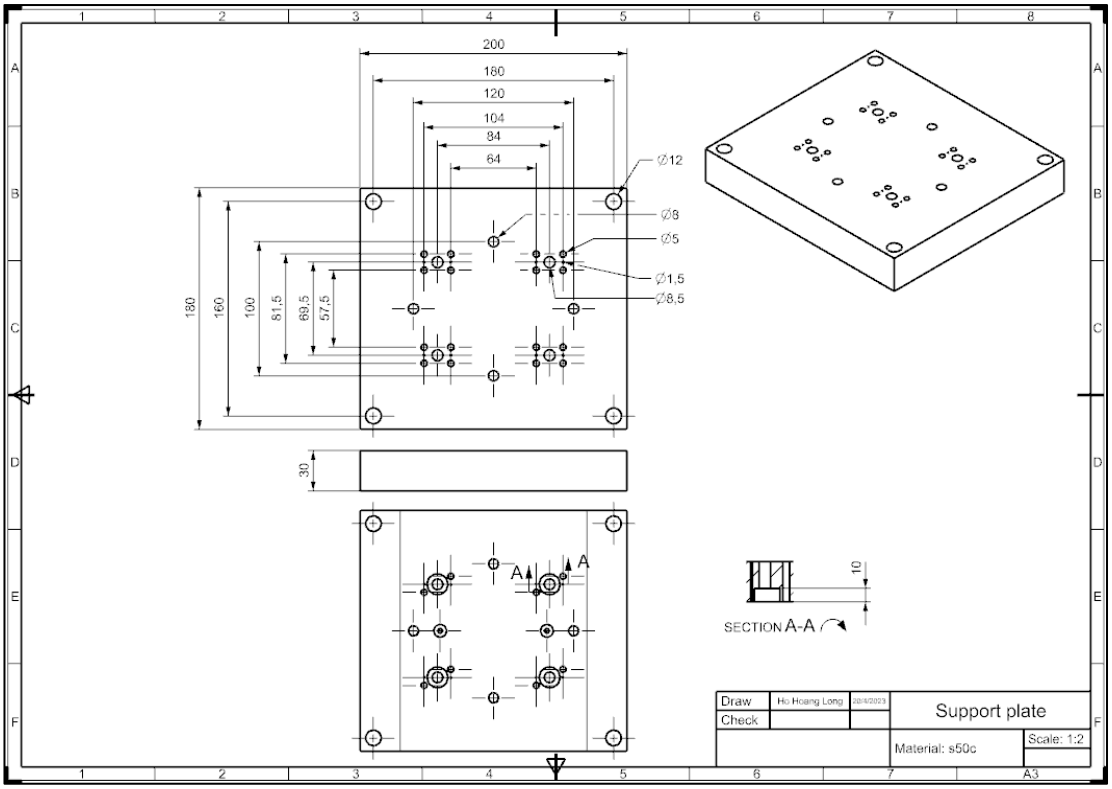

Figure 5-20: The support plate

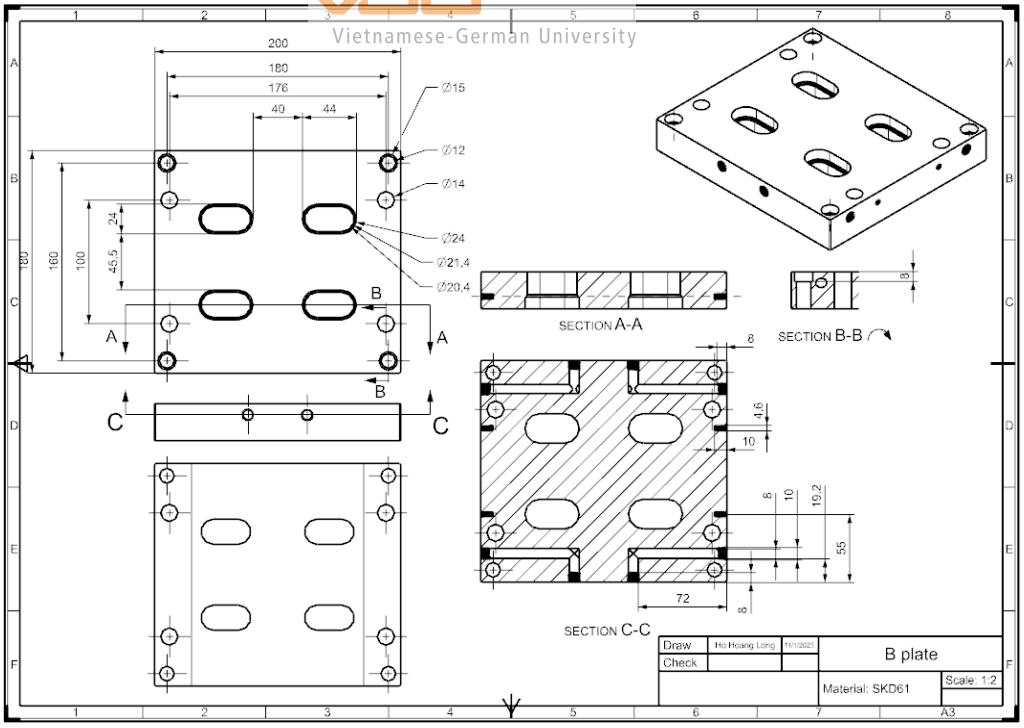

Figure 5-21: The plate B

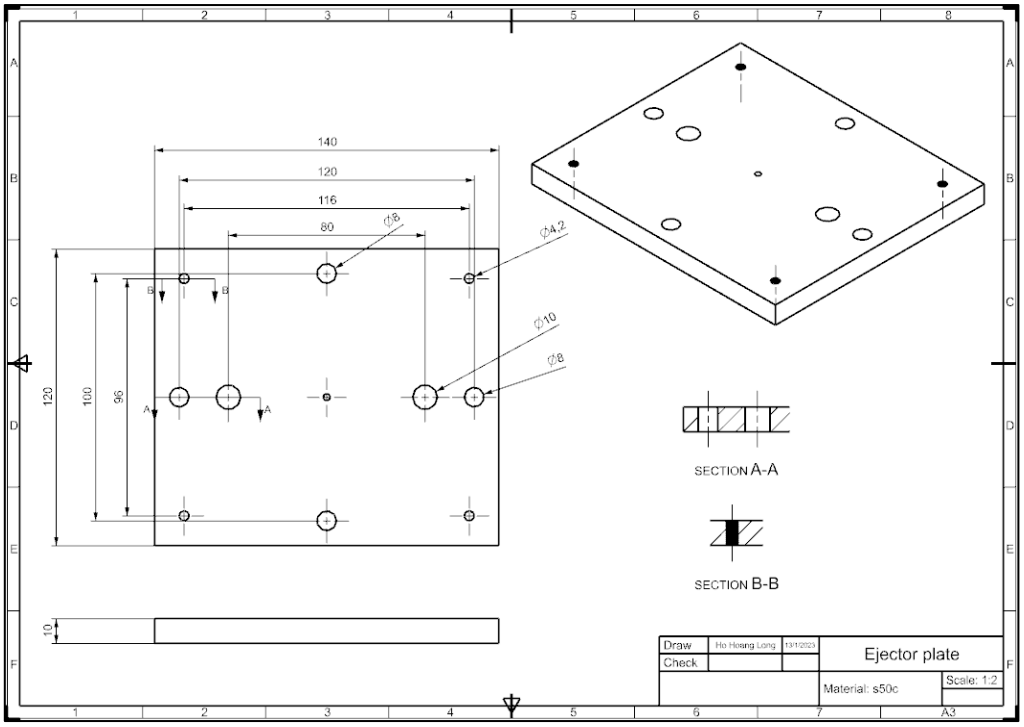

Figure 5-22: The ejector plate

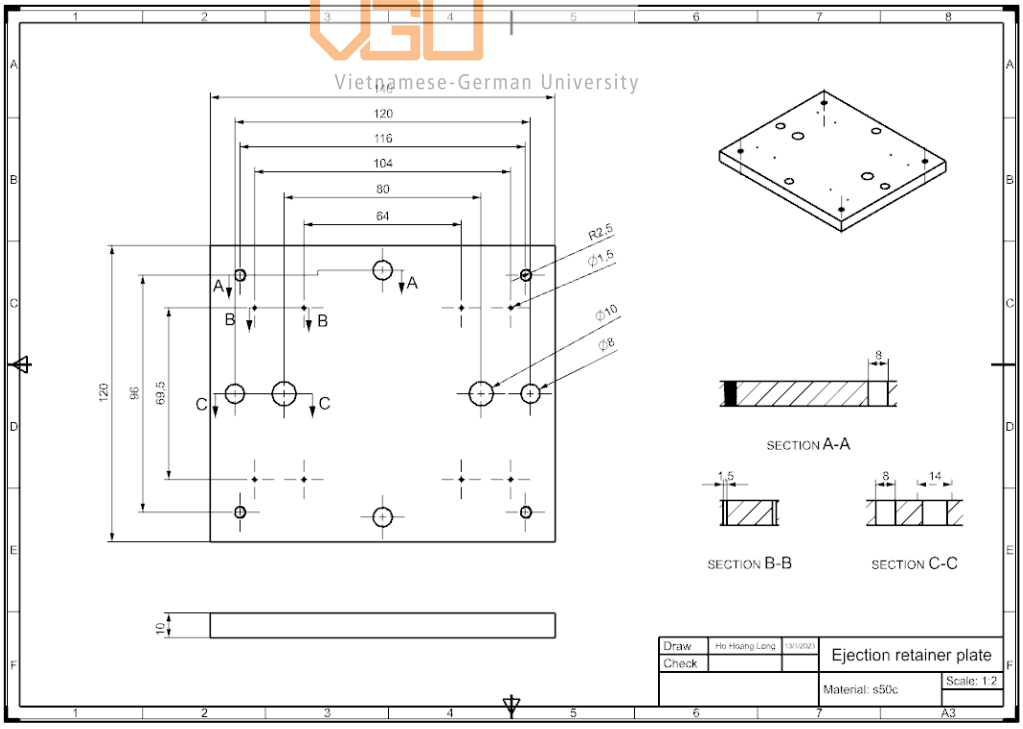

Figure 5-23: The ejector retainer plate

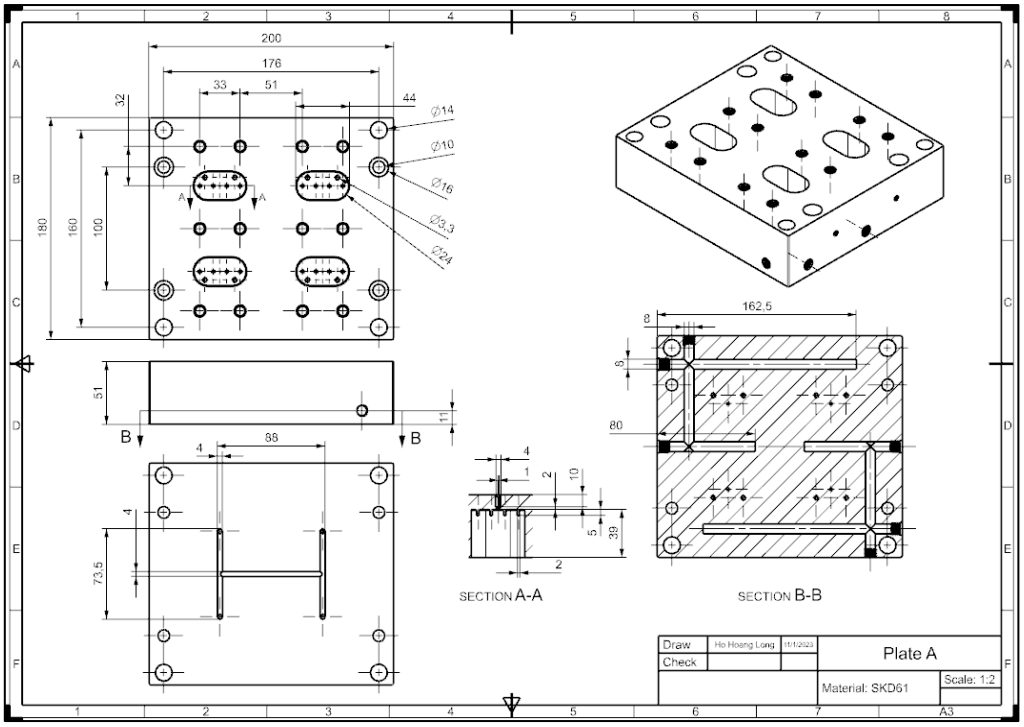

Figure 5-24: The plate A

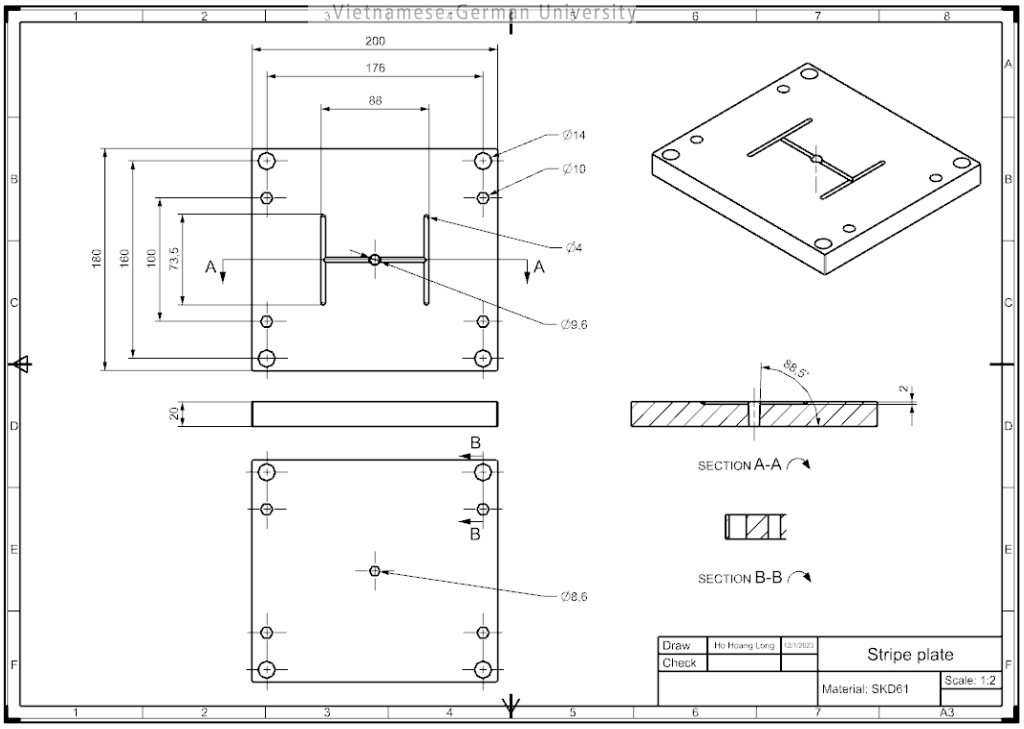

Figure 5-25: The stripe plate

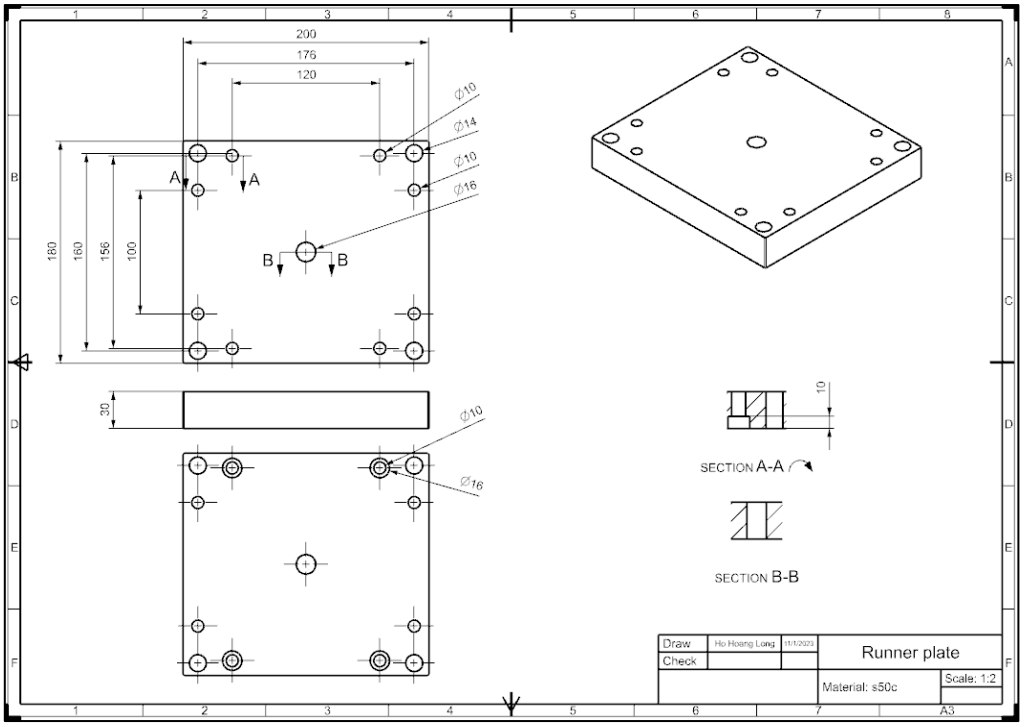

Figure 5-26: The runner plate

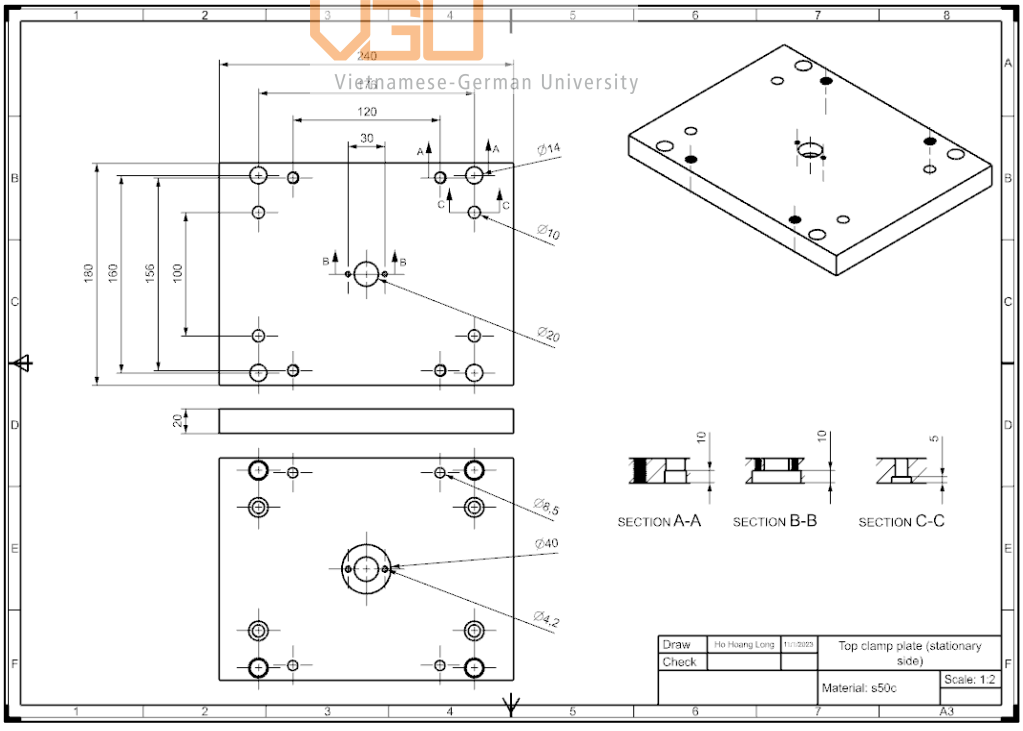

Figure 5-27: The top clamp plate

5.3. Designing the ejector pins

Due to volumetric shrinkage, the molding products generally adhere to the mold cores. The products then must be manually separated from the core, reducing the production efficiency. The automated solution provided by the ejection system is now a requirement for most mold designs.

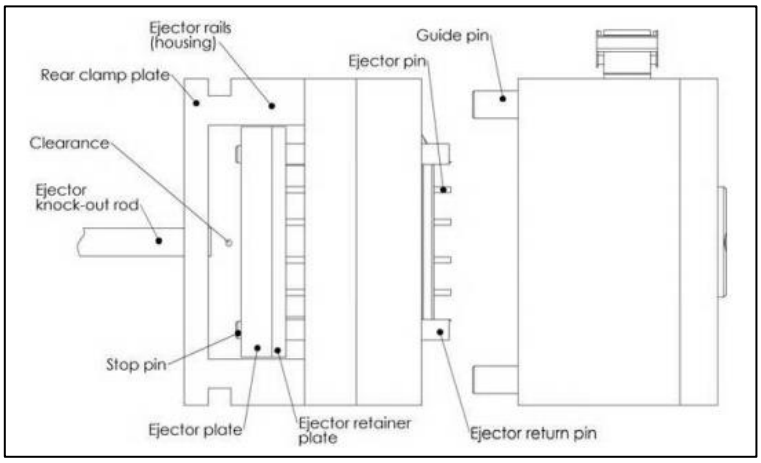

Figure 5-28: The side view of the ejection system

An ejection system generally consists of an ejection plate, an ejector-retainer plate, ejector pins, stop pins, guide pins, return pins and other components. Among these parts, the ejector pins directly contact the product to push it out of the core. Therefore, they have to be designed to be able to push without damaging the product.

5.3.1. Calculating the ejector pin's push area and perimeter

Since the mold products are ejected with the forces applied by the ejector pins, the ejection force is estimated to prevent damaging the products. The ejector pins are subjected to shear and compressive force during the ejection phase, so a poorly designed pin tends to break [10].

The ejection force required to strip the plastic product from the core can be estimated with the following equation:

$$F_{eject} = \mu_s . \cos(\phi) . E . CTE . \left(T_{solidification} - T_{ejection}\right) . A_{eff} \quad (5-7)$$

Where:

μ_s : coefficient of friction

ϕ: the draft angle

E: strain develops with the material at its room temperature modulus

CTE: coefficient of thermal expansion

$T_{solidification}$: solidification temperature

$T_{ejection}$: ejection temperature

A_{eff}: effective area

To estimate the ejection force, the aforementioned parameters have to be assumed or obtained from the CAD drawing, the results of the fill analysis, the material mechanical and thermal properties table. The coefficient of friction of PC plastic is 0.31, the draft angle of the product is 1° according to the CAD drawing. The thermal expansion coefficient is 6.5×10^{-5} 1/°C, the solidification temperature is 143°C, and the ejection temperature is 80°C. These parameters are taken from Appendix A of the book "Injection Mold Design Engineering".

The effective area of each LED base can be assessed from the CAD as 199.8 mm^2. The estimated ejection force is:

$$F_{eject} = 0.31 \times \cos(1°) \times 2.28 \times 10^9 \times 6.5 \times 10^{-5} \times (143 - 80) \times 199.8 \times 10^{-6}$$

$$F_{eject} = 578.2$$

The compressive stress levels must be lower than the critical stress threshold, $\sigma_{fatigue\ limit}$ to avoid fatigue and buckling of the pins. This value depends on the material and the treatment of the pins. A conventional mold design can assume a lower fatigue limit of 450 MPa for P20 steal instead of the hardened steels with the value reaching the order of 800 MPa. [10]

To calculate the total push area of the ejector pins to eject each molding product from a core, the following equation is used:

$$A_{ejector\ pins} > \frac{F_{eject}}{\sigma_{fatigue\ limit}} \quad (5-8)$$

Where:

$A_{ejector\ pins}$: total area of the ejector pins (mm^2)

F_{eject}: required ejection force (N)

$\sigma_{fatigue\ limit}$: stress limit (Pa)

From the required ejection force is 578.2 N, the stress limit is 450 MPa, the total area of the ejector pins is:

$$A_{ejectors} > \frac{578.2\ N}{450\ MPa} = 1.28 \times 6\ m^2 = 1.28\ mm^2$$

Each LED base is separated from the core by 2 ejector pins. Using the minimum total area of the pins, the minimum diameter of each pin is calculated as:

$$D_{min,pin} > \sqrt{\frac{(4 \times 1.28\ mm^2)/\ 2\ pins}{\pi}} = 0.90\ mm$$

The result implies that the appropriate diameter for each ejector pin must be larger than 0.90 mm to not damage the product. The standardized straight ejector pin provided by MISUMI has the value ranges from 1 mm to 30 mm in diameter. This diameter should not be too large to avoid conflicting with the cavities on the core. Hence, the chosen ejector pin's diameter is assumed to be 1 mm.

Because the pins are directly contact with the molten melt during the molding process, expansion and contraction due to either heat, fatigue and impact mold separation resistance during ejection requires a safety factor to be taken into consideration. The safety factor for the ejector pin is calculated by:

$$S = \frac{P}{P_1} \quad (5-9)$$

Where:

S : safety factor

P : buckling strength of an ejector pin (kgf)

P_1 : compression load applied to the ejector pin during filling and packing phase (kgf)

The buckling strength of an ejector pin can be calculated with the Euler's formula:

$$P = n\pi^2 AE(\frac{K}{L})^2 \quad (5-10)$$

Where:

n: terminal condition constant for straight pin (n = 4)

A: cross section (A = $\frac{\pi \times d^2}{4}$ = $\frac{\pi \times 1^2}{4}$ = 0.78 mm^2)

E: modulus of longitudinal elasticity (21000 kgf/mm^2)

K: radius of gyration of area (K = d/4 = 1/4 = 0.25)

L : total length of the ejector pin (L = 107.4 mm)

$$P = 4 \times \pi^2 \times 0.78 \times 21000 \times (\frac{0.25}{107.4})^2 = 5.95\ kgf$$

The compression load to the ejector pin is calculated as:

$$P_1 = p \times A \quad (5-11)$$

Where:

p : internal cavity pressure (p = 45.45 MPa = 4.55 kgf/ mm^2)

A : cross section (A = 0.78 mm^2)

$P_1 = 4.55 \times 0.78 = 3.55\ kgf$

Comparing the two results, the pin's buckling strength is lower than compression load, possibly leading to deformation. Therefore, the area of the pin is increased to 1.5 mm to overcome the load.

$$P = 4 \times \pi^2 \times 1.77 \times 21000 \times (\frac{0.25}{107.4})^2 = 7.95\ kgf$$

The values above imply that the safety factor is:

$$S = \frac{7.95}{3.55} = 2.24$$

With the safety factor calculated, the required diameter of each pin is recalculated as:

$$F_{eject} = 578.2 \times 2.24 = 1295.17\ N$$

$$A_{ejectors} > \frac{1295.17\ N}{450\ MPa} = 2.88 \times 10^{-6}\ m^2 = 2.88\ mm^2$$

$$D_{min,pin} > \sqrt{\frac{(4 \times 2.88\ mm^2)/\ 2\ pins}{\pi}} = 1.35\ mm$$

This result implies that the 1.5 mm in diameter pin is sufficient withstand the compressive load and does not damage the product.

5.3.2. Ejector pin modeling process

To ensure that the ejector pin do not extrude from the core before the ejection phase, the total length of the ejector pin is designed to be 137.4 mm. Using NX 12, the ejector pin model is created based on the 2D drawing provided by MISUMI:

- Drawing 2 circles with the sketch tool. One circle is 1 mm in diameter, and the other is 3 mm in diameter. The circle is drawn on a 2-dimensional XY-plane designated by the program.
- The extrusion tool is used to create the cylindrical shape of the ejector pin. The extrusion distance is 82.4 mm.
- The head of the ejector pin is created with the extrusion tool. The extrusion distance is 4 mm.

The ejector pin from MISUMI has two options of the total length: 100 mm and 150 mm. To obtain the desired total length of 137.4, the 150 mm ejector pin needs to be modified.

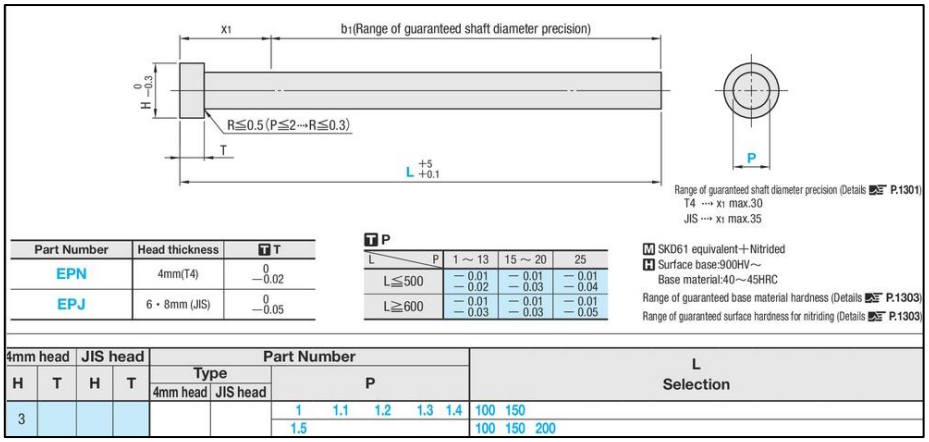

Figure 5-29: Ejector pin's dimension provided by MISUMI

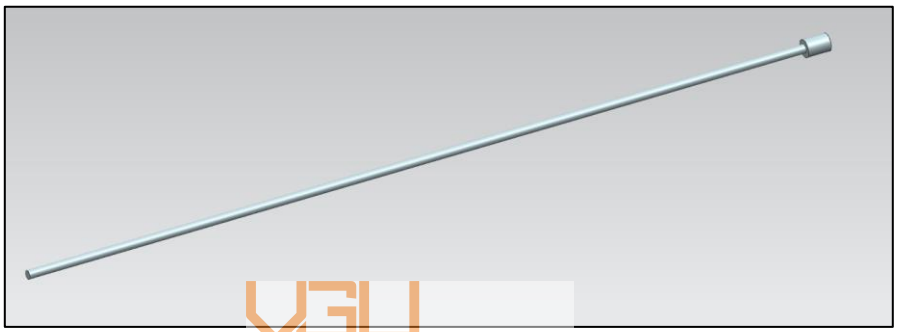

Figure 5-30: The Isometric view of the ejector pin model

5.4. Designing the core insert

The core and the cavity form the shape of the product and define the wall thickness. Plastic melt flows into the space between the core and cavity to form the wall of the product. Therefore, the cavity's depth is equal to the sum of the core's height and the product wall's thickness.

The core forms the LED base cover's hollow interior by preventing the melt from entering that space. To form the screw pillars' shape, there are two cylindrical cavities on each core. Each guide pillar's wall is form by the melt occupying the space between the core's cylindrical cavities and the cylindrical core attached to the A plate's cavity.

For easier ejection, the core is designed to have a 1-degree draft angle. The draft angle is necessary because the plastic inside the mold shrinks as it cools and solidifies. The shrinkage makes it more difficult to eject, and the part's wall rubs against the mold's interior, possibly leading to warpage. The cores are also designed to be able to be separated

from the B plate. During assembly and molding process, they are secured to the B plate with dowel pins. [20]

5.4.1. Core insert modeling process

The mold core is created by:

- Draw the 2D sketch of the core. Use the rectangle, circle sketch tool, and trim tool to create the contour of the core.
- Extrude the sketch to create a 3D body with the extrusion tool. The extrusion distance is 37.4 mm with a 1-degree draft angle. This distance ensures that when the core is attached to the A plate, it creates a space between the core and the cavity to form the wall thickness during the mold's closure.
- The holes are created with extrusion tool.

5.4.2. Core insert stress analysis with NX

The core insert's fatigue and deformation caused by the acting melt pressure are determined with the same FEM analysis provided by the program. Two important results to be considered are the von Mises stress and the displacement. Because the core directly determines the product's shape, the aforementioned results should not surpass their respective limit values to avoid altering with the final product's dimension.

Because the core requires a high fatigue limit and elastic modulus value, strong material such as SKD61 is chosen. The acting pressure reaches 45.6 MPa at the bottom face and reaches 45.4 at the body. The same steps are proceeded to conduct the program's FEM analysis:

- Assign the material (SKD 61)
- Select the 3D tetrahedral mesh
- Assign the fixed constraints and the simply supported constraint
- Apply the melt pressure

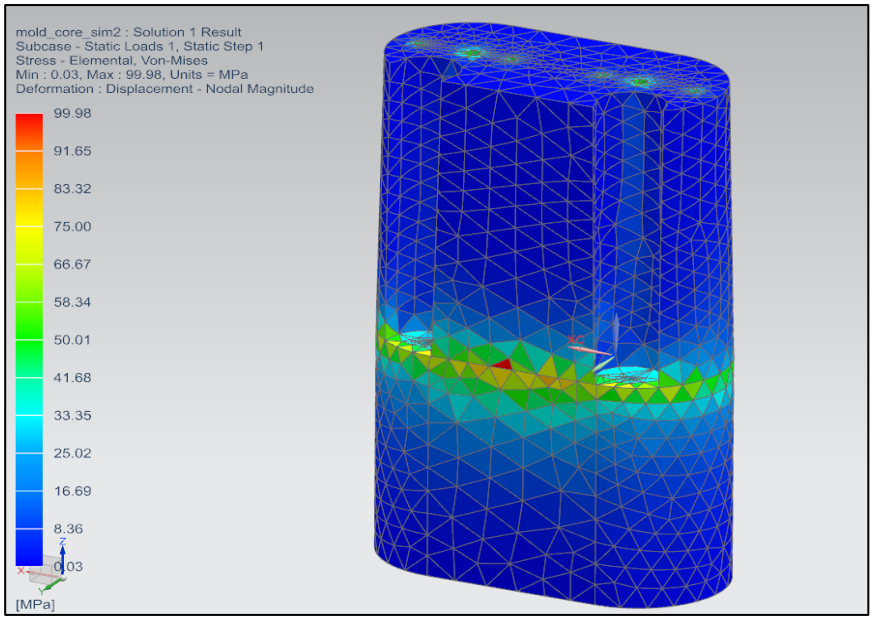

Figure 5-31: The von Mises stress result of the core

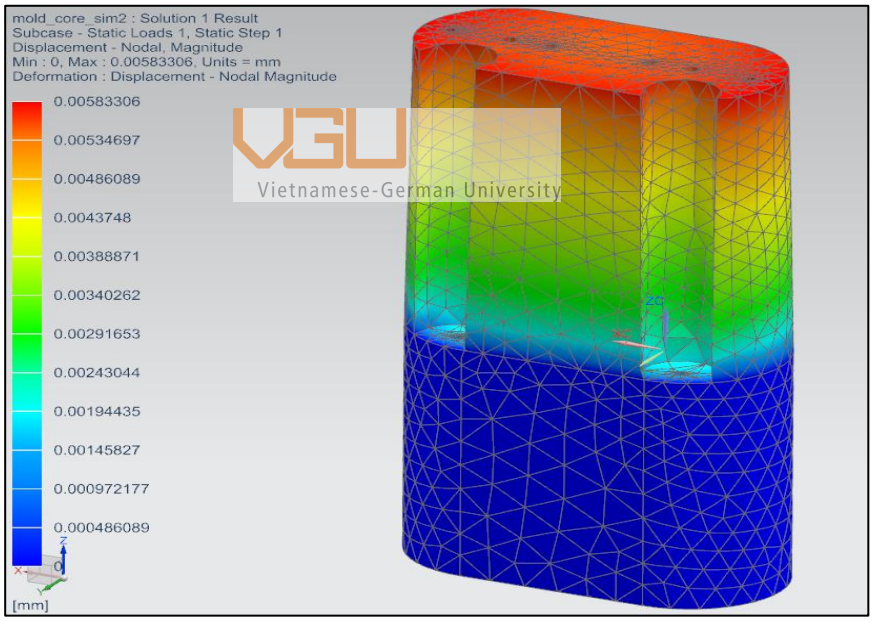

Figure 5-32: The displacement result on the core

The von Mises stress on the core reaches 100 MPa, which is within the stress limit σ_{limit} ranges from 666.7 to 920 MPa. This implies that the core would not experience failure as a result of the acting pressure. The displacement result suggests that deformation only reaches 0.005 mm at the top of the core insert, which is too small to affect the required dimension of the product.

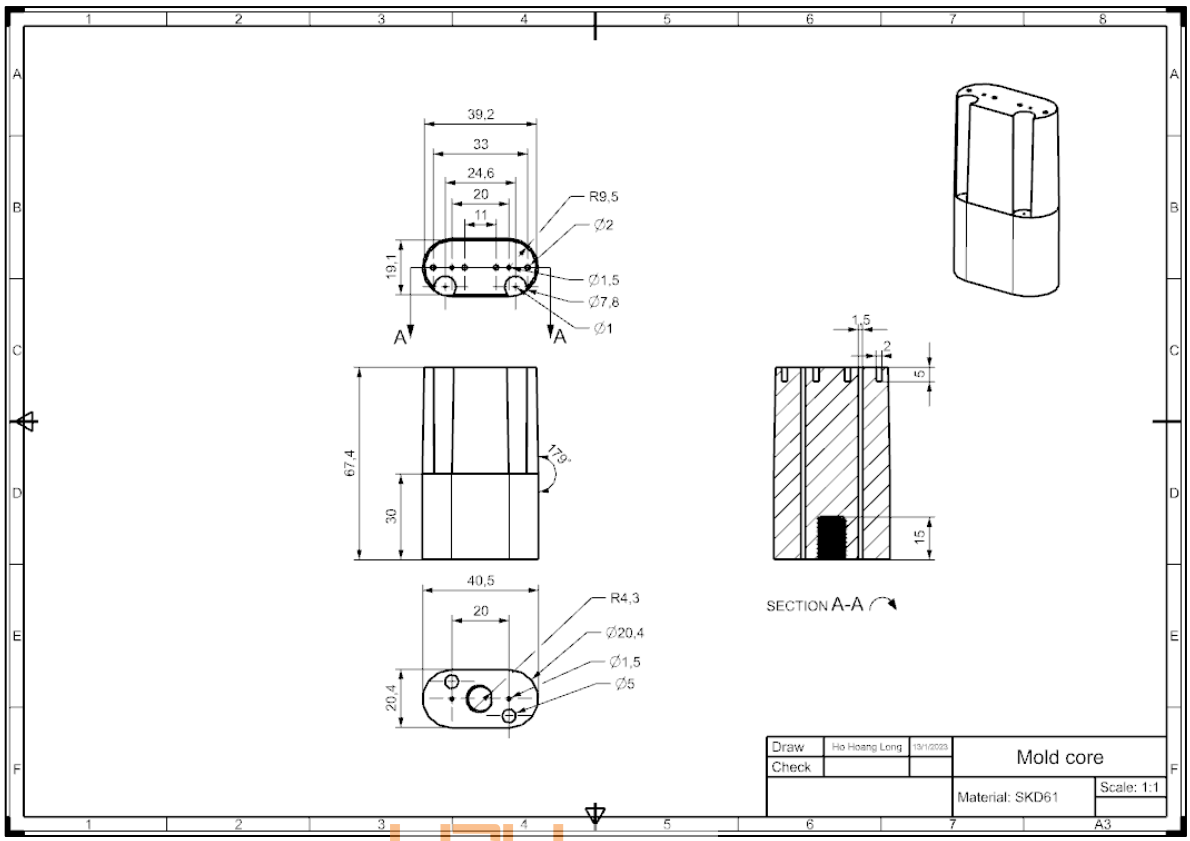

Figure 5-33: The 2D projection views of the mold core

5.5. Selection of the spring for the ejection system

The springs are used to return the ejector plates and pins to their original position at the end of the ejection phase. When the ejector knock-out rod is retracted, the springs decompress, pushing the ejector plates to their original position. The spring's capacity must be capable of overcoming the friction force of the relating ejector plates. For example, the springs of the runner ejector system has to overcome the friction force of the runner ejector support plate and the runner ejector retainer plate against the inner side of the housing plates.

Generally, the die spring is used for injection molding for its capability to support heavy loads in harsh environments, where excessive heat and pressure occurs. The die spring is suitable for application where high force is required, and the installation space is limited. Its capacity is categorized into different color by each manufacturer, depending on the load capacity. A uniform color coded might not be concurred by many producers. Hence, it is advised that a reference card of a particular manufacturer is used.

The ejector system uses two die springs placed between the ejector plates and the A plate. To prevent each spring from dislocating from its position, a spring guide pillar is placed concentrically inside a spring. The friction force of the ejector support plate and the ejector retainer plate can be calculated with the following equation:

$$f = \mu_{steel} \times N \quad (5-12)$$

Where:

f : The friction force (N)

μ_{steel} : steel's coefficient of friction

N : normal force (N)

The normal force in this situation is equal to the total weight of the ejector plate, the ejector retainer plate. The total weight of the two plates can be obtained by multiplying the material's density with the total volume of the plate, because the plates are made of the same material. The total volume of the two plates can be obtained with the measuring tool provided by the NX 12 program. The total weight of the two plates is:

$$V_{total,plates} = V_{ejector\ plate} + V_{ejector\ retainer\ plate}$$

$$= 163.3 + 163 = 326.3\ cm^3$$

$$m_{ejector\ plates} = \rho_{s50c} \times V_{total,plates} = 7.7\frac{g}{cm^3} \times 326.3\ cm^3 = 2512.51\ g = 2.51\ kg$$

The total mass of the ejector pins is relatively small compared to the total mass of the ejector plates. However, it contributes to the total weight that the die springs must push.

$$V_{total,pins} = 8 \times 0.21 = 1.68\ cm^3$$

$$m_{ejector\ pins} = \rho_{SKD61} \times V_{total,pins} = 7.85\frac{g}{cm^3} \times 1.68\ cm^3 = 13.18\ g = 0.01\ kg$$

$$N = W_{total} = m_{total} \times 9.81 = (2.51 + 0.01) \times 9.81 = 24.72\ N$$

Hence, the friction force is equal to:

$$f = \mu_{steel} \times N = 0.7 \times 24.72 = 17.3\ N$$

Since the springs does not directly support the total weight of the plates, but horizontally push the plates back. Hence, the load on the spring is not severe. Assuming that the spring supplier provides with spring made of reliable material, the recommended safety factor is 2.5. The new friction force is:

$$f = 17.23 \times 2.5 = 43.25\ N$$

Therefore, the required spring capacity is:

$$f_{spring,runner\ ejector\ system} = \frac{43}{2} = 21.5\ N$$

According to the datasheet provided by the manufacturer named Raymond, the suitable spring for the runner ejector system is the ASF 8x50 in the extra light load spring category. This spring is capable of enduring the load equal to 58.8 N to achieve the optimal functional life. Another important parameter to be considered is the dimension of the spring. The spring inner diameter must be approximately equal to the guide pillar's diameter. A large difference between the two diameters generates kinking, and causes spring failure. Since the guide pillar's diameter is equal to 4 mm, it is tightly fit inside the ASF 8x50 spring, restricting the spring from kinking during ejection.

Raymond®	EXTRA LIGHT DUTY DIE SPRINGS			JIS B 5012 Series				Yellow	
Outer Dia (mm)	Inner Dia (mm)	Free Length (mm)	Catalog Number	Load at 1mm Def. (kgf)	LOAD DEFLECTION TABLE					
					For Maximum Operating Def. (50%of free length)		For Long Life (45% of free length)		For Optimal Life (40% of free length)	
					Deflection (mm)	Load kgf (N)	Deflection (mm)	Load kgf (N)	Deflection (mm)	Load kgf (N)
A	B	C								
8	4	10	ASF 8 X 10	1.56	5.0	8 (78.5)	4.5	7 (68.6)	4.0	6 (58.8)
		15	ASF 8 X 15	1.04	7.5		6.8		6.0	
		20	ASF 8 X 20	0.78	10.0		9.0		8.0	
		25	ASF 8 X 25	0.62	12.5		11.2		10.0	
		30	ASF 8 X 30	0.52	15.0		13.5		12.0	
		35	ASF 8 X 35	0.44	17.5		15.7		14.0	
		40	ASF 8 X 40	0.39	20.0		18.0		16.0	
		45	ASF 8 X 45	0.35	22.5		20.2		18.0	

Table 5-3: The spring technical datasheet provided by Raymond manufacturer

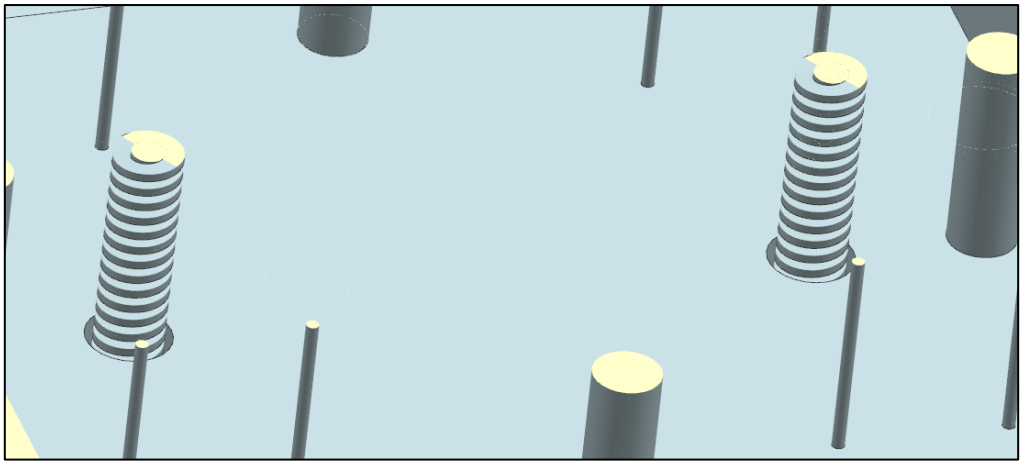

Figure 5-34: The die springs in the ejection system

5.6. Plastic injection mold assembly model

When all of the mold components are designed, analyzed and selected, the components are assembled into a single mold to represent the final result of the designing process. The assembly view helps the designer inspect for design problems such as colliding components, and misalignment of the guide holes. The exploded view of the 3D model, and the section view in the 2D draft visualizes the internal cavities of the mold, which is hidden inside the mold plates.

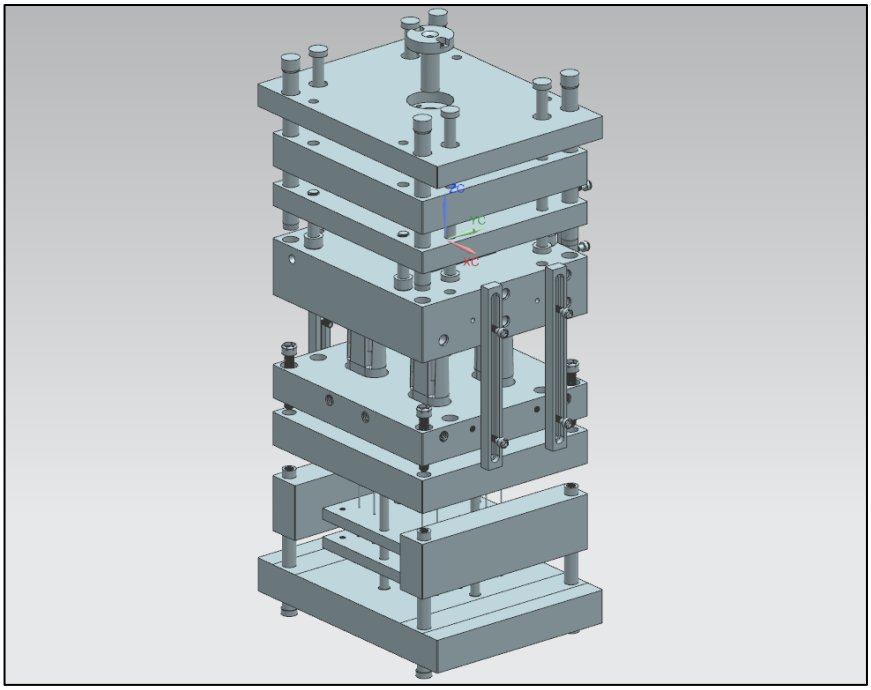

Figure 5-35: The exploded view of the plastic injection mold model

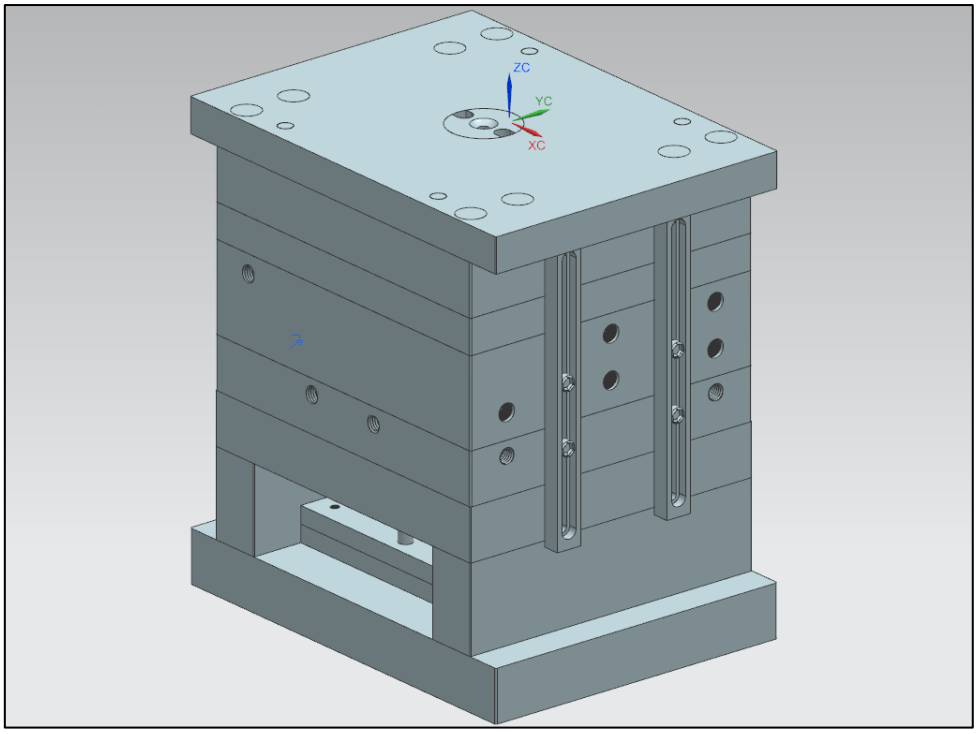

Figure 5-36: The assembly model of the plastic injection mold

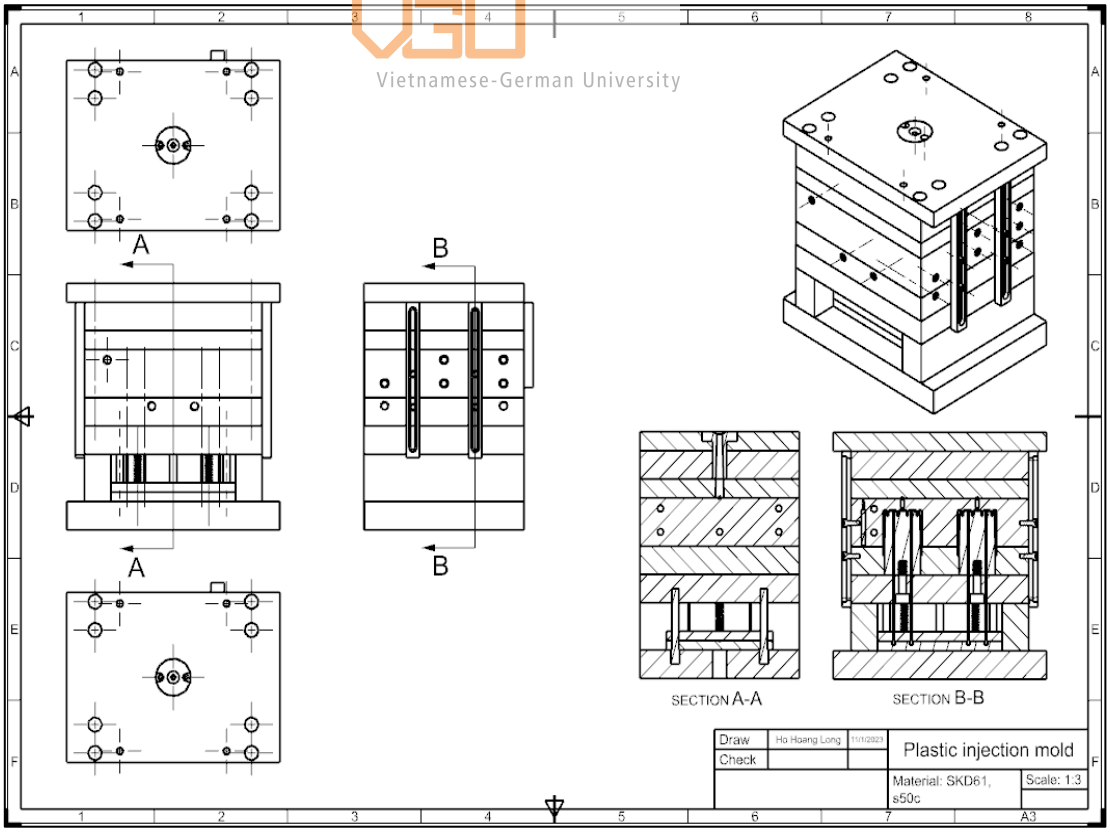

Figure 5-37: The 2D CAD of the plastic injection mold

6. Discussion

This thesis focuses in calculating and designing the feed system to ensure that the material can comfortably flow into the cavity. However, this thesis has not focused in analyzing the volumetric shrinkage that occurs at the product cavity. When the material situates at the cavity is cooled at the end of the packing phase, its volume tends to shrink due to thermal contraction, leading to the dimensional requirement dissatisfaction. The molding will shrink through the thickness and along any unconstrained surface such as rib and side walls. For the LED base cover discussed in this thesis, most of the walls are constrained by the cores and the cavities, the plastic may not shrink but develops internal tensile residual stresses. The products instantaneously shrink when they are ejected from the mold cores. For application that requires tight tolerance, the change in the mold dimensions should be considered when specifying the final dimension of the mold cavity. Another point that should be considered when designing the mold is to apply venting to the design. The primary function of venting is to release the air that is replaced by the pressurized plastic melt. By removing the air inside the cavity, several defects can be prevented. These defects include short shot, burn marks, and the presence of gas between two converging flow front reduces the part strength. Designing the appropriate venting requires the designer to conduct the venting analysis, which consists of air displacement and rates estimation, vents number and location identification. Therefore, the appropriate vent dimension can be specified, and the sufficient airflow rate can be calculated. This thesis has not applied venting in the mold design, which the aforementioned defects have a higher chance to occur on the final product.

7. Conclusion

To conclude this thesis, which focuses in designing an appropriate feed system and a sufficient three-plate injection mold to produce an initially specified product. A suitable feed system is created based on the mold flow analysis, which requires both theoretical calculation and the program's simulation results. Using Autodesk Moldflow Insight, this study determines the appropriate molding conditions and gate location to control melt flow inside the mold cavities. The acquired results provide good quality products and avoid

defects. The feed system is then designed and analyzed to provide the sufficient flow path for the melt to the cavities.

Once the feed system has been designed, the thesis focuses in designing the mold components using the CAD program Siemen NX 12. An understanding of the mold structure, components, and their function during the molding process is important to create the shape of each mold components. Siemen NX 12 provides the necessary tools to construct the 3D model of each mold element. Subsequently, the program's FEM analysis is conducted to evaluate the von Mises stress and the bending value of each mold elements. These values are created by the clamping force generated by the clamping unit, or the plastic melts pressure inside the cavities. The mold components must be robust enough to withstand the acting pressure that leads to plastic deformation, causing permanent damage to the components and affects the product's dimensional requirement.

This thesis can be improved by applying more research about venting to further improve the quality of the products. Venting prevents short shots, burn marks and gas presented between two converging flow fronts, which negatively affects the product's structural integrity and aesthetic. Another improvement to be considered is the volumetric shrinkage of the product, which causes the product's dimensional dissatisfaction. The volumetric shrinkage analysis is more complex and time demanding, but it is possible to satisfy the high demand in the product's final dimension.

8. Reference

1. Melchiorre, M. and Duncan, T. (2021) Study of the Effects of Injection Molding Parameter on Weld Line Formation, The Fundamentals of FEA Meshing for Structural Analysis. Ansys. Retrieved from: https://www.ansys.com/blog/fundamentals-of-fea-meshing-for-structural-analysis.
2. Melito, S. (2021) What you need to know about injection molding gates, What You Need to Know About Injection Molding Gates. Fictiv. Retrieved from: https://www.fictiv.com/articles/what-you-need-to-know-about-injection-molding-gates#:~:text=For%20best%20results%2C%20gates%20should,thick%2Dwalled%20areas%20of%20parts.
3. Gelston, J. (2016) 8 tips for picking a gate location, 8 Tips for Picking a Gate Location. AIM processing. Retrieved from: https://www.aimprocessing.com/blog/8-tips-for-picking-a-gate-location.
4. Molding Window analysis. Autodesk Moldflow Insight 2023. Retrieved from: https://help.autodesk.com/view/MFIA/2023/ENU/?guid=MoldflowInsight_CLC_Analyses_analysis_sequences_Molding_Window_analysis_html.
5. hear rate, maximum result. Autodesk Moldflow Insight 2023. Retrieved from: https://help.autodesk.com/view/MFIA/2023/ENU/?guid=MoldflowInsight_CLC_Results_Fill_or_flow_results_Shear_rate_maximum_result_html.
6. Rheology vs shear rate and ideal processing parameters relating to shear (2019). EntecPolymers.
7. Pressure result. Autodesk Moldflow Insight 2023. Retrieved from: https://help.autodesk.com/view/MFIA/2023/ENU/?guid=MoldflowInsight_CLC_Results_Fill_or_flow_results_Pressure_result_html.
8. Dzulkipli, A.A. and M, A. (2017) Study of the Effects of Injection Molding Parameter on Weld Line Formation.
9. Frozen layer fraction at end of fill result. Autodesk. Retrieved from: https://help.autodesk.com/view/MFC/2023/ENU/?guid=GUID-DA6A0128-0879-4A53-BFC5-A927FC8A9048.

10. KAZMER, D.A.V.I.D.O. (2022) Injection mold design engineering. S.l.: HANSER PUBLICATIONS.
11. Lechner, L. (2020) Injection molding basics: Cold runner systems, Injection Molding Basics: Cold Runner Systems. Echo Engineering. Retrieved from: https://www.echosupply.com/blog/injection-molding-basics-cold-runner-systems/.
12. Worth, J. (2018) Injection molds 101: Cold runner vs. hot runner molds, Injection Molds 101: Cold Runner vs. Hot Runner Molds. The Rodon Group. Retrieved from: https://www.rodongroup.com/blog/injection-molds-101-cold-runner-vs-hot-runner-molds.
13. Rajib (2022) Two plate mold vs three plate mold: Injection mold types, Two Plate Mold Vs Three Plate Mold. RiansClub. Retrieved from: https://www.riansclub.com/two-plate-mold-vs-three-plate-mold/.
14. TYPES OF GATING FOR INJECTION MOLDING (2019). Basilius Inc. Retrieved from: https://www.basilius.com/blog/types-of-gating-for-injection-molding/.
15. Runner Balance analysis. Autodesk Moldflow Insight 2023. Retrieved from: https://help.autodesk.com/view/MFIA/2023/ENU/?guid=MoldflowInsight_CLC_Analyses_analysis_sequences_Runner_Balance_analysis_html/.
16. Beaumont, J.P. (2019) Runner and gating design handbook tools for successful injection molding. Munich: Hanser Publishers.
17. Williams, J. (2019) Injection molding cooling time: A breakdown, Injection Molding Cooling Time: A Breakdown. Design World. Retrieved from: https://www.designworldonline.com/injection-molding-cooling-time-a-breakdown/.
18. Veejayplastic (2020) How to calculate clamping force in injection molding?, Clamping Force in Injection Molding: Introduction, Importance, and Calculation. Veejay Plastic. Retrieved from: http://www.veejayplastic.com/blog/how-to-calculate-clamping-force-in-injection-molding/.
19. Jackie (2020) The types of mold base for plastic injection mold, What Are the Types of Mold base? Ecomolding. Retrieved from: https://www.injectionmould.org/2019/03/23/the-types-of-mold-base/.
20. Neill, B.O. (2023) Draft angles in plastic injection molding. Wevolver. Retrieved from: https://www.wevolver.com/article/draft-angles-in-plastic-injection-molding/.